www.czasopisma.pan.pl PAN www.journals.pan.pl

Acta Geologica Polonica, Vol. 71 (2021), No. 2, pp. 103–152
DOI: 10.24425/agp.2020.134556

Redox conditions, glacio-eustasy, and the status of the Cenomanian–Turonian Anoxic Event: new evidence from the Upper Cretaceous Chalk of England

CHRISTOPHER V. JEANS[1], DAVID S. WRAY[2], C. TERRY WILLIAMS[3], DAVID J. BLAND[4] and CHRISTOPHER J. WOOD*

[1] *Department of Earth Sciences, University of Cambridge, Downing Place, Cambridge, CB2 3EN, UK. E-mail: cj302@cam.ac.uk*
[2] *School of Science, University of Greenwich, Pembroke, Chatham Maritime, Kent, ME4 4TB, UK.*
[3] *Department of Mineralogy, Natural History Museum, Cromwell Road, London, SW7 5BD, UK.*
[4] *15 Pains Close, Pinner, Middlesex, HA5 3BN, UK.*
**Deceased.*

ABSTRACT:

Jeans, C.V., Wray, D.S., Williams, C.T., Bland, D.J. and Wood, C.J. 2021. Redox conditions, glacio-eustasy, and the status of the Cenomanian–Turonian Anoxic Event: new evidence from the Upper Cretaceous Chalk of England. *Acta Geologica Polonica*, **71** (2), 103–152. Warszawa.

The nature of the Cenomanian–Turonian Oceanic Anoxic Event (CTOAE) and its δ^{13}C Excursion is considered in the light of (1) the stratigraphical framework in which the CTOAE developed in the European shelf seas, (2) conclusions that can be drawn from new detailed investigations of the Chalk succession at three locations in England, at Melton Ross and Flixton in the Northern Province where organic-rich 'black bands' are present, and at Dover in the Southern Province (part of the Anglo-Paris Basin) where they are absent, and (3) how these conclusion fit in with the present understanding of the CTOAE. The application of the cerium anomaly method (German and Elderfield 1990) at Dover, Melton Ross and Flixton has allowed the varying palaeoredox conditions in the Chalk Sea and its sediments to be related to the acid insoluble residues, organic carbon, δ^{18}O (calcite), δ^{13}C (calcite), δ^{13}C (organic matter), Fe $^{2+}$ and Mn^{2+} (calcite), and P/TiO_2 (acid insoluble residue). This has provided evidence that the initial stages of the δ^{13}C Excursion in England were related to (1) a drop of sea level estimated at between 45 and 85 metres, (2) influxes of terrestrial silicate and organic detritus from adjacent continental sources and the reworking of exposed marine sediments, and (3) the presence of three cold water phases (named the *Wood*, *Jefferies* and *Black*) associated with the appearance of the cold-water pulse fauna during the Plenus Cold Event. Conditions in the water column and in the chalk sediment were different in the two areas. In the Northern Province, cerium-enriched waters and anoxic conditions were widespread; the δ^{13}C pattern reflects the interplay between the development of anoxia in the water column and the preservation of terrestrial and marine organic matter in the black bands; here the CTOAE was short-lived (~0.25 Ma) lasting only the length of the Upper Cenomanian *Metoicoceras geslinianum* Zone. In the Southern Province, water conditions were oxic and the δ^{13}C Excursion lasted to the top of the Lower Turonian *Watinoceras devonense* Zone, much longer (~1.05 Ma) than in the Northern Province. These differences are discussed with respect to (1) the Cenomanian–Turonian Anoxic Event (CTAE) hypothesis when the ocean-continent-atmosphere systems were linked, (2) limitations of chemostratigraphic global correlation, and (3) the Cenomanian–Turonian Anoxic Event Recovery (CTOAER), a new term to define the varying lengths of time it took different oceans and seas to recover once the linked ocean-continent-atmosphere system was over. The possibility is considered that glacio-eustasy (the glacial control hypothesis of Jeans *et al*. 1991) with the waxing and waning of polar ice sheets, in association with the degassing of large igneous provinces, may have set the scene for the development of the Cenomanian–Turonian Anoxic Event (CTAE).

Key words: Cretaceous; Cenomanian–Turonian Anoxic Event; Eustatic lithocycles; Glacial associations; Redox conditions; Cerium anomalies; Carbon isotopes; NW Europe; Japan.

INTRODUCTION

The concept of the Late Cenomanian–Early Turonian Oceanic Anoxic Event (CTOAE) was put forward 30 years ago by Schlanger *et al.* (1987) and Arthur *et al.* (1987) to explain the widespread and extensive preservation of organic carbon (C_{org}) in ocean sediments of this age in the proto-North Atlantic Ocean basin and their association with a $\delta^{13}C$ spike recorded in the carbonate shell material preserved in the coeval sediments of its shelf seas. It also became an attractive and competing hypothesis to the bolide impact cause for the widespread extinction of numerous faunal and floral species in the marine realm at or close to the Cenomanian–Turonian boundary that was being investigated by many researchers (e.g. Hut et *al*. 1987). It is estimated that 7% of all families, 26% of all genera, and 53% of all species became extinct (Sepkoski 1989; see also Leckie *et al*. 2002; Nagm 2015). The CTOAE was attributed ultimately to a volcano-tectonic event that caused a maximum sea level high stand and the extensive flooding of shelf areas, which resulted in enhanced organic carbon deposition in globally distributed basins under different climatic and ocean circulations. Changes in the patterns of ocean circulation and an increased rate of production of warm saline bottom-waters were considered responsible for an expansion of the oxygen minimum zone and high surface productivity. This resulted in the widespread development of anoxic conditions and the enhanced burial in marine sediments of organic carbon enriched in C^{12}; the record of this enrichment is referred to as the $\delta^{13}C$ Excursion. The general concept of a non-bolide global event has stood the test of time and various challenges. Extensive research has put flesh on the idea and refined its stratigraphical framework. The first challenges were based on correcting the stratigraphy and the detailed interpretation of the lithological record and the conditions under which it occurred. The original mechanism proposed by Schlanger *et al.* (1987) and Arthur *et al.* (1987) linked its development to the great marine transgression of the late Cretaceous Seas as understood at that time that had been mistakenly placed by Hancock and Kauffman (1979) at the base of the Upper Cenomanian *Metoicoceras geslinianum* Zone, the stratigraphic level at which the $\delta^{13}C$ Excursion first appears. In fact the great marine transgression that formed an essential part of the mechanism only reached its acme within the Middle Turonian *Collignoniceras woollgari* Zone (Hancock 1989, pp. 580–581) at a time when the CTOAE had nearly run its course, thus rendering its setting untenable. Four years later a very different setting was suggested. Jeans *et al.* (1991) – based on a detailed reinvestigation of the Cenomanian–Turonian Plenus Marls section at Dover described by Schlanger *et al.* (1987) – drew the conclusions that (1) the initiation of the CTOAE was linked to a facies change associated with a marked drop in sea level, and (2) the development of the $\delta^{13}C$ Excursion was associated with an increasingly shallowing and cooling sea, and (3) the cold water was associated with the boreal or cold water occidental fauna of Jefferies (1962, 1963). An alternative setting – the glacial control hypothesis – was suggested based upon a glacial draw-down mechanism associated with widespread regression resulting in restricted ocean circulation, lower ocean temperatures, enhanced input of terrestrial silicate and organic matter, and the presence of dropstones. Since then researchers have (1) applied various isotopic geochemical proxies to clarify the atmospheric, terrestrial and oceanic conditions leading up to and within the CTOAE (e.g. $^{34}S/^{32}S$: Ohkouchi *et al*. 1999, Owen *et al*. 2013, Gomes *et al*. 2016, Raven *et al*. 2018, 2019; $^{87}Sr/^{86}Sr$: Frijia and Parent 2008; $^{44}Ca/^{40}Ca$: Blättler *et al*. 2011, Du Vivier *et al*. 2015b; $^{144}Nd/^{143}Nd$: Zheng *et al.* 2013; $^{188}Os/^{187}Os$: Turgeon and Creaser 2008; $^{7}Li/^{6}Li$: Pogge von Strandmann *et al*. 2013; $^{53}Cr/^{52}Cr$: Holmden *et al*. 2016, Wang *et al.* 2016; $^{57}Fe/^{56}Fe$: Jenkyns *et al*. 2007, Owen *et al.* 2012; U isotopes: Montoya-Pino *et al*. 2010), and (2) have used refined biostratigraphical zonations, radiometric age determinations of ash bands (e.g. Meyer *et al*. 2012) in association with astrochronology (e.g. Voigt *et al.* 2008) to provide a more precise temporal framework. At the present time the CTOAE is considered to have been a short-lived happening some 94 million years ago that lasted for up to 0.5 million years when both the carbon in the marine calcium carbonate skeletons and in the organic matter of plants and animals that lived in the world's oceans and on the continents had linked and considerably enhanced $\delta^{13}C$ values. This reflected the composition of the carbon dioxide in the world's ocean-atmosphere system that was enriched in ^{13}C. The concentration and variation of carbon dioxide in the atmosphere during the initial part of the CTOAE has been studied by measuring the stomatal index of plant leaves in a sequence of paralic strata of uppermost Cenomanian age in S.W. Utah, USA (Barclay *et al.* 2010). Concentration of carbon dioxide reached estimated levels of $\sim 500^{+400}/_{-180}$ ppm although there were periods when values were little more than background values $(370^{+100}/_{-70}$ ppm. The source of this high concentration of carbon dioxide

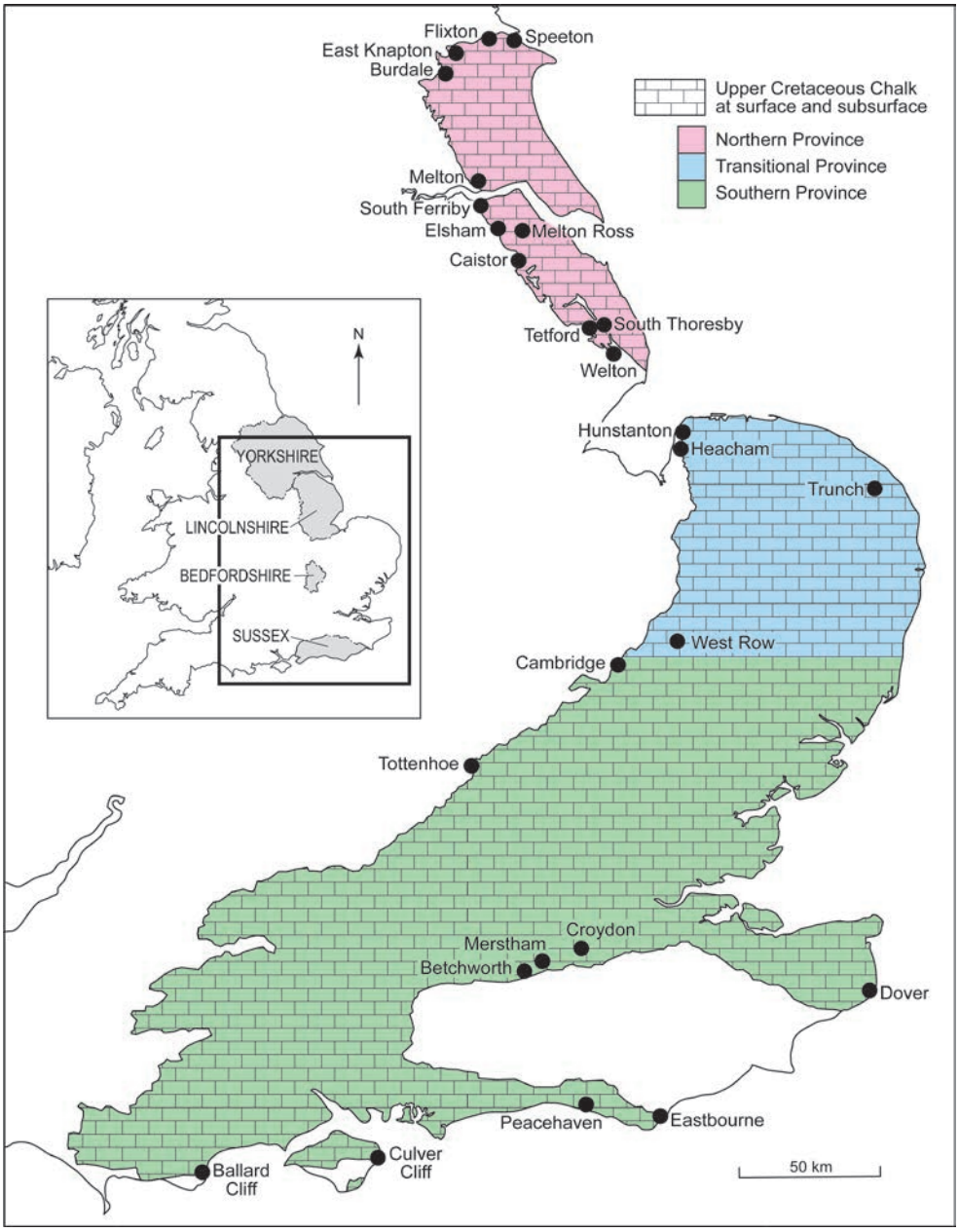

Text-fig. 1. Distribution of outcrop, subcrop and the provinces of the Upper Cretaceous Chalk of England. The strata of the Cenomanian–Turonian Oceanic Anoxic Event (CTOAE) are coextensive within the Chalk. All locations and key localities are shown.

has been linked to the intrusion of one or more large igneous provinces (Black and Gibson 2019) active at the time, particular attention has been given to the Caribbean Large Igneous Intrusion and the role it may have played in triggering the CTOAE (e.g. Turgeon and Creaser 2008) but others such as the Northern Greenland (Tegner *et al*. 2011) and Madagascan (Kuroda *et al*. 2007) may have also played a role. The concept of the CTOAE was based largely upon the stratigraphical idea demonstrated by Scholle and Arthur (1980) that variations of the $\delta^{13}C$ (calcite) values from pelagic limestones were a potential tool for long-range correlation in the Cretaceous strata of the Circum-Atlantic-Western Tethyan region including Chalk sequences in the UK (Kent, Hampshire, Norfolk), North Sea, Netherlands and Germany. The

authors were at pains to discuss possible problems relating to primary controls on the carbon isotope variations related to temperature, water mass and faunal/floral changes, the organic carbon cycle as well as to diagenesis. Unfortunately little serious attention has been given to diagenesis and the changes that may have occurred to an original oceanic signal over the ~90 million years of its burial history. We shall see later that this has led to considerable problems of correlation and interpretation. Global evidence suggests that the Cenomanian–Turonian Oceanic Anoxic Event started at a particular geological "moment" whereas its termination varied considerably depending upon the palaeogeographic situation. This is very evident when comparison is made between the δ^{13} Excursion in our area of detailed investigation of the Chalk sequences in the Northern and Southern Chalk Provinces of England. In order to investigate the significance of this difference it has been necessary to define more precisely the terminology. The Cenomanian–Turonian Oceanic Anoxic Event (CTOAE) is defined here by the $\delta^{13}C$ Excursion preserved in the calcium carbonate skeletons and the organic matter of marine organisms. The Cenomanian Turonian Anoxic Event (CTAE) refers to the conceptual period when there is evidence that both the carbon in the calcium carbonate skeletons and organic matter of organisms that lived in the world's oceans and on the continents had considerably enhanced $\delta^{13}C$ values that were linked and co varied. The Cenomanian–Turonian Oceanic Anoxic Event Recovery (CTOAER) refers to the variable time period between the end of the ocean/continent linkage and the end of the CTOAE when the marine $\delta^{13}C$ Excursion returned to background values. The term Oceanic Anoxic Event 2 (OAE2) is misleading and its use should be discouraged. Oceanic anoxic events are known from Archean and Proterozoic times onwards.

Our paper describes the general setting of the Cenomanian–Turonian Chalk of the Northern Chalk Province of England (Text-fig. 1) and how it is related to the development and decay of the CTOAE in a different setting at Dover in the Southern Province. A precise stratigraphical framework and knowledge of the stratal geochemistry, mineralogy and diagenesis has allowed a much fuller use on a bed-to-bed scale of a range of proxies ((cerium anomalies, acid insoluble residues, organic carbon, $\delta^{18}O$ (calcite), $\delta^{13}C$ (calcite), $\delta^{13}C$ (organic matter), Fe^{2+} and Mn^{2+} (calcite), and P/TiO_2 (acid insoluble residue) in interpreting the changing conditions in the Chalk Sea and its sediment during the CTOAE. Three localities are dealt with in detail, Flixton and Melton Ross in the Northern Chalk Province and Dover in the Southern Chalk Province (part of the Anglo-Paris Basin). The conclusions that can be drawn from these investigations are discussed in relation to recent hypotheses and research on many aspects of the controls and conditions under which the CTOAE and the CTAE developed and decayed on a global scale with particular emphasis on the possibility that glacio-eustacy may have played a significant role.

STRATIGRAPHICAL SETTING OF THE NORTHERN CHALK PROVINCE, ENGLAND

Six transgressive-regressive sedimentary cycles of Upper Albian to Turonian age are recognised in the Northern Chalk Province of England. They provide a detailed record of both local and oceanic events leading up to the CTOAE that took place in the proto-North Atlantic Ocean, its shelf seas and other connected marine areas. Not only can these cycles be matched in considerable detail with the sequences in northern Europe (Text-fig. 2), some can be recognised in North America, Egypt, Sinai, Jordan, Tunisia and the Arabian Plate. They provide the sedimentological setting for the development of the CTOAE and its relationship to changes in the depth of the Chalk Sea. The sediment cycles of the Northern Chalk Province are remarkable for their completeness and lateral consistency in spite of having been deposited in a region of reduced sedimentation, in contrast to the thicker sequences of the adjacent North Sea Basin (Oakman and Partington 1998, p. 298) to the east and the Anglo-Paris Basin (Mortimore 1986, figs 3.3, 3.4) to the south where local tectonics played a more prominent role in controlling the pattern of sedimentation. The cycles are numbered II to VII (Text-fig. 2; Jeans 1980, fig. 3). Five (Cycles II–VI) start with an erosion surface with or without an association of clay enriched chalk strata often with pebble-grade material at the base that pass up through shell fragment-rich and then calcisphere-rich lithofacies into coccolith-rich chalks at the top. The sixth cycle (Cycle VII) – the one associated with the initiation of the CTOAE – is different displaying a coarsening upwards sequence above the basal erosion surface and its immediately overlying basal pebble bed. It starts with a considerable thickness of fine-grained clayey marls and marly chalks that may be laminated (Text-fig. 13) and these pass up into chalks and marls first rich in calcispheres and then fragments of inoceramids. The majority of these cycles are comparable to the standard regres-

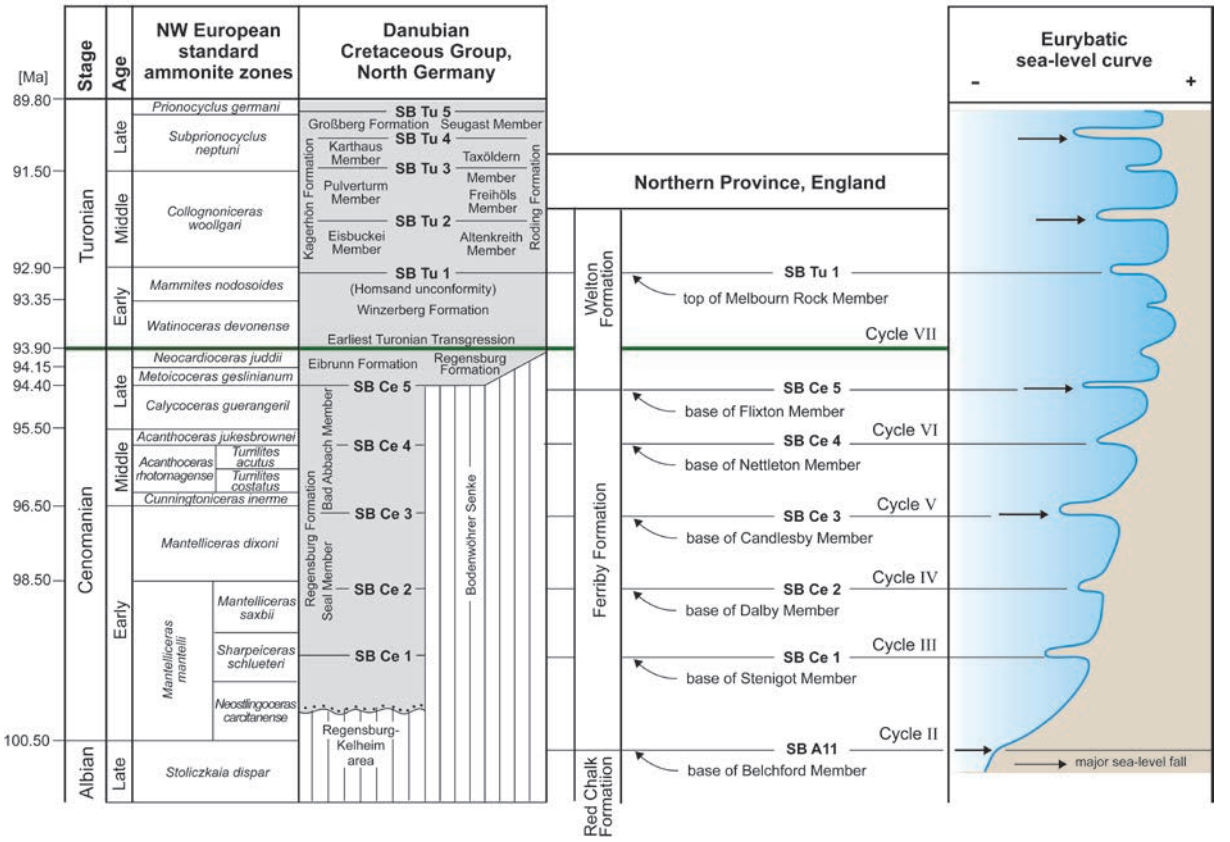

Text-fig. 2. Proposed correlation between the lithofacies Cycles II–VII of the Northern Chalk Province, the sequence stratigraphy (SB Ce 1–5, SB Tu 1–5) of the Danubian Cretaceous Group of northern Germany, and the standard ammonite zones for northwest Europe. Based in part on Janetschke *et al*. (2015). Radiometric dates are based on Ogg *et al.* 2012.

sion-transgression sediment pattern recognised in sequence stratigraphy. The basal erosion surface and its associated complete or patchy hard ground marks the peak of the regression and the maximum lowering of sea level, the overlying bed of chalk pebbles and clay (if present) are deposits of the regressive part of the cycle. The overlying fining upward sequence reflects the transgressive phase with the fine-grained coccolith-rich chalky limestone at the top marking its peak and maximum water depth. The only exception is Cycle VII recording the CTOAE. The basal erosion surface with its pebble bed is overlaid by a coarsening upward sequence ending in chalks rich in inoceramid fragments, a similar pattern is present in the Southern Province at Dover (Jeans *et al.* 1991) and Eastbourne (Keller *et al.* 2001). In both provinces the sequence is broken by a hard chalky limestone, the top of which marks the first appearance of *Praeactinocamax plenus*. This is referred to as the Central Limestone in the Northern Province, Jefferies Bed 3 in the Southern Province, and the "Plenus Bed" in northwest Germany (Text-fig. 4). This upward coarsening sequence is interpreted using the lithofacies models (see below) as reflecting the deposits of an upward shallowing Chalk Sea. The number of cycles and their timing demonstrates a close similarity to the detailed findings of Wilmsen *et al.* (2010a) and Janetschke *et al*. (2015) on the waxing and waning of the Cenomanian–Turonian shelf sea in northern Germany as it encroached upon and partly submerged the Mid-European Island (Text-fig. 2). These authors have used sequence stratigraphy to analyse the relationship between the submergence of the Mid-European Island and the changing lithofacies and biostratigraphy of the Planerkalk, Elbtal and Danubian Cretaceous groups. Six 3rd order sequence bounding unconformities are recognised in the Cenomanian and Lower Turonian strata, each can be matched in the Northern Province of England with the base of different members of the Ferriby

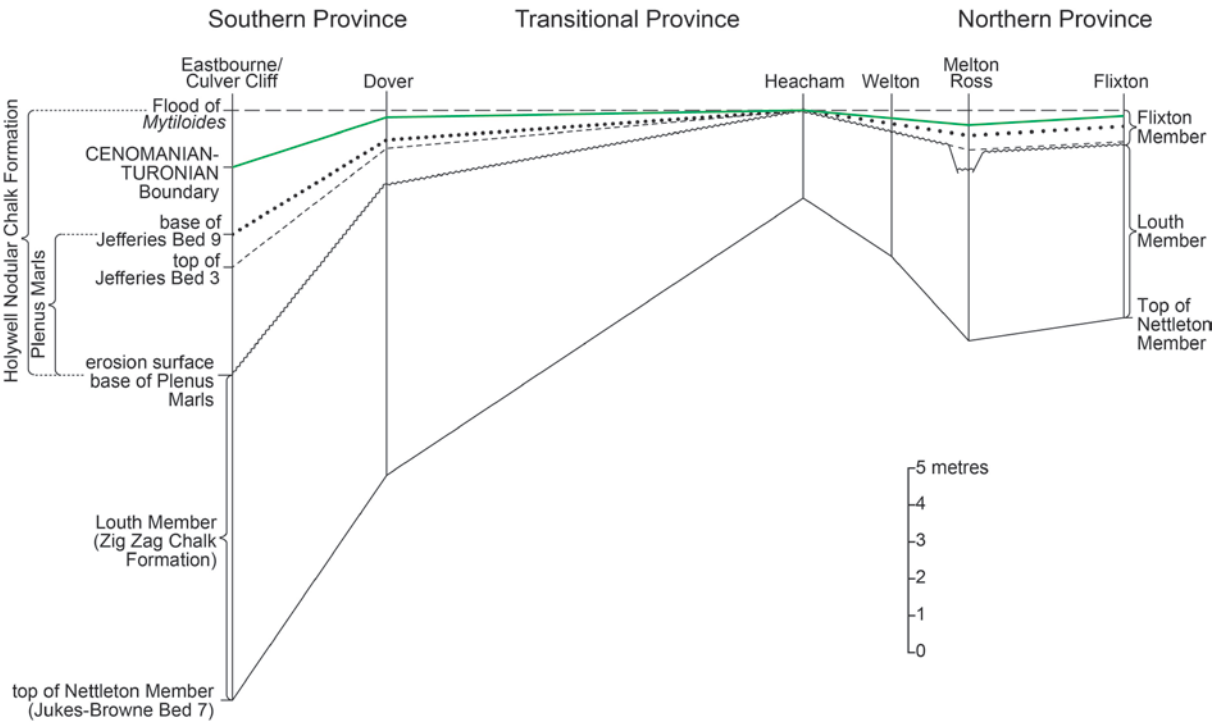

Text-fig. 3. Terminology and general stratigraphy of the Upper Cenomanian and Lower Turonian strata at Dover, Melton Ross and Flixton.

Formation and the overlying Welton Formation (Text-fig. 2). The only exception is the cycle recording the CTOAE and this is an upward-fining cycle in contrast to the upward coarsening cycle in the Southern and Northern Provinces of England.

Some of these transgressive-regressive cycles and in particular the one recording the CTOAE can be recognised in North America (Gale *et al.* 2008; Scott *et al.* 2018), Egypt, Sinai, Jordan, Tunisia and the Arabian Plate (Wilmsen and Nagm 2013; Hairapetian *et al*. 2018). There can be little doubt they represent eustatic changes of sea level and that the CTOAE cycle was initiated by a major drop in sea level and was developed in association with a major transgression that flooded low-lying coastal areas. Why the cycle involving the CTOAE in the Northern and Southern Provinces of England and probably throughout the Anglo-Paris Basin displays evidence of a shallowing and regressive environment needs to be explained. Much of this area was detached from mainland Europe by tectonics during the development of the North Sea Basin on one side and on the other by the early development of the Atlantic Ocean (Oakman and Partington 1998). It would be surprising if the patterns of sedimentation associated with this important transgression were the same on mainland Europe as in England considering their different regional tectonic settings.

An indication of the extent to which the sea level dropped between each cycle in the Northern Chalk Province can be obtained by considering the changes of facies between the top of a cycle and the base of the overlying one by (1) the depth of channelling and, if possible, the regional loss of sediment associated with the basal erosion surface, and (2) the change of lithofacies across this erosion surface using models of Chalk deposition. Two models have been proposed (Black 1980, fig. 13; Wilmsen 2003; Wilmsen *et al.*2005, figs 10, 11). The Black model, originally proposed in 1956, compared the distribution of Chalk lithofacies with three observations in present oceans – the maximum coccolith production at above ~55 metre water depth, the lower limit of abundant pelagic foraminifera at ~185 metre water depth, the lower limit of the presence of shell sand at 185 metres water depth based on observations in the oceans on the Great Bahama Bank, and an average water depth of ~300 metres for a shelf sea. The Wilmsen model is a reconstruction of the facies distribution in the Cenomanian–Turonian seas of northern Germany using a combination of lithofacies with present day fair weather and storm weather wave bases, less stormy seas, and minimal water depths

for particular depositional settings down to a maximum of 100 metres. Black's model allows considerably greater water depths than the Wilmsen model as it does not take into account that the Chalk Sea was perhaps associated with less severe storms – and therefore shallower fair weather and storm weather wave bases – than those of today: this would reduce the lower depth limit for shell sands. Furthermore recent and Cretaceous oceanographies were considerably different with the absence of shelf-break fronts in Late Cretaceous times affecting the distribution of pelagic calcareous plankton (Hay 2008). We have used the Wilmsen model in our estimates of changes of sea level but realising that it may not recognise depth controlled variations in the distal outer shelf facies beyond their 100 metre depth limit. The Black model utilises the decreasing ratio between coccoliths and pelagic foraminifera to establish a contour at ~185 metres water depth making use of the lower limit of abundant pelagic foraminifera to define an outer distal lithofacies with a constant ratio of coccoliths and pelagic foraminifera.

Channelling at the base of Cycles V and VII is absent from the Northern Province and is restricted to the Transitional Province (Text-fig. 1) where the chalk sediment was soft and uncemented unlike the Northern Province where early lithification prevailed (Jeans 1980). At base of Cycle V – the initiation of the Mid-Cenomanian Event – localised channels cut down into the underlying sediment to a depth of 25–30 metres at Tottenhoe in Bedfordshire (Mortimore 2014, fig. 3.10) and to ~10 metres proved in boreholes at Barrington near Cambridge. There is no evidence of the extent of the general loss of sediment represented by the unchannelled erosion surface. This provides a minimum sea level drop of 25–30 metres. The Wilmsen model gives a depth drop of 30–60 metres. It is more difficult to place a minimum value on the sea-level drop associated with the base of Cycle VII marking the initiation of the CTOAE. Evidence from channelling is limited because seafloor conditions were quite different to those at Mid-Cenomanian times. The change in lithofacies ("Facies Change" of German authors) from the coccolith-rich Louth Member (former "poor-rhotomagense Limestones facies", Hoppenstedt Member of the Brochterbeck Formation) at the top of Cycle VI to the bottom of Cycle VII with its marls and chalk rich in clay, calcispheres, shell fragments and chalk pebbles is even more pronounced than between Cycles III and IV. The general depositional setting was further offshore: the coccolith-rich chalk sediment affected by erosion had not undergone early lithification – and this resulted in extensive regional erosion over the Northern Province. This not only removed the Anomalous Black Band sequence (representing Jefferies beds 1, 2), except where preserved at Melton Ross, but also considerable amounts of the underlying Louth Chalk Member particularly in the southern region where it has been reduced from its normal post-erosion thickness of 6–7 m to 2–3 m in parts of Norfolk (Gallois 1994). In the Transitional Province hollows and shoals at the top of the Louth Member in Cambridgeshire are filled by the Plenus Marls (Jefferies 1963, figs 4, 5.); these could represent erosional channels of a few metres depth. The minimum loss of chalk is ~10 metres. It is surprising that evidence of this reworked material, which must have been deposited largely in the Anglo-Paris Basin, has not generally been recognised in the numerous studies of the stratigraphy based on micropalaeontology although Pearce *et al.* (2009, pp. 210–211) has considered this possibility. The Wilmsen model suggests values of 43–86 metres. In Egypt, channels of 30–40 metres depth are associated with this period of erosion (Wilmsen and Nagm 2013).

Of considerable relevance to the geological circumstances leading up to the initiation of the CTOAE is the pulse fauna (Jeans 1968) – this includes the boreal or cold water occidental fauna of Jefferies (1962) – that characterised the early stages in the development of the CTOAE in England and parts of Europe. Representatives of this fauna are linked to the early stages of three of these sediment cycles (Cycles II, V and VII), a fourth example is linked to a lithofacies change within Cycle IV. Associated with the base of these three cycles are $\delta^{13}C$ excursions that are considered to be of worldwide extent: The pattern of $\delta^{13}C$ anomalies at the base of Cycle II – the Albian–Cenomanian boundary at Speeton (Mitchell *et al.* 1996, fig. 5) – has been recognised in the marine environment in many parts of the world: The initial stage of Cycle V, at the base of the Middle Cenomanian ammonite *Acanthoceras rhotomagense* Zone, has a distinctive $\delta^{13}C$ signature first described by Paul *et al.* (1994), which is now recognised as a worldwide event (Mid-Cenomanian Event of Mitchell *et al.* 1996) in both marine and terrestrial environments (Giraud *et al.* 2013). The base of Cycle VII marking the beginning of the much more extensive $\delta^{13}C$ Excursion associated with the CTOAE. These three cycles and their $\delta^{13}C$ excursions have been widely recognised in North America (e.g. Gale *et al.* 2008: Scott *et al.* 2018). So far two of these six cycles and their associated pulse faunas have been investigated by Zheng *et al.* (2013, 2016) in respect to the geochemical changes in the Chalk Sea. Both show the same general pattern and

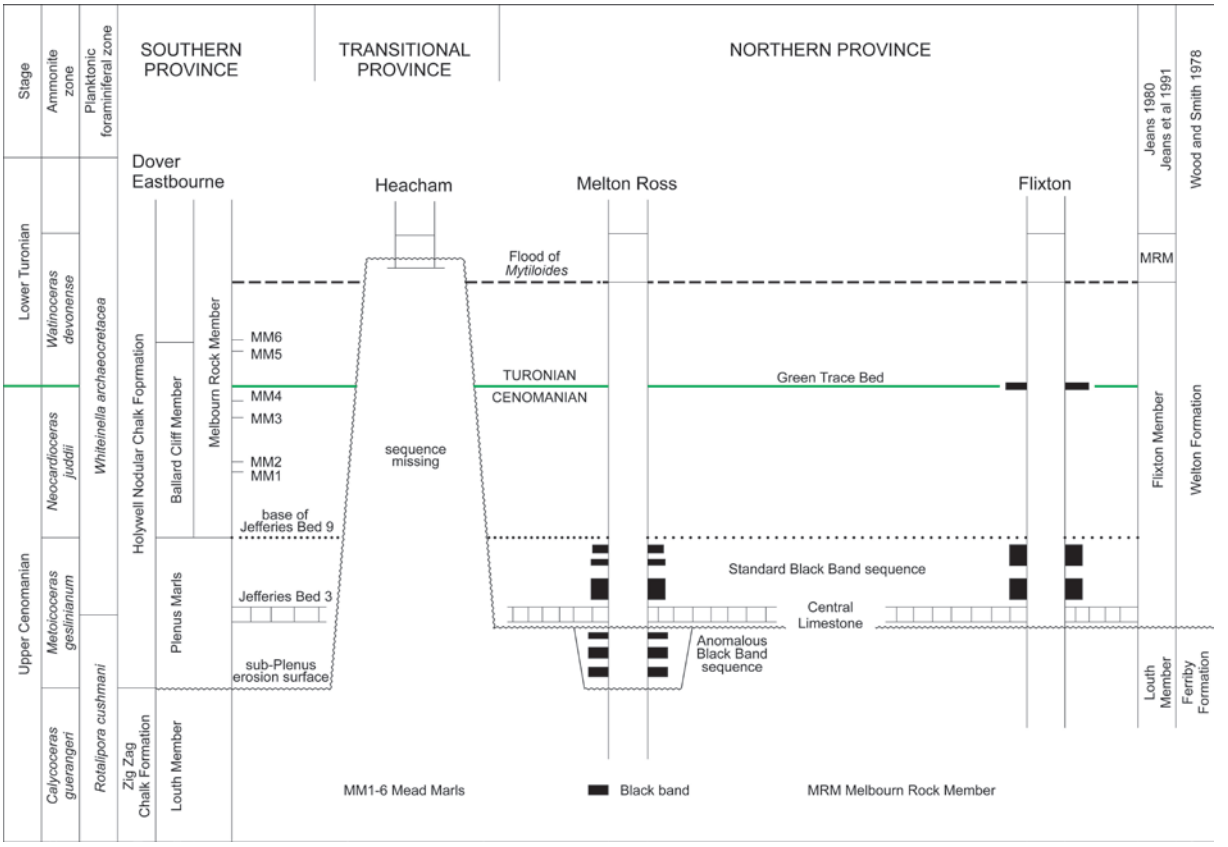

Text-fig. 4. Schematic horizontal section through the Upper Cenomanian and Lower Turonian strata of eastern and southern England showing the main stratigraphic framework in which the investigation was carried out.

we will argue that this is more likely to be related to glacio-eustacy associated with changes in ocean circulation than to changes in the atmospheric concentration of carbon dioxide.

STRATIGRAPHICAL FRAMEWORK

The Plenus Marls and the associated strata that record the CTOAE occur throughout the outcrop and subcrop of the English Chalk (Text-fig. 1). There are regional variations in lithology and thickness as well as the stratigraphical extent of the CTOAE. Text-figs 3 and 4 show how the thicker sequences of Eastbourne and Dover in the Southern Province are related to the much thinner and lithologically more varied successions in the Northern Province at Melton Ross and Flixton that are now referred to as the Variegated Beds (Wood and Mortimore 1995; Wood *et al*. 1997; Jeans *et al*. 2014a) in preference to the Plenus Marls/ Black Band. The Variegated Beds are thinly bedded chalks and marls, sometimes finely laminated, varying in colour between black, grey, green, red and white (Text-fig. 13) are in contrast to the relatively thick units of grey and white marls and chalks that constitute the Plenus Marls of the Southern Province (Text-figs 7, 8). Black bands occur in the Variegated Beds in central and northern Lincolnshire (e.g. Louth, Caistor, Melton Ross, Elsham, South Ferriby) and Yorkshire (e.g. Melton, Burdale, East Knapton, Flixton, Speeton). Two units are recognised in the Variegated Beds; (1) the lower *Anomalous Black Band sequence,* preserved only at Melton Ross within a local down-faulted basin, whereas (2) the upper *Standard Black Band sequence* occurs throughout. Both units have an erosional contact with the underlying Louth Member, but at Melton Ross, the standard sequence overlies the anomalous sequence with an erosional contact (Text-figs 4, 10). There are also laterally extensive black bands and thin marl seams that add to the detailed correlation (Jeans *et al.* 1991, fig. 10; Jeans *et al*. 2014a, text-fig. 5).

The Transitional Province centred on Norfolk (Text-fig. 1) is marked by increasingly reduced sequences as it is approached from either the Northern or Southern Provinces. This represents a loss of the stratal record, probably both by penecontemporaneous erosion and non-deposition. There is no evidence that the whole or parts of the Transitional Province was subaerially exposed, but there is little doubt that it restricted interchange between the waters of the Northern and Southern Provinces. The strata of the Transitional Province, as well as those in the most southerly part of the Northern Province, are conspicuously different from those to the north and south – unless they have been affected by late stage non-intrinsic diagenesis during the Cenozoic (Jeans *et al.* 2016). At Tetford, South Thoresby and West Row (Text-fig. 1) they are red or pink in colour (Text-fig. 5); and are comparable to the CTOAE sediments of the much thicker Rötpläner facies (Söhlde Formation) in northern Germany (Wiese 2009) and the Arowhanan red-coloured marine strata in New Zealand (Hasegawa *et al.* 2013). These coloured sediments never experienced anoxic diagenesis as all the degradable bio matter had already been metabolised in the oxic and suboxic zones of diagenesis (Hu *et al.* 2012). In addition to the presence of organic-rich black bands in the CTOAE strata of the Northern Province and their absence from the Southern Province, there are important differences in the extent to which the strata have been affected by diagenesis. This had to be taken into account when establishing the most suitable stratigraphic framework for our investigation. Much of the strata in the Southern Province are of soft chalks and marls that readily disaggregate into their component grains and have undergone relatively little diagenetic modification. Calcite cements are generally at a very low-level with bulk specific gravities of the chalk in the order of 1.5 to 1.6. However in the upper part of the succession there are nodular chalks rich in inoceramid fragments (Melbourn Rock Member, Holywell Nodular Chalk Formation: Text-fig. 7) that are well cemented by calcite with bulk specific gravities in the region of 1.95 to 2.13 (Mortimore and Pomerol 1998). The strata of the Northern Province Chalk have been affected regionally by calcite cementation, enhanced temperatures and extensive pressure dissolution (check Jeans *et al.* 2014a for an up-to-date review). It is much harder and denser with bulk specific gravities in the region of 2.0 to 2.5. Marl beds are generally uncemented but have been affected by pressure dissolution that may have selectively dissolved the finer-grained calcite fractions.

Little or no stratigraphical use has been made of the pattern of $\delta^{13}C$ variation evident in the bulk carbonate fraction of the strata from the three different localities such as been suggested by Jarvis *et al.* (2006) for a stand-alone means of intercontinental correlation using the Cenomanian–Turonian succession at Eastbourne as a European reference section. Subsequent work has shown that this approach has severe limitations unless detailed knowledge of the type and extent of cement has been determined (Hu *et al*. 2012; Jeans *et al*. 2012) and our study emphasises the importance of the presence of a robust biostratigraphical or chronostratigraphical framework. The stratigraphical framework used in this study is based upon five well-defined lithological and palaeontological marker horizons and units that are of regional or international extent (Text-fig. 4). These include the results of a study on the nannofossil zonal assemblages from the Cenomanian and Turonian Chalk of eastern England (Gallagher, in preparation). The five marker horizons are described below.

Text-fig. 5. Soft pink marly chalk (bed 7, 1.23 m thick, Worssam and Taylor 1969, p. 34) in the upper part of the Plenus Marls at the disused West Row quarry, Cambridgeshire (National Grid ref. TL681752; Text-fig. 1). The mottled appearance is the result of the surface precipitation of soil calcium carbonate. Axe head 23 cm.

(1) The base of the Plenus Marls and the Variegated Beds with their erosional contact with the underlying fine-grained, clay-poor, coccolith-rich chalk. which is referred to as the Louth Member of the Ferriby Formation in eastern England (Jeans 1980) and a similarly named member in the upper part of the Zig-Zag Chalk Formation in the Southern Province (Jeans *et al.* 2014a). This level marks the top of the *Calycoceras guerangeri* Zone and the base of the *Metoicoceras geslinianum* Zone at Dover and Eastbourne in the Southern Province and the base of the Anomalous Black Band sequence at Melton Ross in the Northern Province. At Flixton and

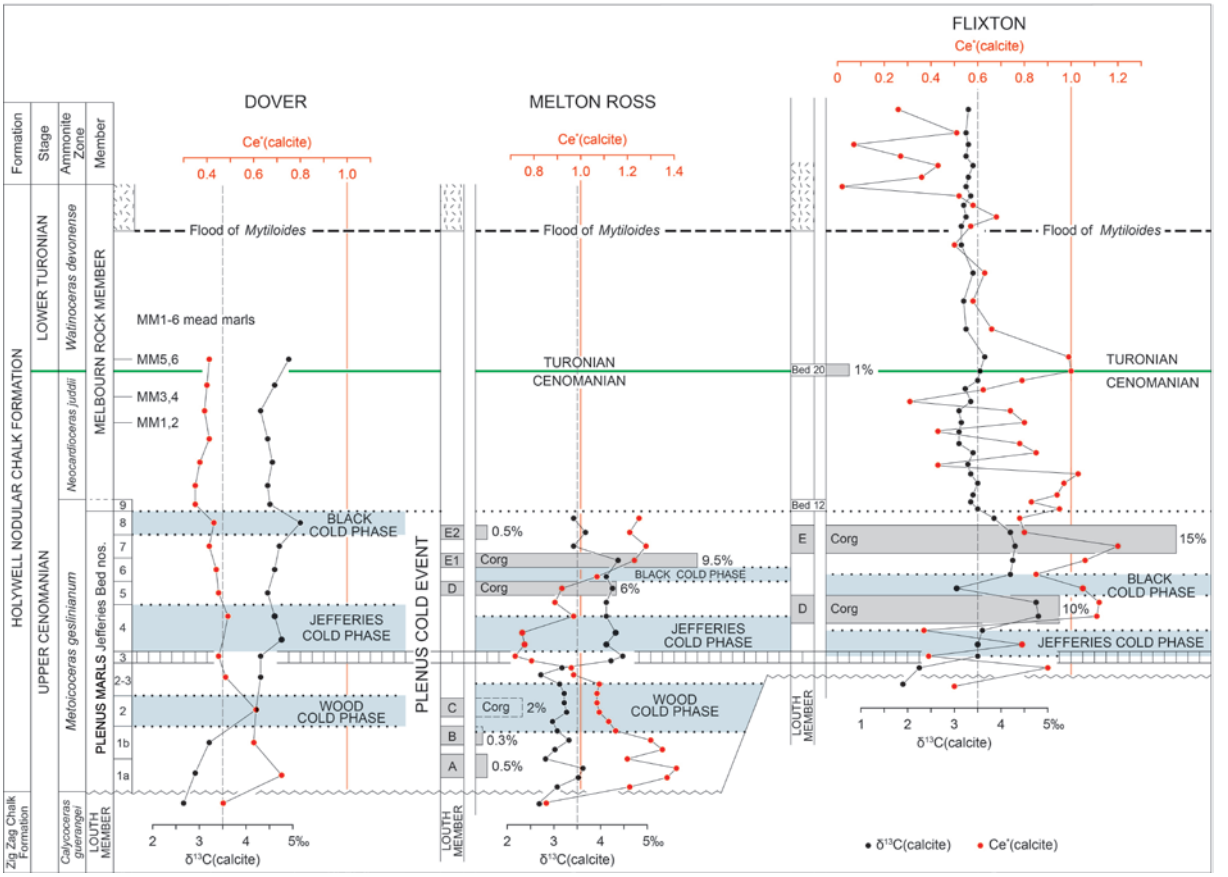

Text-fig. 6. Upper Cenomanian and Lower Turonian sequences at Dover, Melton Ross and Flixton showing the detailed relationships between (a) the general stratigraphy, the distribution of black bands and the C_{org} content of their acid insoluble residues (AIR), the cold events, and (b) the $\delta^{13}C$ and cerium anomalies of the calcite.

other localities in the Northern Province where the Anomalous Black Band sequence is absent, the base of the Standard Black Band sequence is within the lower part of the *Metoicoceras geslinianum* Zone. In north Germany this horizon is referred to as the "Facies-Change" and occurs at the junction of the Hesseltal and Söhlde formations with the underlying coccolith-rich chalks of the Brochterbeck Formation. This "Facies-Change" is a widely recognised quasi-global sequence boundary, possibly caused by a glacio-eustatic sea level fall (e.g., Ernst *et al.* 1983; Owen 1996; Gale *et al.* 1999, 2000; Wilmsen 2003; Wilmsen and Nagm 2013).

(2) Jefferies Bed 3 (Text-figs 4, 6, 8), a prominent bed of massive chalk in the standard Plenus Marls succession of the Southern Province (Jefferies 1963) that is matched with the Central Limestone in the Northern Province (Wood and Mortimore 1995: Text-fig. 10, Bed 3: Text-fig. 13, Bed 3). It is associated with the first appearance of the eponymous belemnite *Praeactinocamax plenus* (Blainville) of the pulse fauna. The Central Limestone is the equivalent of the "Plenus Bed" of the northwest German successions (Wood *et al.* 1997).

(3) The base of nannofossil *Ahmuellerella octoradiata* (Subzone UC5B) and the top of nannofossil *Rhagodiscus asper* (Subzone UC5A) occur at the base of bed 12 at Flixton (Text-figs 6, 13), and in the upper part of the section at Melton Ross (Text-figs 6, 10); these bioevents are recognised at the base of Jefferies Bed 9 at Eastbourne.

(4) The Cenomanian–Turonian stage boundary is taken at close to the inception of nannofossil *Eprolithus eptapetalus* (Subzone UC6B). This was identified in bed 20 at Flixton (Text-figs 6, 13) where it coincides with the Green Trace Bed (referred to as the sticky green clay by Wood and Mortimore 1995), which has been traced over the whole Northern Province (Jeans 1967; Jeans *et al.* 2014a). At Dover/Eastbourne the Turonian–Cenomanian stage bound-

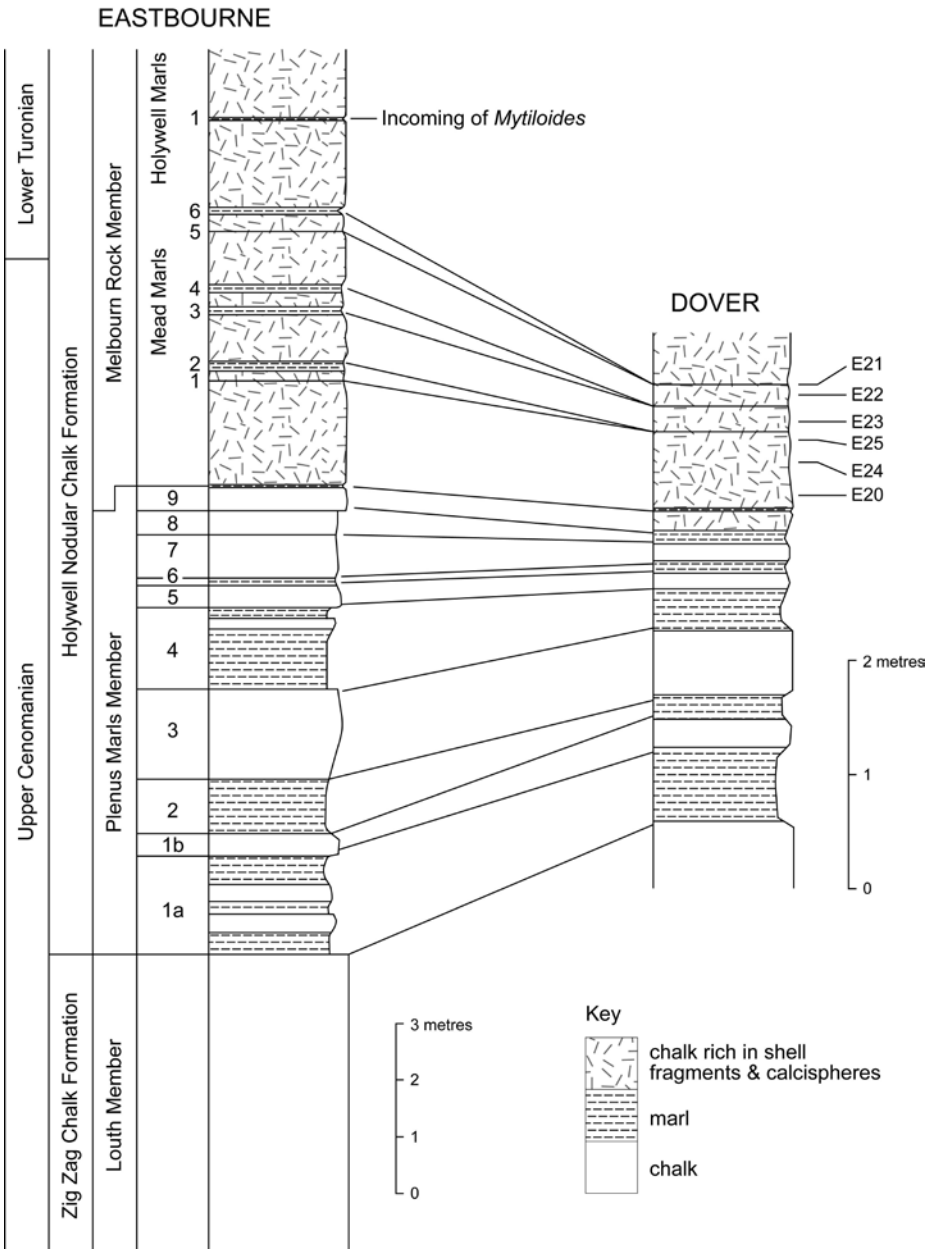

Text-fig. 7. Lithostratigraphy and correlation of the Plenus Marls, lower part of the Melbourn Rock and the six Mead Marls at Eastbourne (based on Paul *et al.* 1999) with the section at Dover. Sample horizons (E20–E25) in the lower part of the Melbourn Rock at Dover are shown.

ary is placed between Mead Marls 4 and 5 (Text-figs 6, 7).

(5) The flood appearance of the inoceramid bivalve *Mytiloides* (Text-fig. 6). This is within the *Watinoceras devonense* Zone of the Lower Turonian. This is recognised throughout the Southern, Transitional, and Northern provinces. It occurs in the upper part of the Melbourn Rock Member at Dover and Eastbourne (Text-fig. 7).

Within this stratigraphical framework various marker beds and horizons based on their lithology and geochemistry are recognised and these further refine correlation. Of particular significance is the recognition of the Plenus Cold Event in both the Northern and Southern Chalk Provinces. This time-stratigraphical term was first used by Gale and Christiansen (1996) in referring to the widespread occurrence in England and western Europe of the

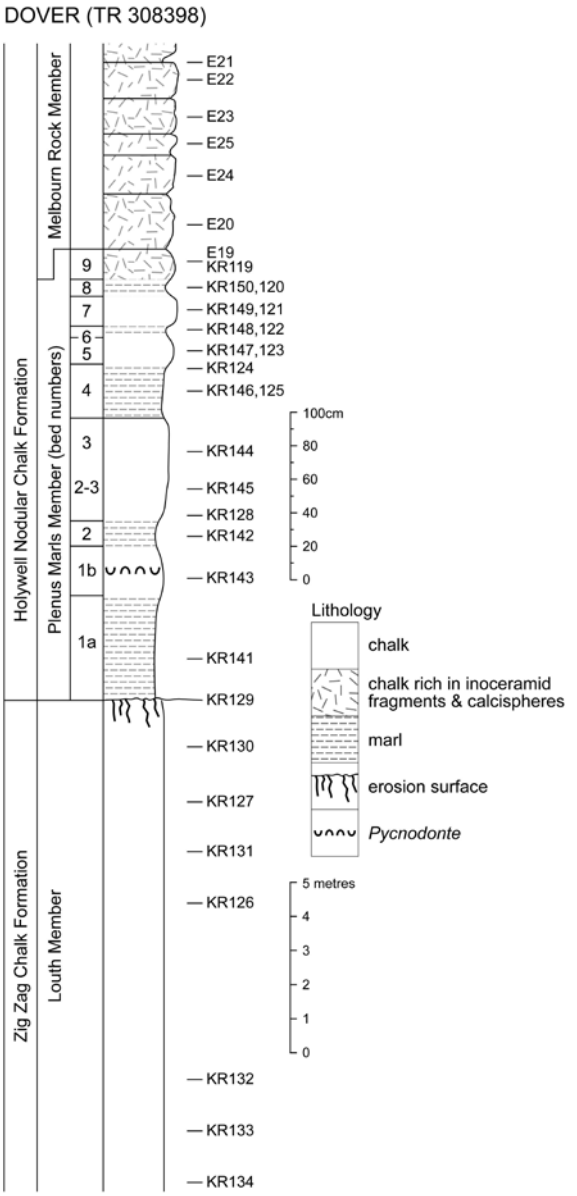

Text-fig. 8. The Plenus Marls section and adjacent strata at Shakespeare Cliff, Dover (National Grid ref: TR308393) showing lithological sequence and sample horizons.

cold water occidental fauna of Jefferies (1962) and its association with chalk with relatively heavy $\delta^{18}O$ (bulk calcite) values in Jefferies Bed 4 of the Plenus Marls succession. We have extended stratigraphically the use of the term Plenus Cold Event to include much of the standard Plenus Marls succession (from Jefferies Bed 2 to Bed 8) with two other cold phases we recognise in the CTOAE sequences of both the Northern and Southern Chalk Provinces – the *Wood Cold Phase* (at the level of Jefferies Bed 2 (Jenkyns *et al.* 2017, p.19) and the *Black Cold Phase* (at the level of Jefferies Bed 8). The original Plenus Cold Event of Gale and Christiansen (1996) is renamed the *Jefferies Cold Phase* (Text-fig. 6). The three cold phases are named in honour of three scientists who have advanced the understanding of the Upper Cretaceous Chalk – Chistopher J. Wood, Richard P.S. Jefferies, and Maurice Black.

Durations of the various Upper Cenomanian and Lower Turonian ammonite zones used in Text-fig. 2 and in the text are based largely on Ogg *et al.* (2012):
- *Collignoniceras woollgari* Zone, base at 92.90 Ma;
- *Mammites nodosoides* Zone, base at 93.35 Ma, duration 0.45 Ma;
- *Watinoceras devonense* Zone, base at 93.90 Ma, duration 0.55 Ma;
- Boundary of the Cenomanian and Turonian at 93.90 Ma;
- *Neocardoceras juddii* Zone, base at 94.15 Ma, 0.25 Ma;
- *Metoicoceras geslinianum* Zone, base at ~94.40 Ma, duration 0.25 Ma,

ANALYTICAL METHODS

Some or all of 95 samples of chalks and marls have been investigated for (1) their content of rare earth elements and a range of elements including titanium and phosphorus, their acetic acid insoluble residue (AIR) and organic carbon (C_{org}); (2) the $^{18}O/^{16}O$ and $^{13}C/^{12}C$ ratios of their bulk calcite; and (3) the $^{13}C/^{12}C$ ratio of their organic carbon. Part of the analytical data is from Jeans *et al.* (1991, 2015). The new rare earth element analyses (Tables 1–6) are based in part on two methods (Jeans *et al.* 2015). The acid insoluble residues (AIR) were extracted by dissolving the calcite fractions of crushed chalk samples in cold 1 molar acetic acid, whereas calcite for analysis was prepared by dissolving crushed chalk samples in 2% nitric acid. Rare earth element analysis was carried out in two phases: prior to 1995 the acid insoluble residues of samples were analysed by CTW using the instrumental neutron activation method (Henderson and Williams 1981) with the following coefficients of variation (CV = 100 × standard deviation/mean analysis (%)) for the rare-earth elements based on the analysis of basalt USGS BCR-1–La, 6.2: Ce 3.6; Nd, 4.4; Sm, 4.7; Eu, 4.3; Gd, 11.5; Tb, 3.2; Ho, 16.7; Tm, 9.8; Yb, 2.5; Lu, 7.1 (see Potts 1987, tables 12–14). From 1995 onwards the calcite fractions and the acid insoluble residues were analysed by DSW using Inductively Coupled Plasma-Mass Spectroscopy

(ICP-MS). The limit of determination for all rare earth elements was found to be less than 0.1 mg/kg. A determination of expanded uncertainty (K = 2, 95% confidence) derived from eleven measurements of duplicate preparations of a number of reference materials over five and a half days established uncertainty values of ±10–12% for the rare earth elements.

The calculation of the cerium anomalies has in this account been based on the following procedures:

$$\text{Ce anomaly} = \frac{\text{Ce s/n}}{(0.8 \times \text{La s/n}) + (0.2 \times \text{Sm s/n})}$$

Ce s/n, La s/n and Sm s/n refer respectively to the shale-normalised values of cerium (Ce), lanthanum (La) and samarium (Sm) for the particular sample relative to the Cody Shale (SCo-1) standard. Ce*(calcite) and Ce*(AIR) refer to the cerium anomalies associated, respectively, with the calcite fractions and acid insoluble residues of the Chalk.

The percentage weight of acid insoluble residue in chalk samples was determined by dissolving 1g of oven-dried sample (105ºC) in exactly 25 ml standard volumetric 1 molar HCl. The excess acid was titrated against standard volumetric 1 molar NaOH using Bromocreosol Green as indicator. From this the weight per cent $CaCO_3$ was calculated and the acid insoluble residue was obtained by difference. Prior to titration it is essential that the acid insoluble residue be removed by filtration through Whatman no. 42 filter paper. Organic carbon (C_{org}) within the acid-insoluble residues was measured by Tinsley's method (1950) for Flixton and Dover, whereas for Melton Ross they were determined using a Costech Elemental Analyser (see below).

DJB carried out the analysis of P_2O_5 and TiO_2 as well as a range of other trace elements in the AIRs by X-ray fluorescence at the British Geological Survey. Stable isotope analysis was performed at the Godwin Laboratory for Palaeoclimate Research, Department of Earth Sciences, University of Cambridge. Samples were analysed for $^{18}O/^{16}O$ and $^{13}C/^{12}C$ of carbonates using either a Micromass Multicarb Sample Preparation System attached to a VG SIRA Mass Spectrometer (prefix S) or a Thermo Electron Kiel Preparation Device attached to a MAT 253 Mass Spectrometer (prefix K). Each run of 30 samples was accompanied by ten reference carbonates and two control samples. The results are reported with reference to VPDB standard and the precision was better than +/-0.6 per mil for $^{18}O/^{16}O$ and +/-0.06 per mil for $^{13}C/^{12}C$. The $^{13}C/^{12}C$ of organic carbon (C_{org}) in the AIRs of Melton Ross samples was analysed by continuous flow using a Costech Elemental Analyser attached to a Thermo Electron MAT 253 mass spectrometer. The results were calibrated to the VPDB standard using international organic standards. The precision was better than +/-0.05 per mil.

UPPER CENOMANIAN–LOWER TURONIAN SEQUENCE AT SHAKESPEARE CLIFF, DOVER, ENGLAND

The succession is exposed in the sea cliffs at Dover (National Grid ref. TR308398). It extends from the top of the Louth Member of the Zig-Zag Chalk Formation – across the 'Facies Change' of north German authors – through the Plenus Marls into the Melbourn Rock, both members of the overlying Holywell Nodular Chalk Formation. The thickness of the Plenus Marls is ~2.2 metres displaying little lateral local variation and is very similar to the type section at Merstham (Jefferies 1963). Text-fig. 7 shows the correlation between the Dover section and the expanded sequence at Eastbourne where particularly the Holywell Nodular Chalk Formation is better developed with much clearer definition of the Mead and Holywell Marls. The stratigraphy and micropalaeontology of the Dover sequence is well known from Jefferies (1963), Robinson (1986), Jarvis *et al.* (1988), Bralower (1988), Koutsoukos *et al.* (1990) and Lamolda *et al.* (1994). Many aspects of its geochemistry have been studied; $\delta^{13}C$ and $\delta^{18}O$ values of bulk samples have been investigated by Schlanger *et al.* 1987, Jarvis *et al.* (1988, 2006), Jeans *et al.* (1991) and Lamolda *et al.* (1994). Various aspects of the geochemistry of separated calcitic bioclastic size fractions, inoceramid fragments and specific foraminifera species have been studied, including the variation in their $\delta^{18}O$ and $\delta^{13}C$ values, concentration of Fe, Mn, Mg and Sr as well as their rare earth element and P content (Corfield *et al*, 1990; Jeans *et al.* 1991, 2015; Mitchell *et al.* 1997). Text-fig. 8 shows the lithological section and sampled horizons. Text-fig. 9 is a schematic section showing the *Wood*, *Jefferies* and *Black cold phases* and the variation in acid insoluble residue, content of C_{org}, the cerium anomalies and the $\delta^{13}C$ and $\delta^{18}O$ values of the bulk calcite. The REE data on which the cerium anomalies are based are in Tables 1 and 2. The rest of the geochemical data is from Jeans *et al.* (1991) excluding the uppermost seven samples (E19–E25) from the Melbourn Rock Member that are new. The clay mineralogy and geochemistry of the acetic acid insoluble residues are known from Jeans (1968, 2006) and Jeans *et al.* (1991) as well as extensive unpublished data.

Sample no.	La	Ce	Pr	Nd	Sm	Eu	Gd	Tb	Dy	Ho	Er	Tm	Yb	Lu	Ce* (calcite)
E 21	13.55	10.66	2.80	11.67	2.27	0.50	2.24	0.31	1.72	0.35	0.91	0.12	0.67	0.10	0.41
E 22	8.20	6.06	1.46	5.92	1.13	0.24	1.14	0.17	0.94	0.19	0.53	0.07	0.42	0.06	0.40
E 23	7.61	5.53	1.29	5.17	0.98	0.23	1.02	0.15	0.86	0.18	0.51	0.07	0.43	0.06	0.39
E 24	6.60	4.52	1.09	4.46	0.84	0.20	0.92	0.13	0.81	0.17	0.48	0.07	0.40	0.06	0.37
E 20	6.01	3.87	0.97	3.93	0.75	0.17	0.80	0.12	0.71	0.15	0.41	0.05	0.34	0.05	0.35
KR 152	7.65	5.70	1.28	5.22	0.99	0.23	1.08	0.15	0.92	0.18	0.52	0.07	0.43	0.06	0.40
E 19	6.54	4.27	1.07	4.30	0.83	0.20	0.92	0.14	0.83	0.18	0.52	0.07	0.46	0.07	0.35
KR 119	12.16	5.94	1.43	5.80	1.09	0.27	1.21	0.18	1.09	0.23	0.65	0.09	0.56	0.08	0.28
KR 120	12.86	11.03	2.73	11.56	2.39	0.56	2.40	0.35	1.94	0.38	1.01	0.13	0.75	0.11	0.43
KR 121	11.61	8.99	2.05	8.44	1.69	0.40	1.77	0.27	1.58	0.33	0.90	0.13	0.80	0.11	0.41
KR 122	14.88	12.36	2.79	11.47	2.26	0.54	2.37	0.35	2.06	0.42	1.16	0.16	0.98	0.14	0.44
KR 123	12.50	10.53	2.20	8.95	1.78	0.42	1.86	0.28	1.64	0.34	0.97	0.13	0.81	0.12	0.45
KR 124	15.65	14.72	3.15	13.11	2.66	0.61	2.71	0.39	2.25	0.45	1.21	0.16	0.97	0.14	0.49
KR 125	16.35	14.82	3.24	13.42	2.66	0.61	2.71	0.39	2.21	0.43	1.17	0.15	0.89	0.13	0.47
KR 144	9.78	8.28	1.72	6.98	1.35	0.31	1.48	0.22	1.30	0.27	0.76	0.10	0.62	0.09	0.45
KR 145	9.26	8.31	1.67	6.71	1.32	0.30	1.41	0.21	1.22	0.26	0.70	0.10	0.60	0.08	0.48
KR 142	10.66	12.31	2.27	9.21	1.79	0.41	1.85	0.26	1.48	0.29	0.77	0.10	0.60	0.08	0.60
KR 143	9.71	11.21	1.96	7.97	1.60	0.35	1.54	0.23	1.26	0.25	0.69	0.09	0.54	0.08	0.60
KR 141	10.72	14.95	2.39	9.60	1.94	0.43	1.86	0.27	1.49	0.29	0.79	0.10	0.62	0.09	0.71
KR 130	5.59	4.96	0.96	3.87	0.76	0.17	0.81	0.12	0.73	0.16	0.44	0.06	0.38	0.06	0.48
KR 126	7.48	6.35	1.38	5.70	1.11	0.25	1.18	0.18	1.04	0.21	0.59	0.08	0.49	0.07	0.45
KR 133	8.46	7.78	1.64	6.78	1.37	0.30	1.38	0.21	1.20	0.24	0.68	0.09	0.55	0.08	0.48
KR 134	8.18	6.81	1.51	6.33	1.20	0.27	1.33	0.19	1.11	0.23	0.64	0.08	0.50	0.07	0.44

Table 1. Rare earth element concentrations (in ppm) and cerium anomalies (Ce*) in the bulk calcite of samples from the Cenomanian–Turonian sequence at Dover, England (Text-figs 8, 9). Analysed by ICP-MS.

Sample no.	La	Ce	Pr	Nd	Sm	Eu	Gd	Tb	Dy	Ho	Er	Tm	Yb	Lu	Ce* (AIR)
E21*	74.83	86.61	17.67	71.58	13.33	3.07	12.61	1.75	9.72	2.04	4.96	0.63	3.48	0.48	0.59
E22*	90.16	100.66	21.07	87.10	16.94	3.97	16.81	2.33	12.94	2.76	6.60	0.79	4.11	0.56	0.56
E23*	68.57	81.41	15.95	65.49	12.54	2.93	12.26	1.68	9.38	1.95	4.82	0.59	3.26	0.45	0.60
E25*	126.6	128.3	27.09	112.68	21.91	5.36	23.93	3.39	19.81	4.41	10.72	1.27	6.33	0.84	0.52
E24*	88.91	93.56	19.97	83.31	16.13	3.95	17.33	2.43	13.68	2.91	6.97	0.80	4.19	0.56	0.54
E20*	65.18	74.88	15.03	61.43	11.94	2.87	12.20	1.70	9.27	1.92	4.69	0.55	2.08	0.41	0.58
KR 152	60.56	65.99	14.59	55.80	10.01	2.58	12.48	1.76	8.93	1.86	4.64	*n.a.*	2.97	0.44	0.57
KR 120*	35.40	44.28	8.87	35.40	7.26	1.72	7.01	0.97	5.30	1.11	2.57	0.32	1.85	0.24	0.62
KR 121*	39.86	51.05	9.86	39.37	7.87	1.94	7.75	1.09	6.11	1.29	2.98	0.37	2.05	0.29	0.64
KR 122	43.35	55.82	11.17	45.11	8.83	2.07	9.82	1.35	6.84	1.41	3.43	*n.a.*	2.57	0.31	0.64
KR 148	27.08	34.89	7.21	28.20	5.20	1.32	6.53	0.85	4.51	0.95	2.12	*n.a.*	1.81	0.23	0.65
KR 123	48.86	70.55	11.96	46.52	9.12	2.24	8.95	1.25	6.87	1.44	3.51	0.45	2.63	0.37	0.73
KR 125*	66.74	93.43	16.02	62.85	12.13	2.87	11.52	1.60	8.94	1.94	4.57	0.57	3.46	0.48	0.71
KR 142	47.72	71.20	11.57	43.82	7.49	1.69	8.01	1.12	6.21	1.29	3.35	*n.a.*	2.96	0.41	0.78
KR 130	73.38	88.38	16.16	60.84	11.00	2.53	12.70	1.83	9.93	2.20	5.74	*n.a.*	4.51	0.65	0.64
KR 126	63.62	80.24	15.54	59.86	11.13	2.71	12.55	1.77	9.37	2.09	4.91	*n.a.*	4.13	0.55	0.65
KR 133	68.94	85.85	17.45	70.99	13.42	3.28	15.17	2.10	10.97	2.30	5.60	*n.a.*	4.24	0.60	0.63
KR 134	76.97	89.85	18.89	74.65	13.45	3.35	16.54	2.31	11.72	2.50	5.91	*n.a.*	4.32	0.62	0.60

Table 2. Rare earth element concentrations (in ppm) and cerium anomalies (Ce*) in the acid insoluble residues of samples from the Cenomanian–Turonian sequence at Dover, England (Text-figs 8, 9). Analysed by the instrumental neutron activation method (*) or by ICP-MS; *n.a.* – no analysis.

Stable isotopes of bulk calcite

The stratigraphical pattern of $\delta^{13}C$ values is an increase from ~2.5‰ in the upper part of the Louth Member to 4.0–4.5‰ in the Melbourn Rock Member. The pattern for $\delta^{18}O$ starts with values between -2.5‰ and -3.0‰ in the upper part of the Louth Member, reaching values between -3.0‰ and -4.0‰ in the Melbourn Rock Member. At four levels in the section (samples KR142, KR125, KR120, E21) there are increases in $\delta^{13}C$ values associated with relatively heavy $\delta^{18}O$ values and these are associated with beds enriched in acid insoluble residues.

Cerium anomalies of bulk calcite and acid insoluble residues

The upper part of the Louth Member has Ce*(calcite) values of 0.44 to 0.48 and Ce*(AIR) values of 0.60 to 0.64. Jefferies Bed 1A, immediately above the sub-plenus erosion surface (Text-fig. 9), exhibits the highest cerium anomalies in the sequence – Ce*(calcite) 0.71 and Ce*(AIR) 0.92. As the succession is followed upwards the cerium anomalies decrease gradually, reaching values in Beds 5–8 similar to those of the underlying Louth Member. This gradual decrease continues into the Melbourn Rock Member, where values stabilise at Ce*(calcite) 0.3–0.4 and Ce*(AIR) 0.5–0.6. The stratigraphical pattern of the cerium anomalies displays an overall antipathetic relationship with the $\delta^{13}C$ values of the bulk calcite.

Organic carbon of acid insoluble residues

The organic carbon contents of the AIR are low (<0.6%), representing values of <0.1% for the total sediment. The stratigraphical variations do not correlate consistently with the variations in either the AIR, $\delta^{18}O$ (calcite), $\delta^{13}C$ (calcite), or cerium anomalies.

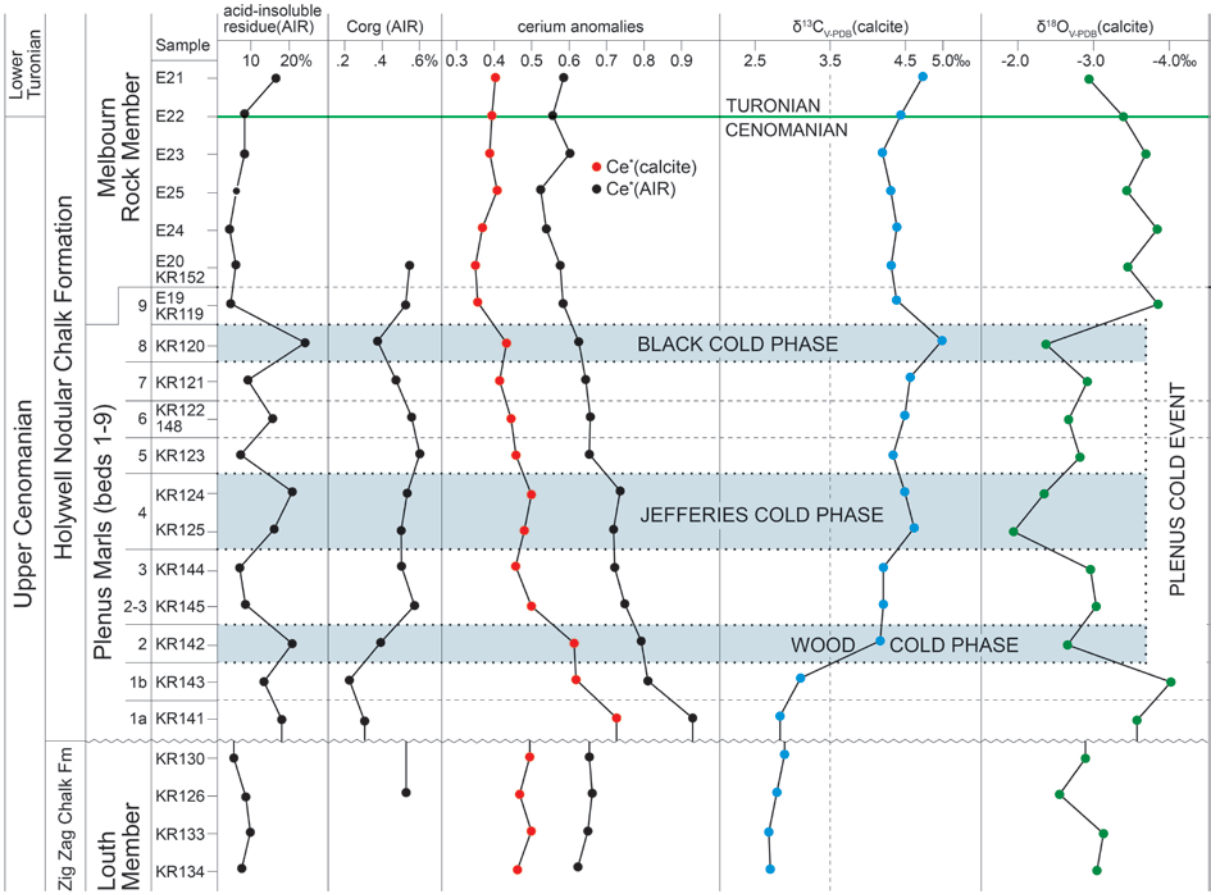

Text-fig. 9. The Plenus Marls and adjacent strata at Shakespeare Cliff, Dover. Stratigraphically arranged samples showing the variations in (a) weight per cent of acid insoluble residues (AIR), (b) organic carbon content of the acid insoluble residue (C_{org}) AIR, (c) cerium anomalies of the bulk calcite (Ce*(calcite)) and the acid insoluble residue (Ce*(AIR)), and (d). $\delta^{13}C$ and $\delta^{18}O$ of the bulk calcite.

UPPER CENOMANIAN–LOWER TURONIAN SEQUENCE AT MELTON ROSS, LINCOLNSHIRE, ENGLAND

This location (National Grid ref. TA 080115) is of particular importance in unravelling the CTOAE in the Northern Province (Wood and Mortimore 1995; Wood *et al.* 1997). Not only does it show the Standard Black Band sequence in the Variegated Beds of central and northern Lincolnshire and of Yorkshire, deep excavations carried out in 1994 revealed an anomalous sequence beneath an erosion surface, representing a record of the earlier part of the CTOAE preserved in a local down-faulted basin that is otherwise absent from the Northern Province. This Anomalous Black Band sequence consists of three black bands and interbedded dark coloured marls that rest on the eroded top of the Louth Member (Text-figs 4, 6). It is possible that similar beds were originally present over much of the Northern Province before being eroded prior to the deposition of the Central Limestone. They are correlated with (a) Jefferies Beds 1 and 2 of the Plenus Marls in southern England and (b) the beds in northern Germany between the "Facies Change" and the base of the "Plenus Bank".

The succession is shown in Text-fig. 10. The Standard Black Band sequence is separated from the underlying anomalous sequence with its three black bands (A, B, C) by an erosion surface and this is overlain by the Central Limestone (bed 3) – equivalent to Jefferies Bed 3 of the Southern Province and the 'Plenus Bank' of northern Germany. This is overlain by a sequence of marls, containing two well-defined black bands (D, E1) and a thin black band (E2), which passes up into chalks of the upper part of the Flixton Member of the Welton Formation. The *Wood*, *Jefferies* and *Black cold phases* are represented (Text-fig. 11). Details of the biostratigraphy, clay mineralogy, aspects of the organic carbon content and the REE patterns of bulk samples of the composite section are in Wood and Mortimore (1995) and Wood *et al.* (1997). Analysis has been carried out on the 26 samples examined by DSW (in Wood *et al.* 1997). The new analyses include $\delta^{18}O$ and $\delta^{13}C$ of the bulk calcite, $\delta^{13}C$ of organic carbon, Ce*(calcite), Ce*(AIR), AIR and organic carbon (C_{org}). The REE data are shown in Tables 3 and 4. The stratigraphical variation in the geochemistry is shown schematically in Text-fig. 11.

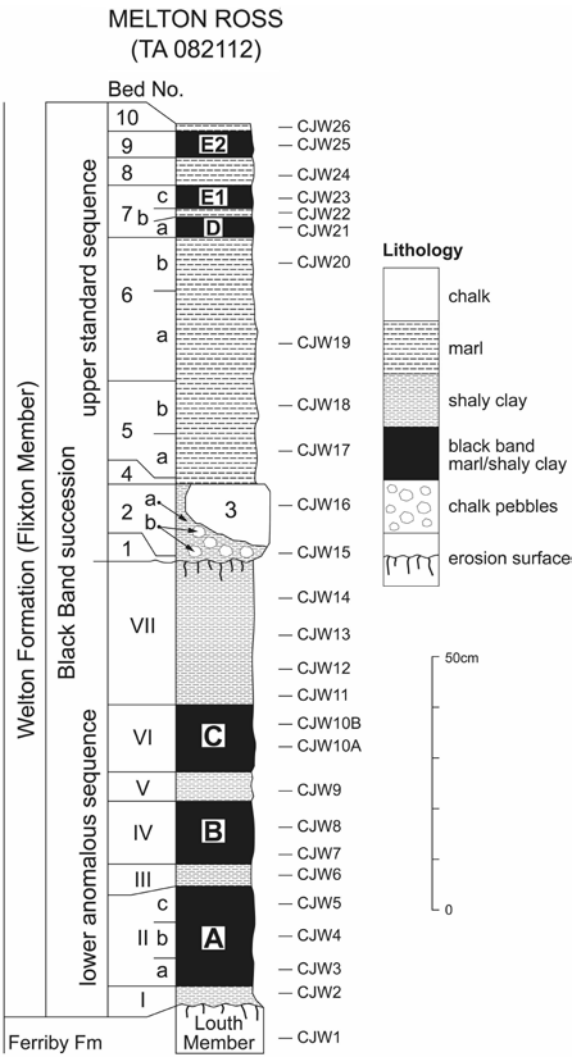

Text-fig. 10. The Anomalous and Standard Black Band sequences in the Variegated Beds at Melton Ross, Lincolnshire (National Grid ref: TA082112) showing the lithological sequence and sample horizons based upon Wood *et al.* (1997, fig. 5).

Stable isotopes of bulk calcite

Anomalous Black Band sequence (beds I–VII): There is little change in the $\delta^{18}O$ and $\delta^{13}C$ values between the top of the Louth Member and sample CJW 2 at the base of this black band sequence. The $\delta^{18}O$ values are generally between -3.5‰ and -4.0‰ but reach -5.2‰ in sample CJW 5. The $\delta^{13}C$ values vary between 2.5 and 3.5‰ displaying no sensitivity to lithological variation, including the three black bands (A, B, C).

Standard Black Band sequence (beds 1–10): The $\delta^{18}O$ values show a distinctive stratigraphical pattern. There are particularly heavy values (~ -3.0‰) in beds 2–5. Above, they decrease, reaching -6.1‰ in black band D. Values rise sharply in bed 7b between black

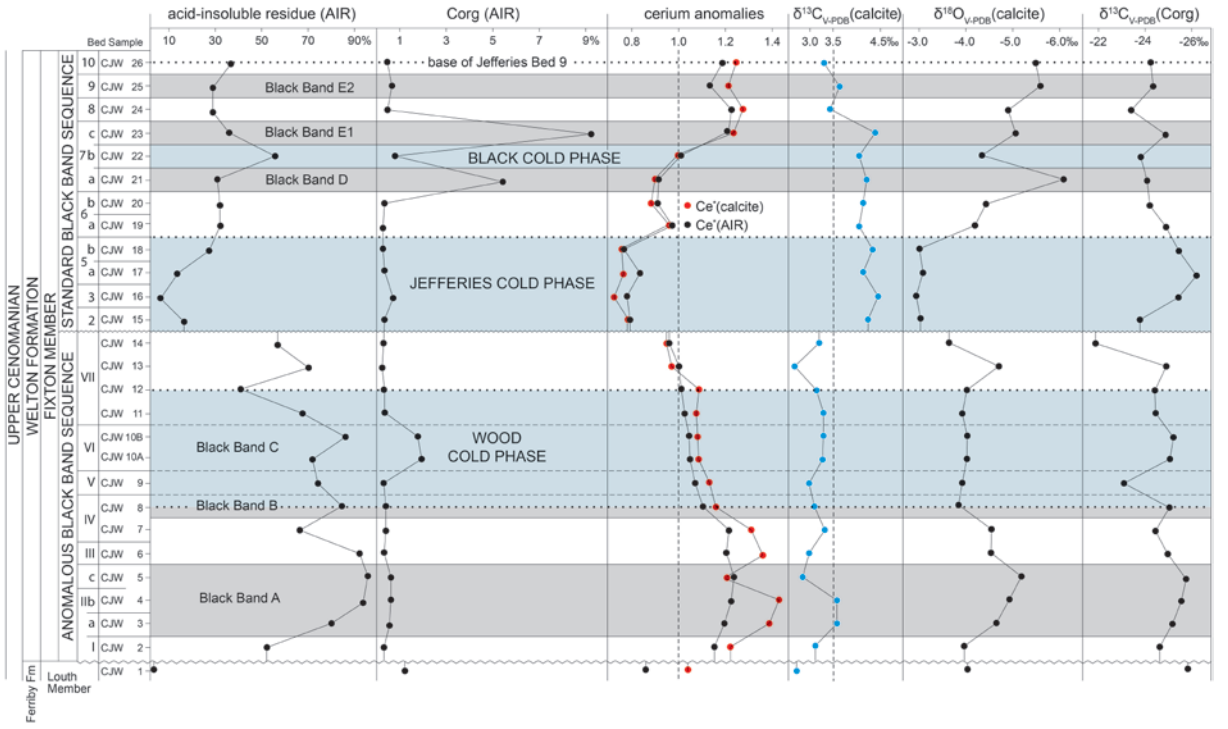

Text-fig. 11. The Anomalous and Standard Black Band sequences in the Variegated Beds at Melton Ross, Lincolnshire. Stratigraphically arranged samples showing the variations in (a) the acid insoluble residue (AIR), (b) organic carbon content of the acid insoluble residue (AIR), (c) cerium anomalies of the bulk calcite (Ce*(calcite)) and the acid insoluble residue (Ce*(AIR)), (d) $\delta^{13}C$ and $\delta^{18}O$ of the bulk calcite, and (e) $\delta^{13}C$ of the organic carbon.

bands D and E1 but decrease generally to the top of the section, showing low values in black bands E1 and E2. The $\delta^{13}C$ values are markedly higher than in the lower sequence, with most of the section (beds 2a–7c) showing values between 4.0‰ and 4.5‰. Above bed 7c (black band E1), values fall to 3.3‰ at the top of the section. All three black bands (D, E1, E2) are characterised by slightly enhanced $\delta^{13}C$ values compared to the immediately underlying and overlying samples. Similar minor variations of $\delta^{13}C$ occur in beds 2 and 5 but are unrelated to variations in the organic carbon (AIR) content.

Stable isotopes of organic carbon

Values of $\delta^{13}C$ (organic carbon) range from -22‰ to -26‰; they show no clear correlation with lithology, $\delta^{18}O$ (calcite), $\delta^{13}C$ (calcite), Ce*(calcite), Ce*(AIR) and AIR. Black bands A, B, C, E1 and E2 are associated with somewhat enhanced negative values of $\delta^{13}C$ (organic carbon). This suggests a greater contribution from marine-derived organic carbon than for black band D.

Cerium anomalies of bulk calcite and acid insoluble residues

Anomalous Black Band sequence (beds I–VII): The top of the Louth Member has Ce*(calcite) and Ce*(AIR) values of 1.03 and 0.85 respectively. The overlying sequence of black bands is divided into three main sections: (1) a gradual build-up in the values of Ce*(AIR) from ~1.18 to 1.25, followed by a gradual decrease to 1.09 (beds II–IV). In contrast, the Ce*(calcite) displays a more rapid build-up to 1.45; this is interrupted in sample CJW 5 by a sudden drop to values similar to those of Ce*(AIR), only to return to previously high values (1.35) before decreasing relatively rapidly to 1.5 in bed IV. (2) A gradual decrease between samples CJW 8 and 12 of both anomalies (Ce*(AIR) from 1.09 to 1.00 and Ce*(calcite) from 1.15 to 1.11). (3) At the top of the sequence (samples CJW 13, 14) the two types of cerium anomalies have similar values as they drop below 1.0.

Standard Black Band sequence (beds 1–10): There is a stratigraphical pattern which starts at the base

Sample no.	La	Ce	Pr	Nd	Sm	Eu	Gd	Tb	Dy	Ho	Er	Tm	Yb	Lu	Ce* (calcite)
CJW 26	23.32	61.03	6.53	27.39	5.67	1.29	5.30	0.78	4.35	0.83	2.16	0.27	1.58	0.22	1.25
CJW 25	19.48	48.88	5.31	22.13	4.58	1.04	4.27	0.64	3.57	0.69	1.82	0.24	1.42	0.20	1.21
CJW 24	30.41	81.72	8.29	34.89	7.36	1.68	6.93	1.06	6.03	1.17	3.13	0.41	2.51	0.34	1.28
CJW 23	28.43	72.84	7.73	32.42	6.82	1.55	6.19	0.93	5.12	0.98	2.56	0.33	2.05	0.28	1.23
CJW 22	23.73	55.28	7.19	30.72	6.70	1.49	5.96	0.87	4.78	0.89	2.32	0.29	1.67	0.23	1.07
CJW 21	21.89	40.93	5.14	21.40	4.57	1.04	4.07	0.60	3.31	0.63	1.69	0.23	1.44	0.21	0.92
CJW 20	37.00	68.31	9.70	40.98	8.56	1.98	7.97	1.19	6.65	1.28	3.40	0.44	2.65	0.36	0.89
CJW 19	21.16	42.24	5.46	22.65	4.78	1.14	4.52	0.68	3.85	0.75	1.96	0.26	1.64	0.23	0.97
CJW 18	13.76	20.64	3.18	13.26	2.80	0.67	2.65	0.42	2.39	0.47	1.29	0.18	1.16	0.16	0.75
CJW 17	14.87	21.55	2.84	11.60	2.31	0.54	2.26	0.35	2.06	0.41	1.15	0.16	1.02	0.15	0.76
CJW 16	10.60	14.51	2.03	8.50	1.67	0.40	1.75	0.27	1.61	0.34	0.93	0.13	0.81	0.12	0.72
CJW 15	22.70	36.68	5.58	23.57	4.97	1.16	4.79	0.73	4.25	0.85	2.36	0.32	2.05	0.30	0.79
CJW 14	62.94	128.5	17.40	74.38	15.93	3.71	15.06	2.28	12.89	2.49	6.59	0.85	5.02	0.69	0.96
CJW 13	45.69	94.56	12.56	54.16	12.00	2.75	10.74	1.60	8.69	1.62	4.11	0.51	2.92	0.39	0.97
CJW 12	30.37	69.16	8.36	35.23	7.55	1.72	6.97	1.06	5.90	1.14	3.05	0.40	2.46	0.35	1.08
CJW 11	40.68	93.17	11.48	48.69	10.52	2.42	9.77	1.48	8.24	1.59	4.16	0.53	3.15	0.44	1.07
CJW 10B	50.48	114.9	14.00	59.74	13.00	3.00	12.01	1.83	10.20	1.95	5.16	0.66	3.97	0.56	1.07
CJW 10A	50.59	117.2	14.38	61.57	13.37	3.07	12.47	1.88	10.49	2.01	5.30	0.68	4.11	0.57	1.08
CJW 9	57.47	135.4	15.50	66.13	14.30	3.31	13.58	2.04	11.53	2.25	6.03	0.78	4.69	0.65	1.12
CJW 8	47.88	119.4	13.86	59.53	13.29	2.99	12.03	1.81	9.95	1.89	4.98	0.64	3.79	0.52	1.15
CJW 7	42.05	117.4	12.10	51.53	11.19	2.60	10.51	1.58	8.81	1.70	4.48	0.57	3.42	0.47	1.30
CJW 6	38.29	113.7	11.64	49.94	11.16	2.55	10.20	1.53	8.41	1.60	4.19	0.53	3.17	0.43	1.35
CJW 5	45.59	114.6	11.42	49.25	11.15	2.57	9.93	1.50	8.17	1.53	3.96	0.50	2.97	0.40	1.20
CJW 4	27.04	87.24	8.93	38.54	8.80	2.00	7.73	1.16	6.26	1.16	2.98	0.38	2.21	0.30	1.42
CJW 3	27.47	84.31	8.96	38.11	8.39	1.91	7.45	1.09	5.85	1.06	2.70	0.33	1.90	0.26	1.37
CJW 2	37.17	97.68	11.27	47.76	10.27	2.31	9.40	1.38	7.47	1.40	3.54	0.43	2.44	0.33	1.21
CJW 1	12.06	19.04	2.12	8.31	1.65	0.39	1.68	0.28	1.72	0.37	1.14	0.18	1.28	0.19	0.85

Table 3. Rare earth element concentrations (in ppm) and cerium anomalies (Ce*) in the bulk calcite of samples from the Cenomanian–Turonian sequence at Melton Ross, England (Text-figs 10, 11). Analysed by ICP-MS.

of the sequence with values of both cerium anomalies at just below 0.8. Upwards the values diverge (0.72–0.83), with the Ce*(AIR) having the lower value (i.e. returning to the relationship at the top of the Louth Member) but showing no clear trend. The main part of the pattern is a general increase in values with fluctuations to the top of the sequence: the lower portion (beds 5b–7a) is characterised by both cerium anomalies having the same value, whereas in bed 7b and above (as in much of the lower sequence) the Ce*(AIR) trails the Ce*(calcite) values by less than 0.1.

Organic carbon in acid insoluble residues

There is a background value of 0.2–0.7%. There are three beds with distinct peak values – (1) black band C (samples CJW 10A, B) with a little below 2%, (2) black band D (sample CJW 21) with 5.5%, and (3) black band E1 (sample CJW 23) with 9.4%. Black bands A and B have low C_{org} values similar to or just above background levels. There is no systematic correlation between the percentage C_{org} and variations in the $\delta^{13}C$ (organic carbon) values.

UPPER CENOMANIAN–LOWER TURONIAN SEQUENCE AT FLIXTON, YORKSHIRE, ENGLAND

The Standard Black Band sections at Flixton, East Knapton and Burdale are typical of the Variegated Beds in the most northern part of the Chalk in England (Text-fig. 1: Jeans *et al.* 1991, fig. 10; Dobsworth 1996, fig. 2). They are somewhat thicker and contain a higher proportion of finely laminated chalks and marls than sections farther to the south at Melton, South Ferriby, Melton Ross and Caistor (Text-fig. 1). The succession at Flixton (National Grid ref. TA 039791) is shown in Text-figs 12–14. It contains the two main black bands (D and E) of Melton Ross, but these are now more clearly separated and have a higher C_{org} content, and a third thin black band F just above the Cenomanian–

Sample no.	La	Ce	Pr	Nd	Sm	Eu	Gd	Tb	Dy	Ho	Er	Tm	Yb	Lu	Ce* (AIR)
CJW 26	83.41	204.6	22.53	91.93	18.72	4.20	16.78	2.55	13.98	2.66	6.90	0.87	5.12	0.71	1.19
CJW 25	83.44	193.8	21.86	88.85	18.11	4.06	16.04	2.48	13.79	2.66	6.96	0.88	5.23	0.74	1.14
CJW 24	117.9	300.3	31.68	130.6	27.20	6.12	24.79	3.80	21.34	4.15	10.91	1.41	8.35	1.16	1.23
CJW 23	92.59	235.3	26.27	107.6	22.14	4.98	19.54	2.95	16.28	3.09	8.03	1.04	6.14	0.85	1.22
CJW 22	67.92	140.2	18.59	74.94	15.73	3.45	13.46	2.07	11.30	2.12	5.57	0.73	4.45	0.60	1.00
CJW 21	67.18	142.1	18.75	76.00	16.14	3.59	13.44	2.05	11.09	2.08	5.50	0.72	4.34	0.60	1.01
CJW 20	121.5	226.8	32.22	133.8	28.06	6.39	24.84	3.84	21.10	4.02	10.58	1.31	7.79	1.05	0.90
CJW 19	58.33	119.5	15.98	66.55	14.31	3.27	12.60	1.90	10.45	1.95	5.00	0.62	3.52	0.49	0.97
CJW 18	28.82	45.47	7.54	31.32	6.70	1.53	5.89	0.90	4.85	0.91	2.37	0.29	1.72	0.24	0.76
CJW 17	48.23	83.48	12.97	55.33	11.56	2.56	10.30	1.49	7.94	1.47	3.73	0.43	2.53	0.35	0.83
CJW 16	99.27	154.3	24.26	103.5	21.13	4.85	19.77	2.84	15.27	2.90	7.21	0.87	4.91	0.67	0.77
CJW 15	145.6	240.4	38.80	164.5	34.55	7.86	31.81	4.78	26.53	5.09	13.19	1.63	9.35	1.28	0.79
CJW 14	139.0	275.8	37.83	157.5	33.41	7.65	30.64	4.73	26.92	5.18	13.93	1.81	10.72	1.49	0.95
CJW 13	83.37	172.7	22.72	94.79	19.87	4.43	17.50	2.66	14.63	2.79	7.31	0.96	5.71	0.82	0.99
CJW 12	94.00	192.5	23.95	98.38	20.50	4.60	18.45	2.79	15.67	2.97	7.88	1.02	6.20	0.86	1.00
CJW 11	86.71	179.2	22.26	91.30	18.69	4.29	16.82	2.62	14.68	2.79	7.55	0.99	5.92	0.84	1.01
CJW 10B	100.8	217.3	26.96	111.5	23.47	5.23	20.97	3.24	18.00	3.49	9.40	1.24	7.56	1.06	1.04
CJW 10A	101.4	217.1	27.13	111.3	23.61	5.20	20.76	3.22	18.11	3.48	9.47	1.23	7.59	1.08	1.03
CJW 9	116.6	253.1	29.87	124.1	25.74	5.84	23.69	3.67	20.83	4.14	11.16	1.47	9.06	1.28	1.06
CJW 8	91.29	202.8	23.75	95.65	19.85	4.46	17.51	2.76	15.45	3.00	8.05	1.08	6.73	0.94	1.09
CJW 7	106.0	264.3	28.61	117.3	24.61	5.54	21.77	3.38	18.99	3.65	9.76	1.29	7.93	1.12	1.20
CJW 6	88.16	212.7	22.89	91.90	18.95	4.22	16.73	2.60	14.67	2.88	7.74	1.03	6.53	0.92	1.19
CJW 5	80.58	200.8	21.10	85.53	17.63	3.93	15.31	2.37	13.12	2.56	6.80	0.92	5.79	0.83	1.22
CJW 4	77.37	193.4	20.72	83.46	17.17	3.83	14.74	2.29	12.53	2.42	6.50	0.88	5.42	0.78	1.22
CJW 3	74.87	182.8	20.45	82.92	17.06	3.85	14.38	2.16	11.96	2.23	5.76	0.75	4.78	0.67	1.18
CJW 2	101.3	241.6	28.24	116.4	24.22	5.40	20.99	3.20	17.52	3.27	8.50	1.05	6.17	0.87	1.14
CJW 1	155.3	328.5	40.97	172.5	35.41	8.27	33.55	4.90	27.46	5.31	13.26	1.61	9.21	1.21	1.02

Table 4. Rare earth element concentrations (in ppm) and cerium anomalies (Ce*) in the acid insoluble residues of samples from the Cenomanian–Turonian sequence at Melton Ross, England (Text-figs 10, 11). Analysed by ICP-MS.

Text-fig. 12. The old quarry face showing the Standard Black Band sequence at Flixton, Yorkshire (National Grid ref: TA039791). D and E are black bands, F is a band of black blobs. The section excavated in 1960 is in the foreground. The scale rule is 60 cm.

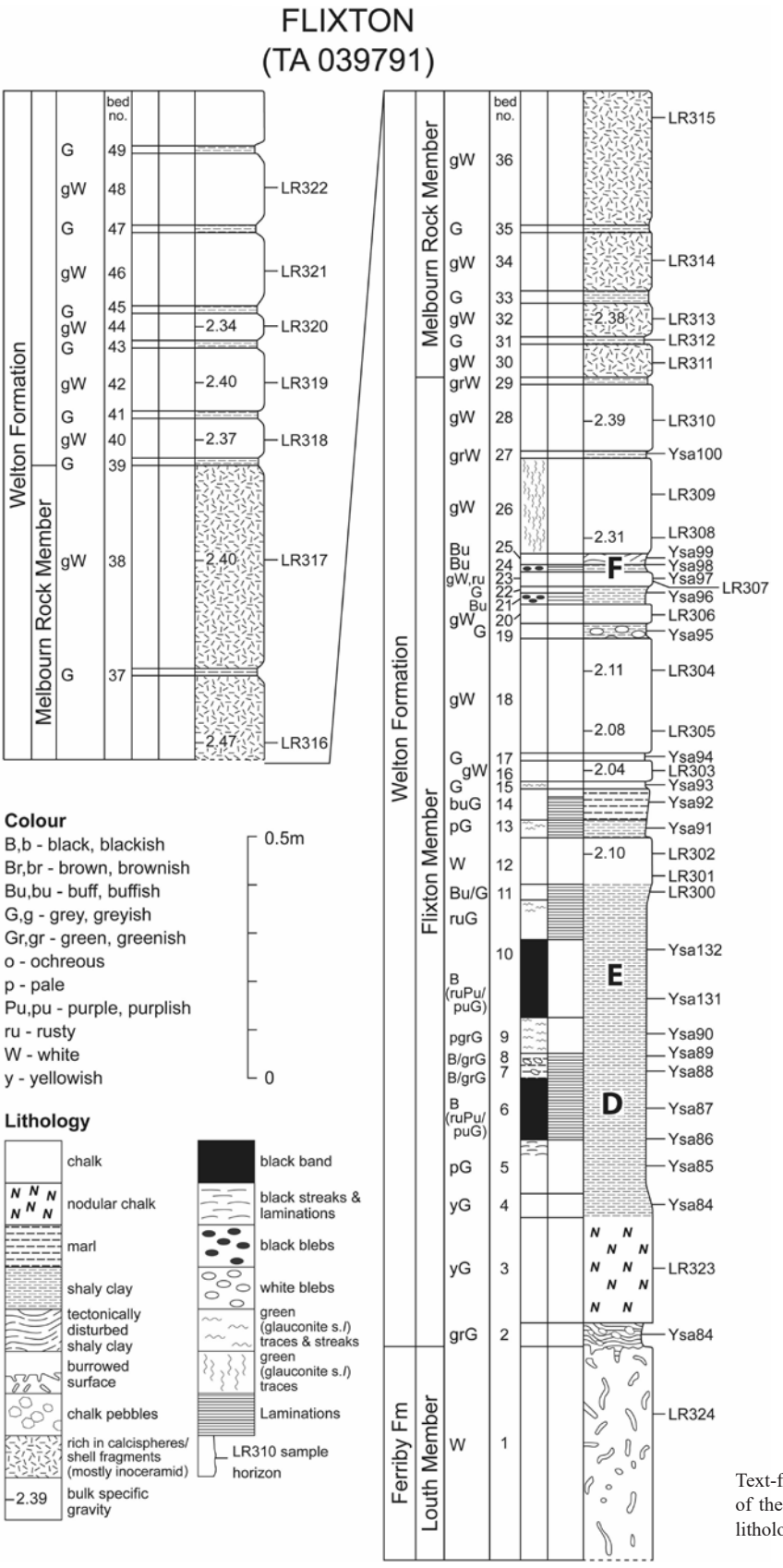

Text-fig. 13. The Standard Black Band sequence of the Variegated Beds at Flixton, showing the lithological sequence, sample horizons and bulk specific gravities.

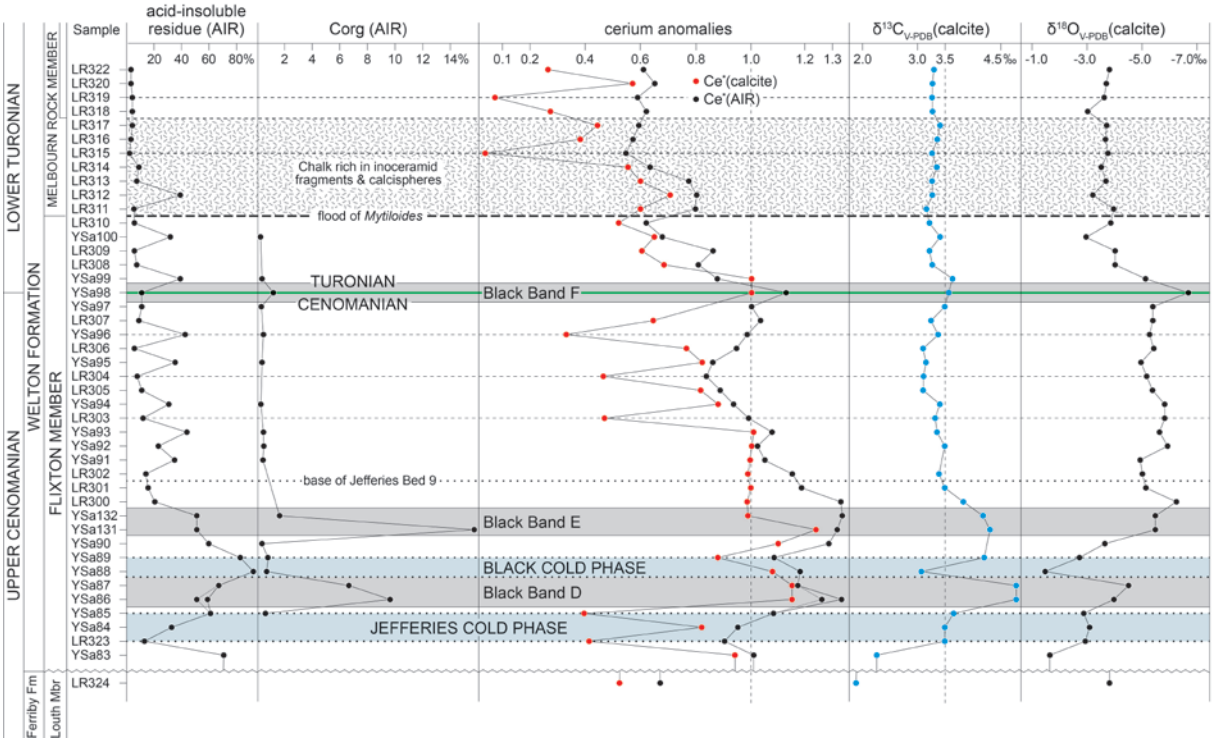

Text-fig. 14. The Standard Black Band sequence of the Variegated Beds at Flixton, Yorkshire. Stratigraphically arranged samples showing the variations in (a) weight per cent of the acid insoluble residue (AIR), (b) content of organic carbon in the acid insoluble residues (AIR), (c) cerium anomalies of the bulk calcite (Ce*(calcite)) and the acid insoluble residue (Ce*(AIR)), and (d) $\delta^{13}C$ and $\delta^{18}O$ of the bulk calcite.

Turonian boundary (bed 20, Text-fig. 13). The investigated section extends from the eroded top of the underlying Louth Member of the Ferriby Formation, through the complete Flixton Member with the Central Limestone (bed 3) near its base and into the flint-bearing chalks of the main part of the Welton Formation above the inoceramid-rich shelly Melbourn Rock (Wood and Smith 1978). Two cold phases are recognised in the $\delta^{18}O$ record (Text-fig. 14), *Jefferies Cold Phase* (Text-fig. 13, beds 4, 5) and *Black Cold Phase* (Text-fig. 13, beds 7, 8). Various aspects of the lithology, geochemistry and palynology of this succession have already been described (Jeans *et al.* 1991; Dodsworth 1996). The clay mineralogy and geochemistry of the acetic acid insoluble residues are known from Jeans (1968, 2006) and Jeans *et al.* (1991, 2000, 2001) as well as extensive unpublished data. Text-fig. 14 is a schematic section displaying the variations between the acid insoluble residues, content of C_{org}, $\delta^{18}O$ and $\delta^{13}C$ of the bulk calcite, and the cerium anomalies of the bulk calcite and acid insoluble residues. The REE data are shown in Tables 5 and 6.

Stable isotopes of bulk calcite

The Standard Black Band sequence has $\delta^{13}C$ values ranging from 2.25 to 4.75‰. The top of the Louth Member has a $\delta^{13}C$ value of ~1.9‰. The base of the sequence has a slightly higher value (~2.25‰) and this increases rapidly up-section to 3.5‰ and above, forming a broad peak coincident with black band D. The $\delta^{13}C$ value drops sharply to ~2.75‰ at the level of maximum acid insoluble residue (sample Ysa 88). It then recovers to values above 3.5‰ in black band E and then decreases gradually upwards to values between 3.00 and 3.25‰, before once again increasing to above 3.5‰ at the thin black band F (samples Ysa 98, Ysa 99). Above this, $\delta^{13}C$ values range between ~3.1 and ~3.4‰. There is no systematic correlation between AIR-rich layers and enhanced $\delta^{13}C$ values.

Oxygen isotope ($\delta^{18}O$) values range from ~ -1.4‰ to ~ -6.75‰; the overall pattern of variation can be divided into three sections. The value at the top of the Louth Member is -3.75‰. The first section shows a pattern of variation practically parallel to that displayed by the $\delta^{13}C$ values. There is a rapid decrease

Flixton. calcite	La	Ce	Pr	Nd	Sm	Eu	Gd	Tb	Dy	Ho	Er	Tm	Yb	Lu	Ce* (calcite)
LR 322	3.11	1.44	0.27	1.02	0.21	0.05	0.24	0.03	0.22	0.04	0.12	*n.a.*	0.10	0.02	0.26
LR 320	2.08	2.11	0.38	1.43	0.29	0.06	0.35	0.04	0.32	0.06	0.17	*n.a.*	0.17	0.02	0.53
LR 319	15.85	1.81	0.37	1.45	0.27	0.06	0.32	0.04	0.29	0.05	0.15	*n.a.*	0.14	0.02	0.07
LR 318	4.36	2.11	0.40	1.53	0.29	0.07	0.36	0.05	0.35	0.06	0.19	*n.a.*	0.18	0.03	0.27
LR 317	0.98	0.82	0.16	0.65	0.12	0.03	0.15	0.02	0.15	0.03	0.08	*n.a.*	0.07	0.01	0.44
LR 316	1.34	0.94	0.19	0.74	0.15	0.03	0.18	0.02	0.17	0.03	0.09	*n.a.*	0.08	0.01	0.38
LR 315	24.36	0.76	0.14	0.57	0.10	0.02	0.14	0.01	0.11	0.02	0.06	*n.a.*	0.05	0.00	0.02
LR 314	1.24	1.25	0.21	0.80	0.15	0.04	0.20	0.02	0.17	0.03	0.10	*n.a.*	0.08	0.01	0.53
LR 313	1.60	1.83	0.30	1.12	0.22	0.05	0.27	0.03	0.25	0.05	0.14	*n.a.*	0.13	0.02	0.59
LR 312	10.40	16.29	3.25	13.28	2.85	0.60	3.04	0.36	2.33	0.38	0.95	*n.a.*	0.64	0.09	0.70
LR 311	2.45	2.83	0.48	1.83	0.37	0.08	0.45	0.06	0.43	0.08	0.23	*n.a.*	0.24	0.04	0.59
LR 310	2.10	2.13	0.42	1.65	0.34	0.07	0.37	0.05	0.34	0.06	0.17	*n.a.*	0.15	0.02	0.51
Ysa 100	7.77	11.30	2.44	10.21	2.18	0.45	2.10	0.25	1.55	0.26	0.62	*n.a.*	0.42	0.06	0.65
LR 309	1.87	2.10	0.30	1.20	0.23	0.05	0.29	0.04	0.27	0.05	0.15	*n.a.*	0.13	0.02	0.59
LR 308	2.37	3.11	0.41	1.60	0.33	0.07	0.39	0.05	0.37	0.07	0.20	*n.a.*	0.19	0.03	0.68
Ysa 99	10.65	23.31	3.11	12.31	2.51	0.52	2.64	0.29	1.85	0.30	0.72	*n.a.*	0.48	0.07	1.02
Ysa 98	3.31	7.15	0.95	3.53	0.70	0.14	0.72	0.08	0.54	0.09	0.22	*n.a.*	0.16	0.02	1.04
Ysa 97	3.45	5.65	0.81	3.05	0.59	0.13	0.66	0.08	0.57	0.10	0.29	*n.a.*	0.28	0.04	0.82
LR 307	4.28	5.31	0.73	2.78	0.58	0.12	0.68	0.08	0.61	0.11	0.31	*n.a.*	0.30	0.04	0.65
Ysa 96	30.26	17.07	2.57	10.34	2.23	0.47	2.18	0.25	1.58	0.25	0.61	*n.a.*	0.44	0.07	0.32
LR 306	3.57	5.56	0.84	3.27	0.69	0.15	0.73	0.10	0.66	0.12	0.33	*n.a.*	0.31	0.05	0.76
Ysa 95	8.88	15.79	2.63	10.53	2.19	0.47	2.28	0.26	1.70	0.27	0.70	*n.a.*	0.49	0.08	0.82
LR 304	3.89	3.26	0.51	2.00	0.42	0.09	0.49	0.06	0.43	0.08	0.22	*n.a.*	0.20	0.03	0.45
LR 305	2.55	4.17	0.57	2.22	0.47	0.11	0.55	0.07	0.48	0.09	0.25	*n.a.*	0.23	0.04	0.81
Ysa 94	6.22	11.67	1.72	6.92	1.46	0.32	1.50	0.17	1.11	0.18	0.47	*n.a.*	0.35	0.05	0.88
LR 303	5.99	4.83	0.65	2.55	0.54	0.11	0.62	0.08	0.53	0.10	0.27	*n.a.*	0.27	0.04	0.44
Ysa 93	9.13	21.31	2.75	11.06	2.38	0.52	2.39	0.29	1.84	0.31	0.79	*n.a.*	0.58	0.08	1.06
Ysa 92	4.76	10.11	1.31	5.12	1.07	0.23	1.10	0.13	0.88	0.16	0.41	*n.a.*	0.34	0.05	1.00
Ysa 91	8.00	16.76	2.28	9.10	1.94	0.42	1.98	0.24	1.55	0.26	0.67	*n.a.*	0.51	0.08	0.97
LR 302	3.63	6.23	0.77	2.99	0.62	0.14	0.72	0.09	0.65	0.12	0.34	*n.a.*	0.33	0.05	0.86
LR 301	4.00	7.87	0.86	3.35	0.70	0.15	0.83	0.10	0.72	0.13	0.37	*n.a.*	0.35	0.05	0.98
LR 300	5.66	8.66	0.90	3.44	0.71	0.15	0.15	0.15	0.15	0.15	0.32	*n.a.*	0.29	0.04	0.81
Ysa 132	14.60	22.12	2.23	8.66	1.78	0.37	1.87	0.22	1.41	0.24	0.60	*n.a.*	0.50	0.07	0.80
Ysa 131	11.62	30.04	3.06	11.79	2.43	0.52	2.54	0.31	1.98	0.34	0.89	*n.a.*	0.77	0.11	1.24
Ysa 90	40.26	91.48	9.86	39.45	8.29	1.85	9.25	1.10	7.35	1.29	3.44	*n.a.*	2.70	0.38	1.10
Ysa 89	40.65	73.16	9.19	36.70	8.09	1.79	8.19	0.98	6.15	1.00	2.56	*n.a.*	1.89	0.26	0.87
Ysa 88	61.20	145.6	18.25	73.82	16.43	3.60	16.71	1.97	12.18	1.99	5.08	*n.a.*	3.64	0.49	1.08
Ysa 87	23.77	57.77	6.31	24.46	5.25	1.13	5.62	0.68	4.35	0.74	1.91	*n.a.*	1.58	0.23	1.15
Ysa 86 (white)	16.63	39.58	4.22	16.48	3.44	0.75	3.65	0.44	2.86	0.48	1.28	*n.a.*	1.03	0.15	1.15
Ysa 85	32.78	21.91	2.72	10.80	2.41	0.52	2.51	0.30	1.85	0.30	0.77	*n.a.*	0.59	0.08	0.38
Ysa 84	5.28	8.51	1.08	4.16	0.87	0.20	0.94	0.11	0.76	0.13	0.36	*n.a.*	0.33	0.05	0.81
LR 323	8.29	5.96	0.77	2.86	0.59	0.13	0.69	0.08	0.60	0.11	0.31	*n.a.*	0.27	0.04	0.40
Ysa 84	5.28	8.51	1.08	4.16	0.87	0.20	0.94	0.11	0.76	0.13	0.36	*n.a.*	0.33	0.05	0.81
LR 324	1.18	1.14	0.19	0.71	0.13	0.03	0.18	0.02	0.16	0.03	0.09	*n.a.*	0.08	0.01	0.52

Table 5. Rare earth element concentrations (in ppm) and cerium anomalies (Ce*) in the bulk calcite of samples from the Cenomanian–Turonian sequence at Flixton, England (Text-fig. 14). Analysed by ICP-MS; *n.a.* – no analysis.

starting with ~ -1.6‰ at the base, reaching ~ -4.5‰ in black band D, and increasing to ~ -1.4‰ at peak acid insoluble residue value. From here the values decrease rapidly to -5.5‰ (sample Ysa 131). From this point up to sample Ysa 99, values vary from ~ -4.9‰ to ~ -6.75‰, forming the second or middle section of the pattern. Above, values increase, varying between -3.0 and -4.0‰.

Flixton. AIR	La	Ce	Pr	Nd	Sm	Eu	Gd	Tb	Dy	Ho	Er	Tm	Yb	Lu	Ce* (AIR)
LR 322	47.21	57.28	12.73	52.37	9.31	1.94	8.89	1.29	6.77	1.38	3.15	*n.a.*	1.88	0.22	0.61
LR 320	65.08	88.34	19.33	81.23	15.66	3.33	13.73	2.12	10.97	2.10	4.76	*n.a.*	3.16	0.42	0.65
LR 319	20.20	22.79	5.19	20.05	3.56	0.71	3.31	0.49	2.43	0.49	1.26	*n.a.*	0.93	0.10	0.58
LR 318	38.35	51.01	12.13	49.98	10.36	2.05	8.40	1.31	6.65	1.36	3.02	*n.a.*	2.00	0.26	0.62
LR 317	12.34	14.93	3.51	14.82	2.76	0.58	2.65	0.34	1.75	0.33	0.80	*n.a.*	0.49	0.04	0.59
LR 316	23.03	27.23	7.06	29.79	5.54	1.11	5.18	0.72	3.42	0.64	1.40	*n.a.*	0.93	0.11	0.57
LR 315	26.29	28.91	7.01	30.26	5.57	1.13	5.47	0.72	3.58	0.70	1.63	*n.a.*	0.94	0.13	0.54
LR 314	25.88	33.36	7.15	30.17	5.43	1.16	5.61	0.80	4.26	0.78	1.81	*n.a.*	1.25	0.15	0.64
LR 313	57.0	94.9	*n.a.*	69.0	13.65	3.03	*n.a.*	*n.a.*	*n.a.*	*n.a.*	*n.a.*	*n.a.*	2.93	0.40	0.78
LR 312	75.0	136.8	*n.a.*	104.1	22.88	6.18	*n.a.*	*n.a.*	*n.a.*	*n.a.*	*n.a.*	*n.a.*	4.94	0.72	0.85
LR 311	59.96	104.5	19.85	81.69	16.91	3.39	14.39	2.16	12.00	2.32	5.33	*n.a.*	3.85	0.48	0.80
LR 310	42.91	55.90	12.88	53.58	11.46	2.25	9.76	1.46	8.00	1.57	3.74	*n.a.*	2.62	0.34	0.61
Ysa 100	80.46	120.4	28.31	118.7	24.11	5.40	25.13	3.34	17.06	3.40	7.94	*n.a.*	5.49	0.72	0.67
LR 309	27.3	47.9	*n.a.*	30.1	5.10	1.13	4.40	0.69	*n.a.*	*n.a.*	*n.a.*	0.26	1.44	0.20	0.59
LR 308	41.22	76.82	12.91	53.60	10.72	2.23	8.94	1.42	7.31	1.47	3.43	*n.a.*	2.34	0.29	0.87
Ysa 99	90.17	203.7	29.08	116.8	21.86	5.16	24.69	3.31	16.52	3.31	7.43	*n.a.*	4.95	0.66	1.39
Ysa 98	58.0	136.0	*n.a.*	62.1	12.30	2.61	10.80	1.87	*n.a.*	*n.a.*	*n.a.*	0.49	2.60	0.38	1.12
Ysa 97	69.92	148.6	23.56	92.96	18.41	4.28	19.98	2.77	13.45	2.62	6.19	*n.a.*	4.90	0.61	0.99
LR 307	59.76	136.0	20.25	82.26	16.88	3.28	13.58	2.14	10.92	2.16	5.08	*n.a.*	3.79	0.53	1.04
Ysa 96	64.6	144.6	*n.a.*	90.0	19.56	4.56	*n.a.*	*n.a.*	*n.a.*	*n.a.*	*n.a.*	*n.a.*	4.56	0.65	0.98
LR 306	81.3	171.4	*n.a.*	111.9	22.98	5.02	*n.a.*	*n.a.*	*n.a.*	*n.a.*	*n.a.*	*n.a.*	5.61	0.85	0.94
Ysa 95	95.19	176.8	31.24	127.5	26.43	5.94	26.63	3.73	19.53	3.92	9.45	*n.a.*	6.69	0.92	0.85
LR 304	64.90	116.2	19.83	82.59	17.42	3.60	14.57	2.26	12.37	2.55	6.02	*n.a.*	4.36	0.55	0.83
LR 305	51.25	109.9	16.83	68.63	14.74	3.00	11.67	1.90	10.63	2.10	5.10	*n.a.*	4.07	0.57	0.69
Ysa 94	67.50	134.6	21.78	88.70	18.06	4.29	18.75	2.66	13.52	2.79	6.75	*n.a.*	5.08	0.73	0.93
LR 303	46.76	100.4	15.53	63.24	12.88	2.62	9.98	1.63	8.44	1.70	4.11	*n.a.*	3.35	0.44	0.99
Ysa 93	78.22	179.6	25.01	101.2	20.84	4.61	22.13	3.14	15.76	3.34	8.00	*n.a.*	5.88	0.84	1.07
Ysa 92	70.0	155.0	*n.a.*	81.8	18.30	3.68	16.50	2.82	*n.a.*	*n.a.*	*n.a.*	0.86	5.50	0.73	1.01
Ysa 91	84.07	189.1	27.67	111.0	23.28	5.46	24.05	3.54	17.15	3.65	8.87	*n.a.*	6.81	0.90	1.04
LR 302	48.0	119.0	*n.a.*	56.7	11.70	2.60	10.50	1.91	*n.a.*	*n.a.*	*n.a.*	0.64	4.20	0.55	1.11
LR 301	74.61	184.2	22.35	90.39	18.79	3.81	15.15	2.56	13.51	2.76	6.68	*n.a.*	5.25	0.67	1.17
LR 300	54.35	149.2	15.77	60.63	12.65	2.53	10.24	1.59	8.80	1.88	4.75	*n.a.*	4.23	0.56	1.32
Ysa 132	56.14	153.0	16.45	64.86	12.54	3.06	13.63	1.95	9.96	2.15	5.50	*n.a.*	4.48	0.68	1.33
Ysa 131	79.0	215.0	*n.a.*	79.1	16.30	3.61	15.50	2.71	*n.a.*	*n.a.*	*n.a.*	1.04	6.70	0.94	1.31
Ysa 90	177.4	460.5	47.51	187.7	38.06	8.79	42.06	6.07	30.99	6.60	17.02	*n.a.*	13.74	1.91	1.28
Ysa 89	75.17	168.1	22.67	88.11	17.75	3.98	18.68	2.74	13.95	2.95	7.40	*n.a.*	6.30	0.84	1.07
Ysa 88	72.5	171.4	*n.a.*	88.4	18.58	5.24	*n.a.*	*n.a.*	*n.a.*	*n.a.*	*n.a.*	*n.a.*	5.87	0.86	1.08
Ysa 87	90.32	214.3	25.43	98.25	19.86	4.53	20.97	3.12	15.84	3.48	8.79	*n.a.*	7.46	1.10	1.16
Ysa 86 (black)	98.0	263.0	*n.a.*	91.8	18.30	4.60	18.90	3.61	*n.a.*	*n.a.*	*n.a.*	1.29	7.50	1.07	1.32
Ysa 86 (white)	118.8	297.7	31.98	126.6	25.94	6.05	27.83	4.12	21.43	4.47	10.92	*n.a.*	9.08	1.30	1.23
Ysa 85	45.34	102.6	13.60	54.52	11.34	2.48	9.64	1.62	8.20	1.60	4.01	*n.a.*	3.41	0.45	1.07
Ysa 84	32.13	63.92	10.15	41.34	8.58	1.88	7.52	1.27	6.02	1.19	2.95	*n.a.*	2.43	0.33	0.93
LR 323	52.8	102.0	*n.a.*	65.4	13.24	3.59	*n.a.*	*n.a.*	*n.a.*	*n.a.*	*n.a.*	*n.a.*	3.29	0.48	0.89
Ysa 84	32.13	63.92	10.15	41.34	8.58	1.88	7.52	1.27	6.02	1.19	2.95	*n.a.*	2.43	0.33	0.93
LR 324	50.4	69.0	*n.a.*	50.6	9.77	2.23	*n.a.*	1.13	*n.a.*	*n.a.*	*n.a.*	*n.a.*	2.52	0.31	0.67

Table 6. Rare earth element concentrations (in ppm) and cerium anomalies (Ce*) in the acid insoluble residues of samples from the Cenomanian–Turonian sequence at Flixton, England (Text-figs 13, 14). Analysed by the instrumental neutron activation method; *n.a.* – no analysis.

Cerium anomalies of bulk calcite and acid insoluble residues

Cerium*(AIR) values range from just below 0.55 to above 1.3, whereas Ce*(calcite) values show a wider range from below 0.1 to above 1.2. For all samples, with the exception of Ysa 99, Ce*(AIR) has a higher value than Ce*(calcite). The overall stratigraphical patterns of variation shown by both types of cerium anomalies are similar. Due to the hiatus

there is a marked difference in values between the top of the Louth Member and the base of the Black Band succession. Values for both Ce*(AIR) and Ce*(calcite) increase rapidly to their highest values (1.2–1.3) in black bands D and E. Above they drop to values of 0.4–0.6 at the top of the section; however, at the horizon of black band F values are again high, 1.1 for Ce*(AIR) and 1.0 for Ce*(calcite). The two cerium anomalies have different patterns of small-scale variation. Cerium (AIR) values tend to exhibit gradual changes spread across a number of samples, whereas Ce*(calcite) values may show sudden and marked changes between samples, suggesting that the sampling interval was too wide to pick up the natural pattern of variation. There is no obvious correlation between variations in the AIR contents and the values of the cerium anomalies. Peak values of cerium anomalies are linked to relatively high contents of C_{org}. Comparison with the $\delta^{13}C$ pattern emphasises that although both cerium anomalies and $\delta^{13}C$ values are enhanced in samples with relatively high C_{org}, the background values are quite different. Background $\delta^{13}C$ values (3.0–3.5‰) are already established in the lower half of the sequence, whereas those for the cerium anomalies are still falling at the top.

Organic carbon of acid insoluble residues

Values range from 0.1 to 15.6%. The background values are typically 0.1 to 0.3%, and it is only in association with the black bands that enhanced values are encountered. The maximum value for black band D is 9.4%, for black band E, 15.6%, and for black band F, 0.8%. These high values are associated with enhanced values of $\delta^{13}C$ (calcite), Ce*(calcite) and Ce*(AIR).

INTERPRETATION

Pattern of cerium anomalies

Jeans *et al.* (2015) have demonstrated that (1) there are two different cerium anomalies preserved in the Chalk, one in the calcite fraction, the other in the carbonate-fluorapatite of the acid insoluble fraction obtained by removing the calcite fraction with 1 molar acetic acid, and (2) each anomaly reflects the average palaeoredox setting of its host mineral phase. The Ce*(calcite) reflects the local conditions of the Chalk Sea in which an organism secreted its calcite skeleton, whereas the Ce*(AIR) reflects the conditions in the sediment when it was incorporated into carbonate-fluorapatite during early diagenesis. The stability of these two cerium anomalies has been tested within different diagenetic settings in the Chalk and this shows that their original values have been preserved until the present day. Our interpretation assumes that the Ce*(AIR) recorded in the acid insoluble residues of our Chalk samples reflects the palaeoredox conditions in the sediment at the time of formation of the carbonate-fluorapatite. In sample preparation no attempt was made to differentiate between the Ce*(AIR) from carbonate-fluorapatite and that from silicate and other insoluble detritus that make up the acid insoluble residues. In our experience of the Chalk there is no evidence that grain-size related changes in the mineralogy of the acetic acid insoluble residues extracted from Chalk samples exhibit any appreciable variation in their Ce*(AIR) values. This has been demonstrated in Jeans *et al*. 2015 (Text-figs 8, 9) for two Turonian marls from Lincolnshire with ~90% of their acid insoluble residue consisting of the smectite-mica clay assemblage of less than 2 μm e.s.d. In spite of the coarser fractions becoming increasingly rich in quartz and minor feldspar there is little or no change in the Ce*(AIR) values. The conclusion is that the host to the Ce*(AIR) is a diagenetic phase developed in the Chalk sediment and reflects the palaeoredox conditions at the time of its precipitation. The same conclusion can be gained by examining the co-variation of the AIR and Ce*(AIR) at Dover, Melton Ross, and Flixton (Text-figs 9, 11, 14) and this demonstrates that there is no overall and consistent correlation between them. If such correlation existed it would mean that Ce*(AIR) pattern reflected variations in the dominantly clay detritus coming into the Chalk Sea. There is however no evidence of variation in this clay detritus. The smectite-mica clay assemblages is the persistent and volumetrically very dominant component of the chalks and marls from Flixton and Melton Ross (Jeans 1968, 2006; Jeans *et al*. 2000, 2001, 2014b; Wray in Wood 1997), whereas the mica-kaolin clay assemblage is the dominant and persistent component at Dover (Jeans 1968, 2006). Additional confirmation of our interpretation are the parallel changes in both the Ce*(AIR) and Ce*(calcite) that match changes in other independent proxies of the palaeoredox conditions. Two particular examples are the parallel changes in (1) the Ce*(calcite), Ce*(AIR), $\delta^{13}C$ (calcite), $\delta^{18}O$ (calcite) and their association with the Plenus Cold Event, and (2) Ce*(calcite), Ce*(AIR), $\delta^{13}C$ (calcite), low Mn^{2+} and Fe^{2+} in the skeletal calcite associated with the development of Corg-rich black bands at Flixton.

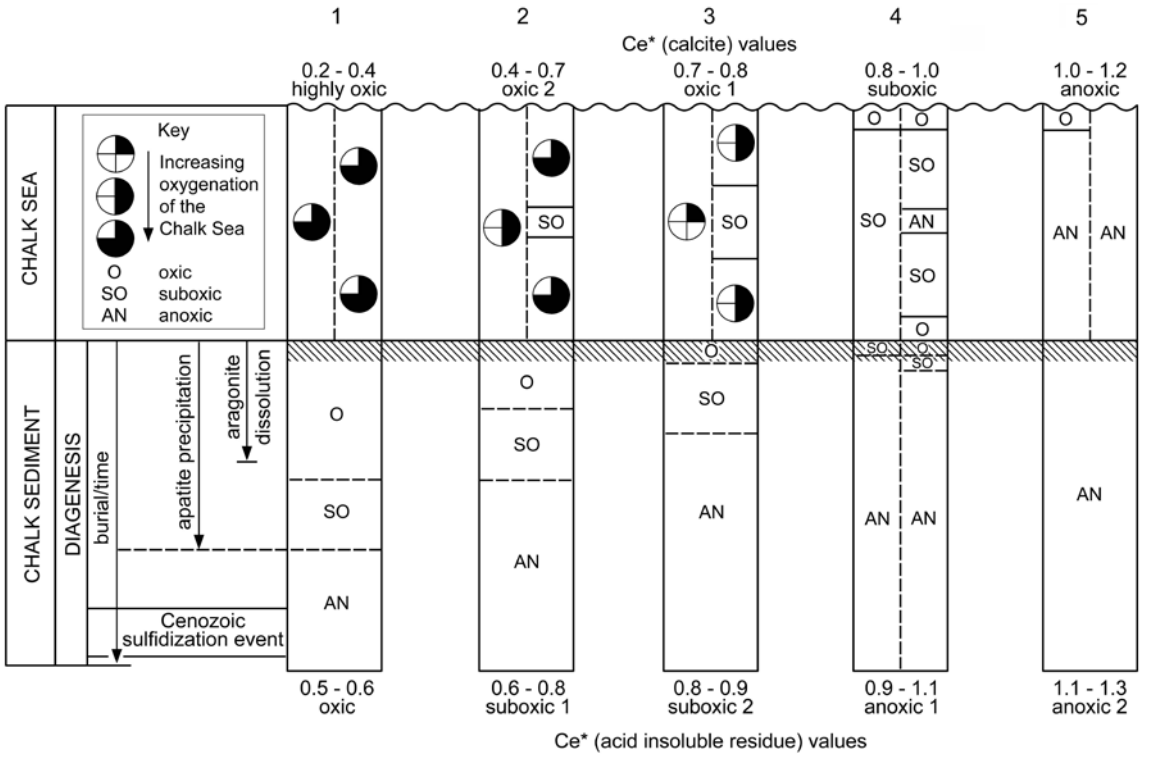

Text-fig. 15. Scheme relating five model situations (1 to 5) of increasing average values of Ce*(calcite) and Ce*(AIR) to hypothetical palaeoredox conditions in the Chalk Sea and its sediment as well as to important diagenetic events. The models covers a range of Ce* anomaly values from model 1 with highly oxic conditions in the water column and oxic conditions in the sediment to model 5 with anoxic conditions in the water column and anoxic 2 conditions in the sediment. Two possible situations in the water column are shown for each model, one where the Ce*(calcite) value represent a well-mixed water mass, the other a stratified water mass. Model 4 shows two possible situations in the sediment for the Ce*(AIR) values.

Interpretation: Text-fig 15 summarises our interpretational model for the range of palaeoredox situations in the Chalk Sea and its sediments that have been determined at Dover, Melton Ross and Flixton from just before, during, and immediately after the CTOAE. It also shows how the various conditions in the Chalk Sea may have been related to those developed in its sediments during diagenesis. Of particular concern is the relationship between the redox conditions of the bottom waters of the Chalk Sea and the redox conditions developed in the underlying sediment. The development and extent of oxic, suboxic and anoxic zones in the chalk sediment would have been controlled by the rate at which oxygen was utilized by microbial action in oxidizing organic matter in the sediment, and whether this could be replaced by diffusion across the water/sediment interface. The amount and type of organic matter in the sediment, permeability, rates of sedimentation and the concentration of oxygen in the bottom waters would have all played a role. If suboxic or anoxic bottom waters were present, there would be effectively little or no oxygen available for the sediment. An oxic zone of diagenesis would have only developed in the sediment associated with an overlying oxic water column. In situations where there was little fine-grained continental detritus and the rates of chalk sedimentation were moderate, there is likely to have been a thick zone of oxic and suboxic diagenesis in which all the utilizable organic matter would have been metabolized by microbial action. In such a situation the sediment would have never experienced anoxic diagenesis, the red and pink chalks of the Transitional Province and the southern part of the Northern Province (Text-fig. 5) are examples.

The relationship between the Ce* anomalies and the palaeoredox conditions (Text-fig. 15) is based on the Ce* profiles recorded from the present oceans in the Cariaco Trench and Saanich Inlet and earlier detailed investigations on the distribution and significance of the Ce* anomalies in the Chalk (Jeans *et al.* 2015 for summary). Five situations (1–5, Text-fig. 15) summarise the range of

values recorded in the Ce*(calcite) and Ce*(AIR) at Dover, Melton Ross and Flixton, and how these Ce* anomalies can be interpretative in different ways. For the Chalk Sea, recorded by the Ce*(calcite) values, the decreasing average degree of oxygenation of the water column illustrated in columns 1 to 5: three oxic zones (0.2–0.4 highly oxic, 0.4–0.7 oxic 2, 0.7–0.8 oxic 1), a suboxic zone (0.8–1.0) and an anoxic zone (1.0–1.2). The chalk sediment for the same five columns show higher, diagenesis related, Ce*(AIR) values: 0.5–0.6 oxic, 0.6-0.8 suboxic 1, 0.8–0.9 suboxic 2, 0.9–1 anoxic 1, 1.1–1.3 anoxic 2. Although the interpretative model shown in Text-fig. 15 is both schematic and simplistic it provides an independent insight into the development, mechanism, and decay of the CTOAE and how the variations in the palaeoredox conditions are related to other features of the sediment. The range in values of the Ce* anomalies for a particular chalk bed or sequence provides indication of the general redox conditions of their deposition, whereas differences between the Ce*(calcite) and Ce*(AIR) reflects the interplay between the conditions in the water column and the pore waters of the chalk sediment. Each sample analysed for their Ce* anomalies displays one of three patterns – *pattern 1* [Ce*(AIR)<Ce*(calcite)] – the values of Ce*(AIR) exceed those of the Ce*(calcite); *pattern 2* [Ce*(AIR) = Ce*(calcite)] – the values of Ce*(calcite) and Ce*(AIR) are the same; *pattern 3* [Ce*(AIR)>Ce*(calcite)] – Ce*(calcite) has a higher value than Ce*(AIR). The patterns, their trends in value, and their relationship to variations in the $\delta^{13}C$ (calcite) and C_{org} form the basis of our interpretation.

The Ce*anomalies of the pre-CTOAE Louth Member display pattern 1 and records a highly oxic/oxic 2 water column and suboxic sediment pore water. At Dover (Text-fig. 9) in the Southern Chalk Province there is slight upward trend to higher palaeoredox values in both the water column and the sediment to the pre-Plenus Marls erosion surface, across which there is a marked increase in values. In the Northern Chalk Province the Ce* anomaly values are generally similar as far as they are known (Jeans *et al.* 2015, table 6). At Flixton (Text-fig. 14) only the very top of the Louth Member is exposed beneath the Variegated Marls and this could have been affected by bioturbation and the mixing-in of sediments from the CTOAE. In spite of this the Ce* anomalies display pattern 1 with an oxic 2 water column and the suboxic sediment. Whereas at Melton Ross (Text-fig. 11) there is a single sample from just below the base of the Variegated Marls with Ce* anomalies of pattern 3 showing an anoxic water column and anoxic 1 sediment caused possibly by considerable intermixing of sediment at the initiation of the CTOAE that has been preserved locally from the regional erosion that defines the base of the Upper Black Band sequence in the Northern Area.

The CTOAE sequence at Dover (Text-fig. 9, Holywell Nodular Chalk Formation) is characterised by pattern 1 with palaeoredox values in the water column and the sediment displaying very similar and increasing trends from lower levels of oxygenation at the base to higher levels at the top. At the base of the sequence the water column is oxic 2 grading to highly oxic in the uppermost of the section, whereas the sediment grades from anoxic 1 at the base to oxic at the top.

The CTOAE sequence at Melton Ross (Text-fig. 11) displays patterns 1, 2 and 3 in its palaeoredox values. The base of the Lower Anomalous Black Band Sequence shows a marked decrease in the available oxygen compared to the underlying Flixton Member. The sequence is dominated by pattern 3 (first evident in the very top of the Louth Member) with two levels displaying pattern 2; the water column was anoxic for much of the unit but at the very top became suboxic**,** whereas the pore waters of the sediment ranged from anoxic 2 in the lower part to anoxic 1 in the upper part. There is a marked increase in the level of oxygenation across the basal erosion surface defining the Standard Black Band Sequence with the Jefferies Cold Phase characterised by pattern 1 and pattern 2 with oxic 1 conditions in the water column and suboxic 1 in the sediment. Initially the upper part of the Standard Black Band Sequence displays pattern 2 followed by pattern 3, both the water column and the pore waters of the sediment becoming increasingly anoxic. It is important to note that there is little or no correlation between the presence of black bands and the variations in palaeoredox conditions of either the water column or the pore waters of the sediment at Melton Ross in contrast to the situation at Flixton.

The CTOAE sequence at Flixton (Text-fig. 14) is dominated by pattern 1 palaeoredox values with only one level (Black Band F) displaying pattern 3. Although dominated by pattern 1 the relationship between condition in the water column and the pore waters of the sediment are very variable in contrast to the situations at Dover and to a lesser extent at Melton Ross where the Ce* (calcite) and Ce*(AIR) generally vary in parallel. At the base of the Flixton CTOAE section the conditions in the pore waters of the sediment were anoxic 1 and as the sequence is followed upwards to the horizon of Jefferies Bed 9 the pore waters became increasingly anoxic (anoxic 2) with a

marked sensitivity to Black Bands D and E where the most anoxic conditions developed. Over this interval conditions in the water column varied generally in parallel ranging from oxic 1 to anoxic although there were short intervals at the beginning and at the end of the Plenus Cold Event where the water conditions were highly oxic. Above the level of Jefferies Bed 9 the pattern changed. The sediment pore water displayed gradual changes becoming more oxic (from anoxic 1 to suboxic 1) as the sequence is traced to the top of the section although the conditions returned to anoxic 2 at the level of Black Band F. The conditions in the water column displayed the same overall trend with it becoming increasingly oxic as the sequence is ascended and showing a reversion to suboxic condition at the level of Black Band F. There were, however, frequent phases of highly oxic water conditions indicating short termed invasion by new well oxygenated water masses; This conspicuous detachment between the pattern of palaeoredox conditions of the water column and the pore water of the sediment first occurs in the upper part of Black Band E.

Clay – black band association

An important question for understanding both the early stages and the development of the CTOAE in Europe is the significance of the enhanced quantities of terrigenous clay-rich silicate detritus that are mixed either with enhanced amounts of C_{org} to form black bands or with low C_{org} chalk to form typical grey marls. At Flixton, Melton Ross and Dover there is no appreciable change in the compositions of the clay mineral assemblages as they are traced from the underlying clay poor Louth Member (Ferriby Formation) into the clay-rich overlying Variegated Beds of the Flixton Member (Welton Formation) in the Northern Chalk Region and the Plenus Marls sequence in the Southern Chalk Region. At Flixton the clay mineral fraction belongs to the smectite-mica assemblage, at Melton Ross to the same assemblage but with occasional traces of kaolin, and at Dover, where there is evidence of its derivation from the Central European Island (Jeans *et al.* 2001), it belongs to the kaolin-mica assemblage. This constancy of clay mineralogy suggests that the pattern of clay sources were little or undisturbed by the development of the CTOAE in the English Chalk Provinces. Various hypotheses have been put forward to explain this influx of clay during the early stages of the CTOAE at other locations. In the black band Bonarelli Level in Sicily Scopelliti *et al.* (2004) have suggested that the influx of silicate terrigenous material is related to a sudden change from an arid to a wetter climate, but have provided no mineralogical evidence in support of this hypothesis. In the Bass River borehole on the New Jersey Shelf, van Helmond *et al.* (2014b) have suggested that the increase in the abundance of the dinocyst *Palaeohystrichophora infusoroides* (interpreted as tolerant of low sea-surface salinities) was evidence of wetter climates during the Plenus Cold Event. Some support for a climate change comes from differences in the calcium and lithium isotope ratios in the Chalk's calcite immediately before the CTOAE compared to the values during it (Blätter *et al.* 2011: Pogge von Strandmann *et al*. 2013). The suggested change from arid to wetter climate is likely to have been associated with changes in the soil clays, but we have found no evidence of this in the clay mineral patterns of England (Jeans 2006; Wray in Wood *et al.* 1997). However, its absence could reflect the relatively slow re-establishment of clay mineral assemblages typical of new climatic conditions and their short duration. However Du Vivier *et al*. (2015) draw different conclusions from their investigation of the calcium isotopes from the Portland core (Colorado, USA), Eastbourne (UK), Pont d'Issole (France), and Oyubari (Japan) suggesting that the pattern of variation was caused by a short-lived phase of acidification of the oceans. Neither interpretation has yet any supporting evidence in the sedimentary record. Either interpretation can be accommodated within our geological interpretation that the CTOAE was associated with a major lowering of sea level, a reworking of exposed sediments followed by the Plenus Transgression. Later in this paper we suggest that acid rain, associated with enhanced carbon dioxide concentration in the atmosphere, may have played a role in returning dissolved phosphate to the Cenomanian seas as the stimulant for the excessive production of $Corg_{.}$ in the oceans that triggered the CTOAE.

Early interpretations of black bands considered the possibility that they represented deposition at or below the carbonate compensation depths with the terrigenous silicate detritus being undifferentiated from that occurring much more sparsely in the adjacent limestones. Detailed investigations of such horizons in the Standard Black Band sequence in the North Chalk Province of England (Bralower 1988; Gaunt *et al.* 1992; Wood *et al.* 1997) demonstrate that they contain a very restricted macrofauna and a specific microfauna. The black bands are virtually devoid of macrofossils apart from complete skeletons of fish and their scattered remains and exceedingly rare occurrences of oysters, terebratulid brachiopods and lobsters. They are characterised by a low-diver-

sity dinoflagellate cyst assemblage dominated by *Cyclonephelium compactum* together with common smooth forms of *Deflandrea*, the comparative lack of long-spined taxa point to reduced water temperature. The foraminiferal assemblage is entirely composed of simple agglutinating forms. The nannofossil assemblage is dominated by *Eprolithus floralis* that makes up to 47 per cent of the non-*Watznaueria barnesae* fraction. At Flixton (Jeans *et al.* 1991, fig. 11) and at localities in Lincolnshire (South Ferriby; Elsham; Caistor; Louth) this black band microfauna is characterised by a skeletal carbonate mineralogy with exceptionally low values of Fe^{2+} and Mn^{2+} (<100 ppm, Jeans *et al*. 1991, fig. 11). At the equivalent horizons (Jefferies Beds 4–6, Text-fig. 17) at Dover in the Southern Chalk Province this Fe^{2+} poor skeletal calcite (~150 ppm) is still evident but it is now relatively enriched in Mn^{2+} (≤ 800 ppm). In contrast the clay mineralogy of the black bands cannot be differentiated from other parts of the Variegated Beds in eastern England.

The relationship between the development of black bands, evidence of anoxia in the water column and in the pore waters of the sediment, and the $\delta^{13}C$ Excursion is a critical one for understanding the development of the CTOAE in England. In the Northern Province the lateral changes between two well correlated sections at Melton Ross and Flixton allows the relationship to be examined between the clay-rich silicate detritus, the preservation of organic matter to form black bands, the type of organic matter, the redox conditions in the water column and in the sediment (both expressed by cerium anomaly values) and the pattern of $\delta^{13}C$ (calcite). In both sections there are intervals of clay-rich marls deposited under suboxic and anoxic conditions where there is no enrichment in C_{org} (Text-figs 11, 14), whereas all the black bands with C_{org} enrichment have been deposited under similar redox conditions. At Melton Ross the black bands (A, B, C) in the Anomalous Black Band sequence are associated with somewhat enhanced content of acid insoluble residues of terrestrially derived clays. The C_{org} component is predominantly marine although there is some terrestrial woody matter (Batten in Woods *et al.* 1997) and this has lighter $\delta^{13}C_{org}$ values than the organic matter in the adjacent marls. These black bands are not associated with enhanced $\delta^{13}C$ (calcite) values. Black bands (D, E1, E2) in the Standard Black Band sequence display a different pattern. Their acid-insoluble residues are not enhanced relative to the adjacent marls, and the organic matter is a mixture of marine and terrestrial origin. They display enhanced $\delta^{13}C$ (calcite) values relative to the adjacent marls. All the black bands at Melton Ross are associated with pattern 3 [Ce*(AIR) > Ce*(calcite)] cerium anomalies except for sample CJW 5 that shows pattern 2 [Ce*(AIR) = Ce*(calcite)]: the significance of this has already been discussed. The evidence from the Anomalous Black Band sequence at Melton Ross indicates that black bands A, B and C, each separated by beds of marl laid down under anoxic redox conditions, represent blooms of indigenous dinoflagellates in a relatively open marine environment (Batten in Wood *et al.* 1997). However, black bands D, E and F, which are also separated by beds of marl laid down under similar redox conditions, reflect a more restricted marine environment with a higher proportion of continentally derived organic matter. These are also associated with blooms of a more restricted population of indigenous dinoflagellate cysts. At Flixton the situation is quite different. Black bands D and E are better developed than at Melton Ross and have enhanced C_{org} contents (Text-fig. 14). Their organic matter is dominated by terrestrial material (Cornford in Jeans *et al.* 1991; Dodsworth 1996) and the bands are associated with enhanced cerium anomalies and $\delta^{13}C$ (calcite) values. Marine conditions had become normal with pattern 1 cerium anomalies with little evidence of any influence of cerium-enriched waters. The $\delta^{13}C$ (calcite) excursion is intimately linked with the enhanced preservation of organic matter and the anoxic/suboxic conditions in the water column and in the pore waters of the sediment. The black bands are also associated with a phase of enhanced clay-rich marls.

Combining these three situations (Text-fig. 16) in which black bands developed, a working hypothesis is that the black bands represent spasmodic floods of terrestrial C_{org} matter entering the Chalk Sea during an early phase in the development of the $\delta^{13}C$ Excursion when considerable amounts of continental clay material entered the sea. In the more open parts of the Chalk Sea – such as at Flixton – the microbial breakdown of this terrestrial organic matter in the water column and in the sediment were responsible for the suboxic and anoxic conditions necessary for the development of black bands. In less open parts of the Chalk Sea, such as represented in the Standard Black Band Sequence at Melton Ross, where the water was enriched in cerium and already anoxic or suboxic, the addition of terrestrial organic matter and waters of a different chemistry, perhaps containing nutrients of continental origin, set off ‘blooms’ of dinoflagellates. The marine organic matter derived from these blooms added to the terrestrial organic matter to form the black bands. The black bands in the Anomalous Black Band Sequence at Melton Ross represent a more distal location in a cerium-enriched

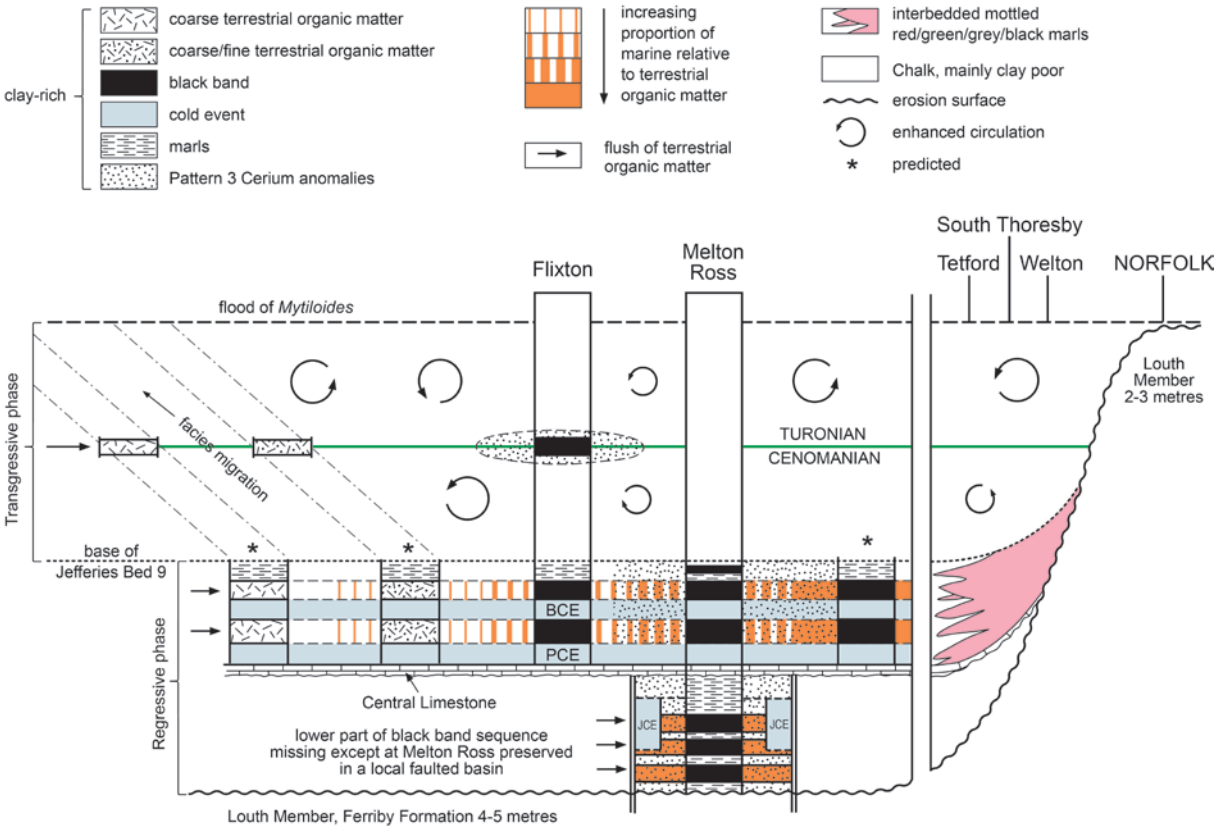

Text-fig. 16. Interpretative and predictive lithofacies model for the CTOAE in the Northern Chalk Province based on the relationships between (1) the red mottled oxic-suboxic facies of southern Lincolnshire and the anoxic facies at Melton Ross and Flixton, and (2) the proposed regressive–transgressive cycle and cerium-enriched sea water (**Pattern 3**). Cold phases (WCP – Wood Cold Phase: JCP – Jefferies Cold Phase: BCP – Black Cold Phase), and the black bands with their lateral changes in the organic carbon components of their acid insoluble residue are shown.

Chalk Sea where there is little evidence of terrigenous C_{org} material; dinoflagellate 'blooms' catalysed by the occasional flush of continentally influenced waters provided the organic matter.

Relations similar to those at Flixton are associated with the numerous and well developed black bands in the Cenomanian–Turonian sequence of the Hesseltal Formation at Wunstorf, near Hannover, Germany (Voigt *et al*. 2008, fig. 4). Here the extent of the $\delta^{13}C$ (calcite) Excursion is similar to Dover and Eastbourne although its form is considerably different. The black bands are not tied to the CTOAE and extend into the overlying upper part of the *Watinoceras devonense* Zone. Blumenberg and Wiese (2012) report that in the black bands there is appreciable amounts of derived terrestrial organic matter mixed with autochthonous organic matter, and there is good correlation between enhanced $\delta^{13}C$ (calcite) values and the black bands – matching our findings at Melton Ross and Flixton. They also suggest that continentally derived reduced phosphate played a role in triggering black band development without any evidence of the actual pattern of phosphorus variation in the succession. In the Northern Province the pattern of phosphorus variation in the acetic acid insoluble residues does not give any clear evidence of variation linked to the black bands, and we have postulated a continentally derived factor – waters of a different chemistry – may have triggered or were capable under suitable conditions of setting off their formation. Further analysis of the black band sequence at Wunstdorf by Van Helmond *et al.* (2015) has demonstrated that (1) these black bands are also enriched in spores and pollen but impoverished in dinocysts relative to the intervening chalks and marls, and (2) both were deposited in a marine setting with a similar sea surface temperature. These authors suggest, based upon the higher values of the P/G ratio (peridinoid dinocysts (heterotrophic)/gonyaulacoid dinocysts (autotrophic)) in the black

bands, that their development was associated with a low salinity, high productivity surface layer resulting from seasonal flushes of freshwater input and later, in the lower part of the water column, anoxic conditions developed particularly conducive for the preservation of organic matter.

The role played by phosphorus as a growth stimulant in the initiation and maintenance of the $\delta^{13}C$ Excursion has been considered by Nederbragt *et al.* (2004) and Mort *et al.* (2007, 2008) for the Tarfaya Basin, Morocco. This was based upon the pattern of P_2O_5 in the total sediment, where there is a marked spike in values (0.6%) just as the $\delta^{13}C$ Excursion was getting under way – as if it catalysed the excessive production of organic matter in the sea – whereas in the main part of the excursion P_2O_5 values are particularly low (~0.2%) only returning to normal values (~0.3%) in the upper part of the Cenomanian. This pattern of variation is not evident at a local level in either the Southern or Northern Chalk Provinces of England. At Dover there are three well defined peaks (Jefferies beds 4, 6, 8) in the P_2O_5 /TiO_2 values within the acid insoluble residues (Text-fig. 17) but there is no evidence of any enhanced organic matter associated with them, however each of these peaks is associated with enhanced chromium values. At Flixton there are numerous P_2O_5/TiO_2 and chromium peaks displaying no clear relationship to the development of black bands or to each other. It is far from clear what role the availability of phosphorus played in promoting the excessive production of organic matter in the proto-North Atlantic. Perhaps a mechanism such as the acidification of oceans suggested by Du Vivier *et al.* (2015b) is a simpler way of recycling phosphorus as a growth stimulant than relying upon global changes in the weathering regime for which, at least from the clay mineral viewpoint, we have found no evidence. The effects of acid rain on the exposed area of Chalk sediment resulting from the major regression preceding the start of the CTOAE may well have released phosphorus from carbonate skeletal matter, phosphatic nodules and phosphatized surfaces to be returned to the oceanic reservoir. This could be an explanation of the marked spike in P_2O_5 reported from Tarfaya Basin in Morocco.

Plenus Cold Event, the $\delta^{13}C$ "trough" and marine extinctions in the Late Cenomanian

The Plenus Cold Event as defined in this paper extended from the early to the late part of the *Metoicoceras geslinianum* Zone (see *Stratigraphical framework*). Its characteristic boreal fauna with *Praeactinocamax plenus* occurs widely along the shelves of the northern Tethyan margin, from Turkistan-Tadzhikistan in the east to the Anglo-Paris Basin and northern England in the west (Wilmsen *et al.* 2010; Jefferies 1963). At locations where this boreal fauna and its geochemical context has been investigated in sufficient detail (e.g. Dover, Jeans *et al.* 1991; Eastbourne, Paul *et al.* 1999; Wunstdorf, Van Helmond *et al.* 2015; Vocontian Basin, Jarvis *et al.* 2011) it is associated with the "trough" section of the $\delta^{13}C$ Excursion and with relatively heavy O^{18}/O^{16} values and/or reduced sea water surface temperatures. Beyond the regional occurrence of this boreal fauna there is evidence that the Plenus Cold Event was more widely felt. It has been identified (Forster *et al.* 2007; Sinninghe Damsté *et al.* 2010; van Helmond *et al.* 2014a) at drilling sites (603, 1276, 641, 386, 367) in the proto-North Atlantic basin as a short interval in an otherwise anoxic sequence of oceanic sediments during which the bottom waters and sediments were either reoxygenated or were deposited under less anaerobic conditions with the sea surface temperature dropping between 5–11ºC based on Tex_{86} palaeothermometry. Off-shore New Jersey, U.S.A., the Plenus Cold Event has also been recognised in the Bass River borehole by a cooling phase in the sea surface temperature from 36–37ºC to 33–34ºC (Tex_{86} palaeothermometry) associated with the influx of boreal dinocyst species that had migrated into equatorial regions from the higher latitudes of the Northern Hemisphere (Van Helmond *et al.* 2014b, 2016).

The Plenus Cold Event and the enhanced occurrence of wildfires (Baker *et al.* 2019) have been linked with the "trough" section of the CTOAE $\delta^{13}C$ Excursion in the $\delta^{13}C$ (organic C) Excursion recorded in the paralic Upper Cretaceous strata of southwest Utah, U.S.A, where Barclay *et al.* (2010) have estimated the carbon dioxide contents of the late Cenomanian palaeo-atmosphere by using the pattern of variations in the stomatal index of leaf cuticles. Here the development of the CTAE was associated with a marked increase in the carbon dioxide concentration from an estimated background value of $\sim 370^{+100}/_{-70}$ ppm. It reached the highest values ($\sim 500^{+400}/_{-180}$ ppm) at the beginning of the "trough" and it returned towards more normal values during the second build-up to the "plateau" although data for the latter part of the CTAE is not available. Interrupting this overall change in the uppermost Cenomanian palaeo-atmosphere were three levels when the carbon dioxide concentration revert to much lower levels, two of which are essential similar to the background levels. Barclays *et al.* (2010) suggested that these two

intervals (A, B of their fig. 2e) are somehow related to the Plenus Cold Event. We suggest that the lowest of these (A in Barclay *et al*. 2010, fig. 2e) – associated with the "first build up" – reflects the *Wood Cold Phase*, whereas the middle one – at the beginning of the "trough" – reflects *Jefferies Cold Phase*, and the upper one (B in Barclays *et al.* 2019, fig. 2e) – associated with the "second build-up" to the "plateau" – reflects the *Black Cold Phase*. What is the significance of our suggested correlation between these three fluctuations in the carbon dioxide concentrations and the Plenus Cold Event? Did fluctuations in the input or extraction of carbon dioxide cause the ocean cooling, re-oxygenation, and the influx of the pulse fauna (Arthur *et al*. 1988; Sinninghe Damsté *et al*. 2010), or were influxes of cold and oxygenated ocean waters responsible for the return to normal carbon dioxide concentrations? A partial answer comes from the study by Zheng *et al.* (2013) of the neodymium isotope values ($^{144}Nd/^{143}Nd$) expressed by ratios to bulk Earth (ε_{nd}) preserved in the fossil fish debris across the marine CTAOE sequence at Eastbourne, England. The general trend across the sequence is from values of -9 ε_{nd} (t) at the base of the sequence to -10.6 ε_{nd} (t) at the top. This is disturbed by four marked oscillations with values varying from -10.6 ε_{nd} (t) to -7.6 ε_{nd} (t) that are associated with the Plenus Cold Event. Two possible explanations are suggested. The first is that these oscillations either represent either major changes in the pattern of ocean circulation with the influx of boreal waters with relatively high ε_{nd} (t) values representing ocean waters with their ^{144}Nd /^{143}Nd signature derived from ancient non-radiogenic rocks, or a marine setting that reflected mixing of waters from the Tethyan and proto-North Atlantic oceans. The second explanation is that it resulted from the development of a water current carrying a radiogenic signature from its suggested volcanic source (Caribbean Large Igneous Province) to Eastbourne. The general stratigraphical setting of the CTOAE in western Europe (see *Stratigraphical framework*) gives little support to this second possibility as its cycle is no different from other Upper Cretaceous stratal cycles associated with widespread and major changes in sea-level that are most simply linked to changes in ocean circulation with the influx of the pulse fauna and cooler waters (see Text-fig. 2). If this is the correct interpretation, the presence of the "trough" section of the $\delta^{13}C$ Excursion in the proto-North Atlantic basin and its surrounds, the Western Interior Seaway, and in the proto-Pacific basin (see later) suggests that the Plenus Cold Event might have been of global extent. Critical evidence for deciding whether variations of the carbon dioxide in the atmosphere were caused by the introduction of cold oxygenated waters into the proto-North Atlantic basin and its surrounding seas or by variation in supply from volcanic degassing would be evidence from the sea surface temperature in the proto-Pacific basin. A marked drop in temperature would support control by volcanic degassing; if not, the influx of cold water into the proto-North Atlantic basin, the European shelf area, the northern margin of the Tethys, and the northern part of the Western Interior Seaway of North America would be the driving force behind of this global drop in the atmospheric carbon dioxide content. Present evidence favours that (1) three influxes of cold oxygenated boreal water were responsible for the three oscillations in the carbon dioxide concentration of the atmosphere in the late stages of the Cenomanian, and (2) the increased solubility of carbon dioxide in the cooler oceans and its enhanced drawn-down from the atmosphere were responsible, and not variations in the input of carbon dioxide into the atmosphere from volcanic sources such has been favoured by Jarvis *et al*. (2011).

An important question is the relationship between the Plenus Cold Event and the well-known faunal and floral extinctions in the microfossil assemblages of the marine realm associated with the CTOAE that were initially described in detail from the Plenus Marls at Dover by Jarvis *et al.* (1988). These changes were considered to be the result of an expanding oxygen minimum zone in the Chalk Sea, however attempts by Jeans *et al.* (1991) to chemically define this zonation by using $^{13}C/^{12}C$ and $^{18}O/^{16}O$ on single foraminifera species failed – although apparently successful at the time but later shown to be marred by the minor but selective growth of diagenetic calcite cement (Mitchell *et al.* (1997). These faunal and floral changes became part of the stepwise mass extinctions associated with the CTOAE (Hut *et al.* 1987; Hart and Leary 1991; Gale *et al.* 2000). Originally Hut *et al.* (1987) have suggested that the CTOAE and its associated extinctions were caused by cometary impact, but subsequent research by Orth *et al.* (1993) indicated that this was unlikely. In contrast, Hart and Leary (1991) argued that the stepwise extinction and the subsequent reappearance of certain groups of foraminifera, ostracods, dinoflagellates and calcareous nannofossils was related to the synchronous development of the $\delta^{13}C$ excursion at many localities around the world, and that this was best explained by the effects of the expanding oxygen-minimum zone of the oceans and its subsequent shrinking. An alternative view (Paul and Mitchell

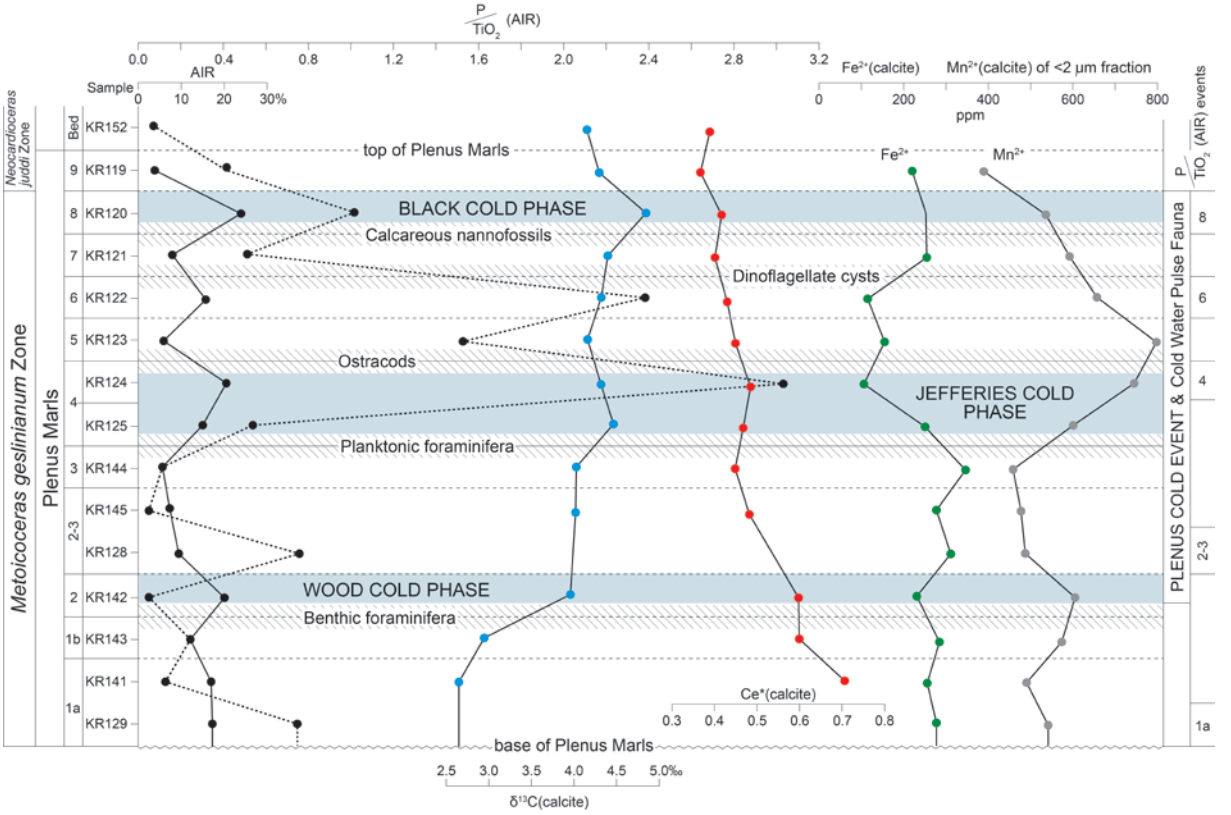

Text-fig.17. The Plenus Marls and adjacent strata at Shakespeare Cliff, Dover showing the stratigraphical relations between the acid insoluble residues (AIR), P/TiO_2, Fe^{2+}(calcite), Mn^{2+}(calcite) and the five stepwise extinctions of the plankton groups described by Hart & Leary (1991) but based on data from Jarvis *et al*. (1988). The hachured areas are zones within which there is a significant loss of species within the named fossil groups. The Plenus Cold Event with its three cold phases, the extent of the pulse fauna and the P/TiO_2 events are shown.

1994) suggested that a widespread reduction in ocean productivity (Coccolithophoridae) during the late Cenomanian could have led to famine among the zooplankton populations higher up the food chain and their "extinction" and subsequent reappearance when conditions improved. It is now generally accepted that marine conditions in the Southern Chalk Province were oxic throughout the deposition of the Plenus Marls and this is confirmed by the pattern of cerium anomalies (Text-fig. 9). If there was an oxygen-minimum zone it was not recorded in the chemistry of the sediments nor within the chemistry of the different groups of foraminifera although diagenetic development of carbonate cements within their chambers may be masking original differences.

At Dover there is now sufficient geochemical data to test critically the relationship between the stepwise extinctions observed in the microfossils and the Plenus Cold Event. Does the famine hypothesis still have a role to play? Text-fig. 17 summarises the relationships between the faunal and floral extinctions in the Plenus Marls at Dover and how these are related to the cold phases, the pulse fauna and the changing geochemistry of the sediment. The extinction of benthic foraminifera (top of Jefferies Bed 1b) is associated with the initial recovery of the Chalk Sea from the relatively poorly oxygenated conditions (Ce* (calcite) 0.71) of Jefferies Bed 1a. The extinction of planktonic foraminifera, ostracods, dinoflagellate cysts and calcareous nannofossils occur at different levels between Jefferies bed 4 and bed 8 during a phase of gradually increasing oxygenation of an already oxic sea (Ce* (calcite) 0.4–0.5). These extinctions are associated with: (1) the Jefferies Beds 2, 4, 8 (Text-fig. 17); (2) the pulse fauna (Jefferies Beds 2, 4, 8); (3) exceptional values of Mn (high) and Fe (low) in the calcite skeletons of the nannofossil-dominated <2µm fraction of Jefferies Beds 4 to 7 (similar values occur also in the 63–125 µm, 8–63 µm and 2–8 µm calcite fractions); and (4) enhanced values of P/TiO_2 (AIR) with peaks in Jefferies Beds 4, 6 and 8. The extinctions are unrelated to the Ce* (calcite) signal,

this suggests an increasingly well-oxygenated water column, but they do relate to the anomalous patterns in the Fe^{2+} and Mn^{2+} contents of the biogenic calcite and the enhanced values of P/TiO_2 (AIR). The very low Fe^{2+} in the biogenic calcite can be matched with the findings of Martin (1990), Boyd *et al.* (2007) and Cassar *et al.* (2007) who demonstrated that a deficiency of Fe^{2+} in seawater is a limiting factor controlling primary productivity (Coccolithophoridae) in the oceans and that this will adversely affect the zooplankton higher up the food chain. Faucher *et al*. (2017) have argued that the size variations and dwarfism in the coccolith *Biscutum constans* during the CTOAE were caused by changes in ocean chemistry. Du Vivier *et al* (2015b) has suggested that the changing pattern of calcium isotopes associated with the CTOAE is related to ocean acidification. These lines of evidence support the famine hypothesis of Paul and Mitchell (1994) and not the expanding oxygen-minimum zone hypothesis of Jarvis *et al.* (1988) and Hart and Leary (1991). Higher values of P/TiO_2 (AIR) in Jefferies Beds 4, 6 and 8 suggest the enhanced development of carbonate-fluorapatite in the sediment. A number of authors (Martin 1990; Filippelli *et al.* 2007; Filippelli 2008) have described similar enhancements of P/TiO_2 ratios and Fe deficiencies associated with the Pleistocene glacial and interglacial phases. An alternative explanation of the low skeletal iron contents is the suggestion that iron was being lost from the shelf region of the proto-Atlantic by the "reactive Fe shuttle" of Owen *et al.* (2012) finding its way into the ocean basin where it was, with phosphorus , an essential and limiting nutrient in the production of organic matter. The regional distribution of iron in Northern and Southern Chalk provinces is complex. The black bands sequences of the Northern Province with their very low Fe^{2+} calcite content of less than 50 ppm pass southwards and laterally into pink chalk of the Transitional Province (Text-figs 5, 16) with an Fe^{2+}(calcite) content of 200–300 ppm (Jeans *et al*. 2014) that contain a fine-grained hematitic pigment possibly of hydrothermal or volcanogenic origin (Jeans *et al.* 2016). Traced southwards these chalks of the Transitional Province pass into those representing the Plenus Cold Event at Dover with their low Fe^{2+}(calcite) of ~100 ppm. This general setting could suggest that Fe was being lost on the "reactive Fe shuttle". There is, however, little evidence that it helped to generate organic matter in the proto-Atlantic as the Plenus Cold Event and its equivalent levels in the ocean basin were characterised by either the reduced production or preservation of organic deposits.

DIAGENETIC MODIFICATION OF PROXY RECORDS OF THE CENOMANIAN–TURONIAN OCEANIC ANOXIC EVENT

The original CTOAE hypothesis (Schlanger *et al.* 1987; Arthur *et al.* 1987) was based on measurements of the carbon and oxygen isotopes preserved in calcite at a number of locations within a stratigraphical framework dependent very largely on biostratigraphy with its hundred and fifty years or more experience of its shortcomings and strengths. Since then there has been refinement in the stratigraphical framework by the radiometric dating of volcanic ash bands when they occur and the use of a whole range of isotopic geochemical proxies to test and define the hypothesis (see *Introduction*). However some proxies have not been tested as to their stability during diagenesis before they have been applied to a particular Cenomanian–Turonian sequence or whether they are suitable for chemostratigraphical application. It has been assumed that they retain the original oceanic signature from Cenomanian and Turonian times. If this assumption is only partially correct and the signal has been totally or patchily modified by post-depositional processes in its 90 Ma year burial history the conclusions drawn from the results can be misleading. Once the range of limitation of a proxy is known its usefulness is much increased. The $^{18}O/^{16}O$ (calcite) proxy, for example, with its sensitivity to modifications by waters of different origins during diagenesis can still be used to obtain temperatures in the Chalk Seas as long as care is taken to select unaltered shell material, or by using relative temperatures to identify the presence of the Plenus Cold Event with its cold phases as long as the bio-and litho-stratigraphy is tightly constrained. There are situations when the use of certain proxies have resulted in misleading conclusions as to correlation or the conditions in the Chalk Sea at the time of the CTOAE. Two examples are discussed.

34S/32S ratios of the sulphate preserved within calcite (CAS)

This isotopic system was used first by Ohkouchi *et al*. (1999) to study the Cenomanian–Turonian Bonarelli sequence in Italy, then by Adam *et al.* (2010) to investigate the USGS No.1 Portland core sequence from Pueblo, Colorado, USA, and later by Owen *et al.* (2013) to study four Cenomanian–Turonian sections in Europe: more recently it has been used by Gomes *et al*. (2016) to investigate the biogeochemical sulfur cycle, and by Raven *et al.* (2018, 2019) to examine the role played by sulfur-

ization of organic matter in causing the variable preservation of organic matter during the CTOAE. Both the Bonarelli sequence and the Portland core demonstrated a sharp increase in $^{34}S/^{32}S$ (CAS) values of 4–5‰ associated with the initiation of the CTOAE as defined by the increased $\delta^{13}C$ (organic) values. In the Bonarelli sequence itself there are no measurement as calcite is very largely absent. The limestones leading up to it display a wide scattering of values increasing upwards from ~14‰ to ~17‰ immediately below the base of the Bonarelli. In the limestone and chert sequence overlying the Bonarelli values start at ~23‰ and then display a broadly scattered trend in the opposite direction to lower values between 18 and 19‰ some 11 metres above. The Portland core displays consistent values of 13–14‰ from 13 metres below, to the base of the CTOAE sequence where values increase to ~19‰ and these are maintained with minor variations into the Turonian *Collignoniceras woolgari* Zone some twelve metres above. The four sections in Europe, three in England and one in Italy, investigated by Owen *et al.* (2013) produced rather variable patterns none of which matched the Portland core. At each locality the $\delta^{13}C$ (calcite) Excursion lies within a general trend of increasingly heavy $^{34}S/^{32}S$(CAS) values. Only at Raia del Pedale, Italy, does this trend revert to lower values after the end of the Excursion. In none of these localities is there a marked increase in values associated with the initiation of the Excursion. At South Ferriby in the Northern Chalk Province (Text-figs 1, 18) this increasing trend continues beyond the end of the Excursion to the Cenomanian–Turonian boundary after which there is insufficient data to see a trend. The same pattern is present in the Trunch borehole (Transitional Chalk Province Text-fig. 1) and at Eastbourne (Southern Chalk Province), at both these locations the trend continues well into the Turonian. At South Ferriby and at Eastbourne there is another feature of particular interest; this is the increase in the scatter of values within certain zones of this general trend. At South Ferriby (Text-fig. 18) it is restricted to the chalk lithology above and below the black bands but not within the clay-rich marls. This chalk is of high bulk specific gravity with values of up to 2.40 compared to the uncemented Standard Louth Chalk with a value of 1.64 (Jeans *et al*. 2014a). The section in the Louth Chalk beneath the black bands (Text-fig. 18) was part of the Upper Pink Band prior to its sulfidization in latest Cretaceous or early Cenozoic times. This sulfidization was associated with iron sulphide nodules with $^{34}S/^{32}S$ values up to as heavy as 40‰ (Jeans *et al.* 2016). Related to this was the regional precipitation of calcite cement in the Northern Chalk Province responsible for the high specific gravity of the chalk. The question is whether the wide range of $^{34}S/^{32}S$ values in these chalk zones reflect an oceanographic signal of short termed variations in the seas in which a homogeneous chalk sediment was being deposited, or is it the result of the late diagenetic modification of the strata some 30 Ma years after its deposition? Present evidence supports a diagenetic origin. At Eastbourne, the European type locality for the CTOAE, a great scattering of $^{34}S/^{32}S$ values from 16 to 20‰ occurs between Jefferies Beds 2 and 8 (Owen *et al*. 2013, fig. 2) and poses the same question that will be explored more fully below.

Marine $\delta^{13}C$ (calcite) record

Stratigraphical correlation between marine Cenomanian–Turonian sections around the world was frequently based on variations in the $\delta^{13}C$ (bulk calcite) curves with more or less use of biostratigraphy. This chemostratigraphical confidence reached a climax with the publication by Jarvis *et al* (2006) suggesting that a $\delta^{13}C$ (calcite) reference curve based upon bulk samples from the Upper Cretaceous Chalk of England can be used as a primary criterion for trans-continental correlation. It was used by Takashima *et al.* (2010) to establish a new biostratigraphical scheme linking the planktonic foraminiferal assemblages of the proto-Pacific region (Yezo Group, Japan) with those of the Upper Cenomanian to Lower Turonian assemblages of Europe. Unfortunately the standard European $\delta^{13}C$ (calcite) curve at Eastbourne (Paul *et al*. 1999) as well as the English Chalk has been relatively little investigated as to either (1) the range of variation related to changes in the dominant fossil material (coccolith, calcisphere, shell fragment) that made up the original sediment although this had been done at the Dover sequence (Jeans *et al.* 1991), or (2) the post-depositional effects of the calcite cement that is extensive at least in certain parts of the Chalk. Reasonable matches between the Cenomanian–Turonian $\delta^{13}C$ (calcite) curve from Eastbourne (Paul *et al.* 1999) and other sequences around the proto-North Atlantic Ocean, in the Western Tethys, and in the Western Interior Sea, USA must have seemed acceptable at the time in spite of evidence of diagenetic effects at Eastbourne discussed by Paul *et al.* (1999). In places where the biostratigraphy was inadequate there was the chemostratigraphy, if both failed there was diagenesis or an incomplete sedi-

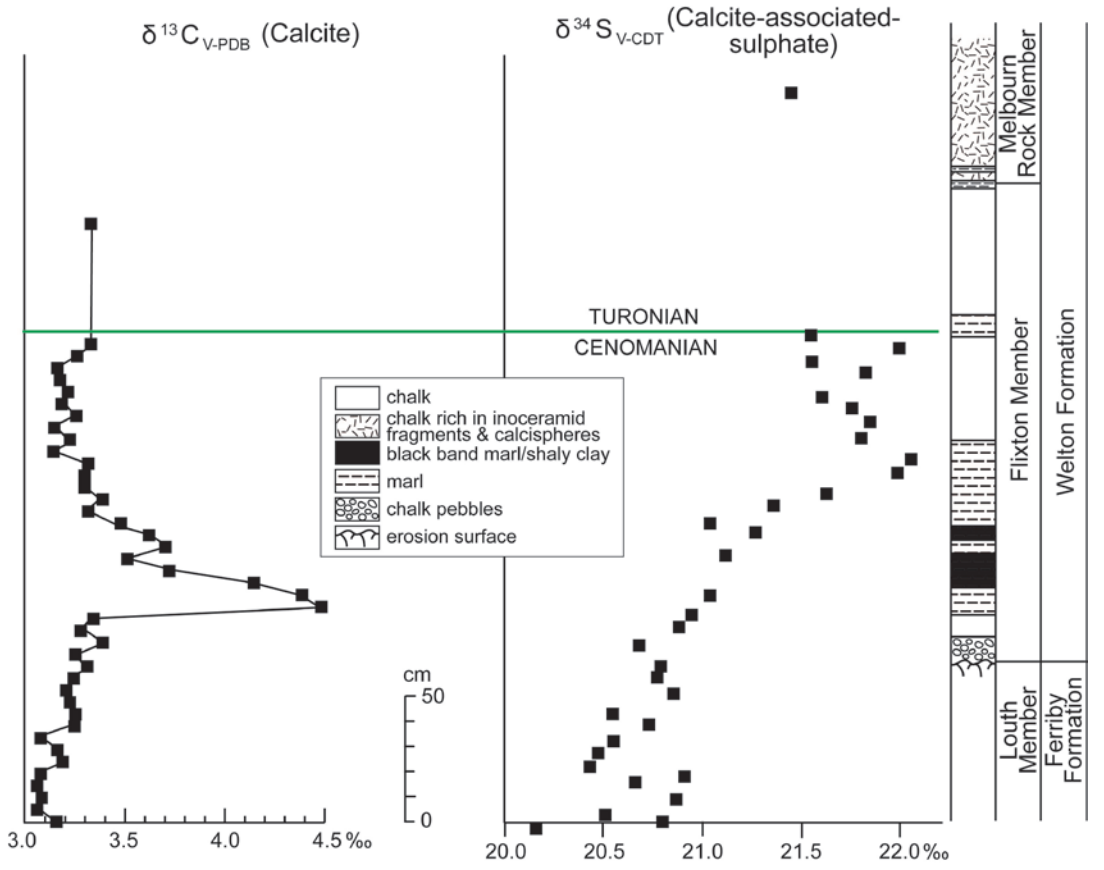

Text-fig. 18. The standard black band sequence at South Ferriby, Lincolnshire showing the d^{13}C (calcite) and the $^{34}S/^{32}S$ (CAS) data from Owen *et al*. (2013) replotted against the lithological log of Jeans *et al*. (1991, fig.10) and the position of the Cenomanian-Turonian boundary. The chalk units in both the Louth and Flixton Members display a wide scattering of $^{34}S/^{32}S$ (CAS) values compared to the marl unit in which the black bands occur.

mentary record to blame, or the inadequacies could just be overlooked. However the general assumption that the $\delta^{13}C$ (calcite) Excursion, based on bulk samples, with its various stages (first and second "build-ups" and the intervening "trough", "plateau", "decay") were essentially immune to diagenetic effects seem to have been derived ultimately from the widely read article by Hudson (1977, p. 649) that suggested diagenesis played little or no role in modifying the $\delta^{13}C$ (calcite) value of the original chalk sediment. Hu *et al.* (2012) demonstrated that this was wrong and Jeans *et al.* (2012) showed that the $\delta^{13}C$ values of calcite cements in the Chalk could range from +3 to -10‰ depending on the oxic or anoxic conditions of the pore waters at the time of precipitation. Such cements can modifiy the $\delta^{13}C$ (calcite) values of the bulk rock, it can reduce or hide even the most pronounced $\delta^{13}C$ (calcite) excursion, and it can cause false excursions. The diagenetic effect is seen in Text-fig. 19 that shows the $\delta^{13}C$ (calcite), δO^{18} (calcite) and the $\delta^{13}C_{org}$ values from a series of closely spaced chalk samples with an average bulk specific gravity of 1.75 from the *Offaster pilula* Zone at Peacehaven Steps, Sussex (Jeans *et al*. 2012, text-figs 14, 15, tables 7, 8, 9). An estimated 5% of their volume has been occupied by an anoxic cement with a $\delta^{13}C$ (calcite) value of ~ -10‰ and a $\delta^{18}O$ (calcite) value of ~ -6‰. The very distinctive parallel variation in the isotopic values from the bulk chalk is characteristic of the major effect of anoxic cements, and these show little correlation with variation in the $\delta^{13}C$ (organic carbon) values from the same samples. These difficulties combined with the limitations imposed by endemic marine faunas and floras have hindered correlation between the proto-North Atlantic and the proto-Pacific regions and the testing of the hypothesis that the CTAE and the CTOAE were global events.

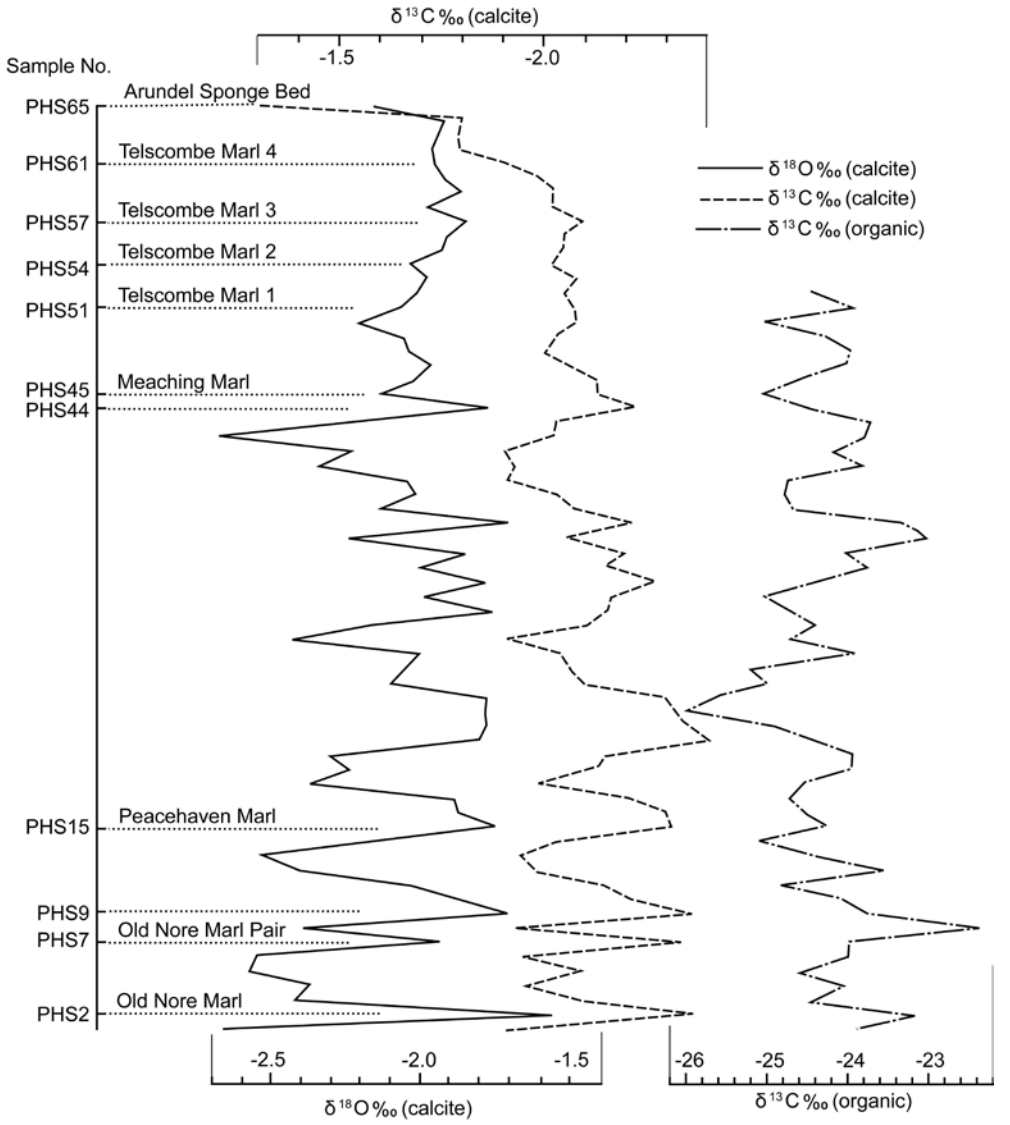

Text-fig. 19. The stable isotope curves for bulk calcite ($\delta^{18}O$, $\delta^{13}C$) and organic carbonaceous matter ($\delta^{13}C_{org.}$) from 65 samples collected at 25 cm intervals through the early Campanian section (*Offaster pilula* Zone), Newhaven Chalk Formation at Peacehaven Steps, Sussex, England. The parallel trend in the $\delta^{18}O$ and $\delta^{13}C$ curves result from the presence of a small amount of an anoxic calcite cement. There is little or no correlation with the $\delta^{13}C_{org.}$ values of the organic matter (data from Jeans *et al*. 2012).

GLOBAL CORRELATION AND THE TIMING OF THE CENOMANIAN–TURONIAN ANOXIC EVENT

Of particular importance for establishing the global extent and duration of the CTOAE and the CTAE is correlation between the proto-North Atlantic region where the sediments are conspicuous by their high content of organic carbon (e.g. Van Helmond *et al*. 2014) and the Cenomanian–Turonian sequences of the proto-Pacific region in which organic rich black shales are rarer and there is evidence that bottom waters and sediments were oxic, other than at a few limited levels when they developed anoxia with the formation of pyrite (e.g. Takashima *et al.* 2011). The proto-Pacific record is based upon stratigraphical and $\delta^{13}C$ investigations of the terrestrial organic matter in the marine Upper Cretaceous part of the Yezo Group, Oyubari and Obira areas, Hokkaido, Japan. It has been undertaken by, among others, Hasegawa (1997, 2003), Hasegawa *et al.* (2010), Uromato *et al.* (2009), Nemoto and Hasegawa (2011) and Takashima

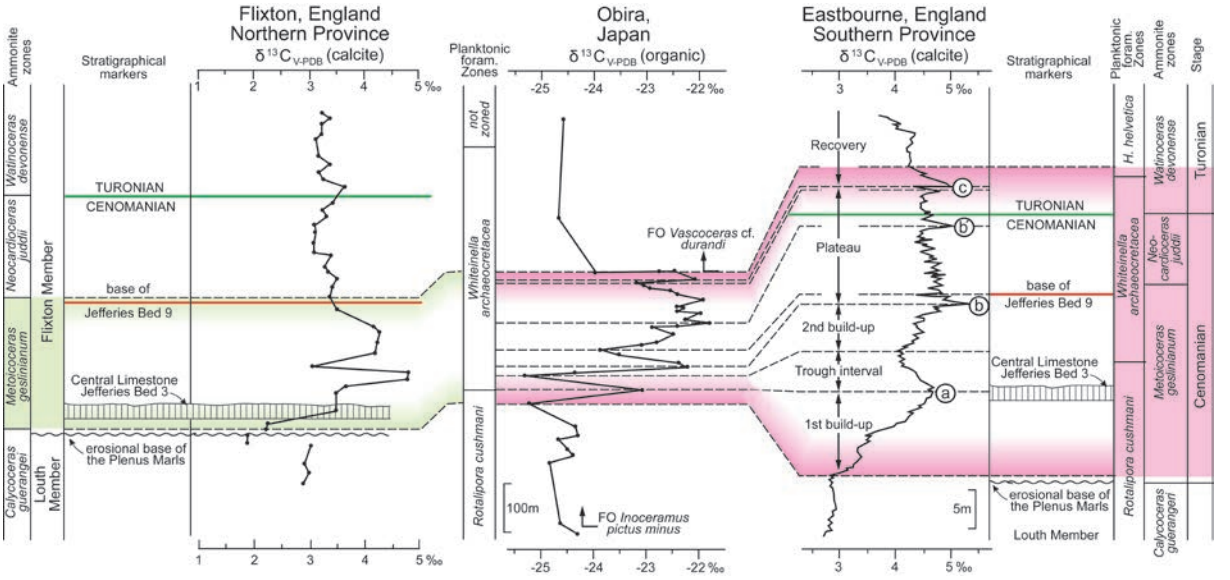

Text-fig. 20. Correlation (red shaded) based on Uramoto *et al.* (2009, fig. 9) between the $\delta^{13}C_{org}$ curve from the Cenomanian–Turonian siliciclastic sequence of Obira, Japan, and the $\delta^{13}C$(calcite) curve of Eastbourne, England using foraminifera zonation and curve matching. The upper limit of the CTOAE is within the *Whiteinella archaeocretacea* Zone at Obira whereas at Eastbourne it is at a higher stratigraphical level within the *Helvetoglobotruncana helvetica* Zone. Revised (green shaded) correlation between Obura and Flixton, England, based on nannofossil and foraminifera zonation suggests that the CTAE as recorded at Obira came to an end at the top of the *Metoicoceras geslinianum* Zone. The Flixton section is not drawn to scale, its total thickness is ~4.5 metres: the first five $\delta^{13}C$ (calcite) values in the main part of the Louth Member are from Speeton.

et al. (2009, 2011). The organic matter is considered to represent the terrestrial vegetation in the hinterland of the NE Asian region and the variations in the $\delta^{13}C$ of its kerogen are taken to reflect changes in the isotopic composition of the atmospheric carbon dioxide. It suffers relatively little from diagenetic effects (Gröcke 1998, Gröcke *et al*. 2005) and the extent of its thermal alteration can be established by its spore colour index, vitrinite reflectance and Rock-Eval pyrolysis (e.g. Collins 1990, Cornford 1998). There are two problems that are difficult to avoid particularly if the strata such as those in the Yezo Group are derived from an extensive region of varied vegetation and these result in a noisy $\delta^{13}C$ record (Takashima *et al*. 2009, 2011). First, older wood or plant debris grown in an atmosphere with different $\delta^{13}C$ characteristics are likely to be mixed with varying amounts of penecontemporaneous material, and second, the penecontemporaneous plant material may represent a number of different species with varying $\delta^{13}C$ characteristics.

The $\delta^{13}C_{org}$ Excursion for the Cenomanian–Turonian sequence in the Obira region of Hokkaido displays values of $\delta^{13}C$ ranging from -25.3 to -21.8‰ (Text-fig. 20) within a stratigraphical framework based on various marker macrofossils as well as on European foraminiferal assemblages (*Rotalipora cushmani*, *Whiteinella archaeocretacea*, *Helvetoglobotruncana helvetica*) that are not well represented in the proto-Pacific region. Uramoto *et al*. (2009) attempted chemostratigraphical correlation with the European standard $\delta^{13}C$ (calcite) curve at Eastbourne not realising that this is, at the best, a record of a marine oceanic signal with unknown limitations related to diagenetic processes. Particular emphasis was placed on the matching of peaks within the "second build-up" and the "plateau region' at Eastbourne (Paul *et al*. 1999, fig.4) with peaks in the Hokkaido $\delta^{13}C$ (organic carbon) curve. However, the "plateau region" at Eastbourne is developed in well-cemented chalks with a bulk specific gravity of ~2.13 (Mortimore and Pomerol 1998, fig. 5) suggesting that approximately 20% by volume of the chalk is cement. These chalks contain iron sulphides or their oxidation residues suggesting that anoxic cements are present – to confirm this more detailed investigation would have to be undertaken. The general level of the "plateau" is at about 4.85‰ showing a slight decrease up section; the "plateau" is subdivided by three peaks, one at ~5.3‰ and two at~5‰. The lowest values of ~ 4.0‰ reported for this zone is in Gale *et al.* (2005, fig. 17).

This sequence of cemented chalks displays clear correlation between the $\delta^{13}C$ (calcite) values of the chalk beds and the marl seams (Paul *et al.* 1999; Jeans *et al.* 2012, Text-fig. 11), with the latter showing consistently higher values. These relationships suggest that most of the "plateau region" has been modified by anoxic cements from perhaps an original plateau at ≥5‰ to values as low as 4‰. If the three present peaks are the result of diagenesis they have no place in stratigraphical correlation. The presence of iron sulphides throughout the Cenomanian–Turonian succession at Eastbourne could suggest that other parts of the $\delta^{13}C$ (calcite) curve may contain a considerable diagenetic signal bearing in mind that only a small proportion of anoxic cement can have a major effect (Text-fig. 19).

When this Hokkaido sequence is compared biostratigraphically to Eastbourne using the European foraminiferal zonal scheme (Uramoto *et al*. 2009, figs 6, 7: Text-fig. 20) there is a good match between the beginning of the $\delta^{13}C$ Excursion at both locations near the top of the *Rotalipora cushmani* Zone (equivalent to the top of the *Calycoceras guerangei* Zone), whereas the upper limit of the zone of positive $\delta^{13}C_{org}$ anomalies at Obira is in the middle of the *Whiteinella archeocretacea* Zone and this approximates to the basal part of the *Neocardioceras juddii* Zone. This is the level at which the "plateau", the main part of the $\delta^{13}C$ (calcite) Excursion at Eastbourne, is just getting under way (Text-fig. 20). Such a correlation is similar to our findings when the Northern Province's $\delta^{13}C$ (calcite) record is compared to Eastbourne (Text-fig. 20). Uramoto *et al*. (2009, fig. 7) also attempted peak matching with the 3 peaks (b, b^1, c) in the "plateau region", the likely limitations of which have already been discussed. This seems to have resulted in a forced matching and cross correlation with the end of the Obira $\delta^{13}C$ (organic carbon) curve representing the continental atmospheric $\delta^{13}C$ Excursion (mid-*Whiteinella archeocretacea* Zone) being linked to a horizon in the lower part of the overlying *Helvetoglobotruncana helvetica* Zone at Eastbourne (Uramoto *et al*. 2009, fig.7) and not, as we consider more likely, to the mid-*Whiteinella archeocretacea* Zone (Text-fig. 20). More recently Takashima *et al*. (2015) have identified the five phases of the CTOAE curve from Eastbourne (Paul *et al*. 1999) in the Kotanbetsu section and the Great Valley Sequence of California, comparing them to the Cenomanian–Turonian sequence in the Vocontian Basin in France. Their $\delta^{13}C$ (wood) record from the Kotanbetsu section, although detailed, is noisy with values varying widely throughout suggesting that this reflects the problem of mixed assemblages of plant/woody matter discussed above. We consider the identification of the "first build-up", "trough", "second build-up", "plateau" and "recovery" in the proto-Pacific region as being only tentative at the best. The study by Du Vivier *et al.* (2015a) of the pattern of $^{188}Os/^{187}Os_{(org.)}$ in the penecontemporaneous marine organic matter at two proto-Pacific localities – the Yezo Group at Hokkaido Japan and the Great Valley Sequence, California using stratigraphical frameworks based on radiometric dates from volcanic ash bands and palaeontological markers – indicates that the CTAE did not extend beyond the Cenomanian–Turonian boundary. The upper limit of the CTAE in the Yezo Group was placed some ~15 metres below the palaeontological Cenomanian–Turonian stage boundary and some 60 metres below the boundary in the Great Valley Sequence. These results and our reinterpretation of the original correlation by Uramoto et al. (2009) between the proto-Pacific region and Eastbourne adds evidence to our findings in the Northern Chalk Province in England that the CTAE with its global isotopic linkage between the continental and oceanic regions had been broken before the end of the Cenomanian. It is also a likely explanation of the short temporal records for the CTOAE at a number of locations in Europe (e.g. Central Poland, Peryt and Wyrwicka 1993; Czeck Republic, Uličný *et al.* 1997; Eastern Switzerland, Wohlwend *et al*. 2015). It also justifies the need for differentiating between the CTAE and the CTOAE and the introduction of the new term (CTOAER) to deal with the variable time period needed for the $\delta^{13}C$ values of the World's oceans and marginal seas to return to normal values. A related conclusion was drawn by Tsikos *et al.* (2004) when they considered the stratigraphical limitations of the CTOAE $\delta^{13}C$ Excursion as a means of chemostratigraphy at four locations (Pueblo, USA; Eastbourne, England; Gubbio, Italy; Tarfaya, Morocco) in the proto-Atlantic and Tethyan regions each with fairly similar excursions. In each they recognised an isotopic plateau ("plateau region" of Paul *et al*. 1999) but the "*Recognition of an unambiguous return to background δC^{13} values above the Plateau is, however, contentious in all sections, hence no firm chemostratigraphic marker for the end-point can be established … This Oceanic Anoxic Event* [CTOAE] *is demonstrated to be largely, if not wholly, confined to the latest part of the Cenomanian stage*." Now that the Cenomanian–Turonian sequences of the Northern Chalk Province in England suggest that the local CTOAE came to an end at the top of the *Metoicoceras geslinianum* Zone well before the end of the Cenomanian, the CTAE is restricted to even

a shorter time frame of perhaps 0.25Ma with the CTOAER lasting for up to another 0.25Ma.

CONTINENTAL ICE SHEETS AND SEA ICE

A major transgression of the seas in the proto-North Atlantic area has always been the backbone of the CTOAE hypothesis since it was put forward by Schlanger *et al.* (1987) and Arthur *et al.* (1987). More recently, Wilmsen *et al*. (2010a). Richardt *et al*. (2013) and Janetschke *et al.* (2015) have emphasised the extent and speed of this transgression associated with *Praeactinocamax plenus* and its associated pulse fauna in northern Europe. The same transgression is known throughout Europe, parts of North America, northern Africa and the Middle East. In Europe it is one of a number of short-termed eustatic changes of sea level that occurred during Cenomanian and Turonian times, some of which are of world-wide extent (see *Stratigraphic setting*). However little attention has been given to the cause of the equally extensive regression that immediately preceded it or to the similar regressions/transgression cycles that had been occurring at intervals of about 1.25 Ma since the beginning of the Cenomanian. Our estimate of the drop of sea level associated with the pre-CTOAE transgression is of the order of 43–86 metre (see *Stratigraphical setting*). The simplest explanation is that these cycles reflect the waxing and waning of polar ice sheets. Although suggested by a number of researchers (Bornemann *et al*. 2008: Galeotti *et al.* 2009) such an explanation is not favoured because there is evidence of exceptionally high sea-surface temperatures (35–38ºC) in the equatorial and tropical areas of the proto-North Atlantic ocean during the Upper Cretaceous (e.g. Wilson *et al*. 2002; Bice *et al.* 2003, 2006; Van Helmond *et al*. 2014) although temperatures in the marginal temperate and subtropical regions of the Chalk Sea, judging by $\delta^{18}O$ values of unaltered brachiopods, were in the order of 19–25ºC (Voigt *et al*. 2003). An alternative cause of the cycles could be some poorly understood process such as aquifer-eustacy (Wagreich *et al.* 2014). There is however evidence that during the Cretaceous there was (1) glaciation in the Antarctic and (2) local sea ice in the western part of the European Chalk Sea in late Cenomanian and early Turonian times. This was part of the evidence put forward by Jeans *et al*. (1991) in support of the glacial control hypothesis and the role of glacio-eustasy in the development of the CTOAE. General evidence for the presence of Antartic glaciation is discussed below, whereas that for sea ice during the deposition of the late Cenomanian and early Turonian chalks of southern England is discussed in an accompanying paper (Jeans and Platten 2021).

Continental ice sheets

The presence and extent of ice sheets during the Cretaceous is a contentious subject. There is doubt whether they existed or not, let alone to have been of sufficient extent to cause the rapid variations in ocean levels (see *Stratigraphical setting*). It is important to consider what evidence there is for major ice development in the Cretaceous. The possible presence of glacio-eustacy in the Cretaceous has been discussed *in vitro* extensively in the late 1990's and the early 2000's (Sahagian *et al.,* 1996; Miller *et al.,* 1999, 2003, 2004; Kominz *et al.,* 2008; Browning *et al.,* 2008). Recent modelling (Flögel *et al.,* 2011) using an Atmospheric General Circulation Model suggested that under certain conditions large volumes of snow might accumulate even under Late Cretaceous greenhouse conditions with the possible build-up of an Antarctic ice sheet large enough to drive sea level fluctuations in the order of tens of metres within ~20,000 years.

There are two regions where the possibility of Cretaceous continental ice sheets have been considered, Australia and, very recently, southeastern Beringia.

Australia is the continent where the battle has been particularly fought on the geological evidence between those who do not accept the likelihood of an ice-free earth during the Cretaceous and those who claim that either there is no definitive evidence in support of ice sheets or, if present, there were none of sufficient size to be responsible for the eustatic changes in sea level postulated by stratigraphers. In the Cretaceous sediments particularly of New South Wales and South Australia there are abundant erratics of sedimentary, metamorphic and igneous rocks some up to 3 metres in diameter – some can be matched with rock types from the late Pre-Cambrian Adelaide System or from the Gawler Range some 200–300 miles (320–480 km) to the south west (David and Browne 1950). There are records of glendonites (De Lurio and Frakes 1999) and a tillite (Alley and Frakes 2003). Although most of the evidence for glacial debris in Australia is concentrated within Lower Cretaceous strata it still persists well into the more distal facies of the Upper Cretaceous as suggested by the erratics present within museum collections of Upper Cretaceous fossils (the late R.M. Carter pers. comm.) and erratic blocks of greensand in the

Santonian Gingin Chalk at Gin Gin, Queensland (K. McNamara, pers. comm.). The non-marine Winton sedimentary series of Cenomanian–Turonian age contains abundant erratics of sedimentary, metamorphic and igneous rocks, some up to 1.7 m in maximum dimension (Woolnough and David 1926). In the Ergomanga Basin within the Great Australian Basin, Morgan (in Hawkes and Cramsie 1984, p. 157) has suggested that the deposition of the Winton Series continued into the Turonian based on palynological data from six fully cored boreholes. The significance of the erratics was recognised by the early surveyors at the end of the 19th and the very beginning of the 20th century long before Wegener's ideas of continental drift were published in 1915 and even longer before palaeomagnetic measurements indicated that these areas were at a palaeolatitude of 60 to 70 degrees south during the early and mid-Cretaceous times (Embleton 1984) – the equivalent of being close to or within the present Antarctic Circle. More recently Frakes and Francis (1988) and Francis and Frakes (1993) have reviewed the evidence from the viewpoint of those most familiar both with the Australian Cretaceous and the Antarctic. The alternative interpretation, developed and reviewed by Markwick and Rowley (1998), manages to cast doubt on all aspects of the case for the proximity of major glaciers and ice sheets. However, this has been achieved by utilising evidence from many parts of the world and from sedimentary sequences ranging in age from the Triassic to the Recent. Such an approach means that all shortcomings of many investigations are heaped upon the Australian case that seems, at least to us, fairly well established although not proved.

Evidence for the possibility of Cretaceous glaciation in Beringia – the regions of Siberia, Alaska and the Yukon in proximity to the Bering Strait – has been discussed recently by Savidge (2020). A remote and inaccessible region in southeastern Beringia between the Klondike Plateau and the Yukon-Tanana highlands of Yukon and Alaska has a particular topography with low elevation ridges that differentiated it from the rest of northwest America. The current interpretation is that it is an "unglaciated" region representing glaciated alpine locales and periglacial areas in the context of localized Pliocene–Pleistocene montane ice caps, alpine glaciers, and periglacial changes. However, Savidge (2020) considers these low elevation ridges to be relict arête/cirque remnants. He recognizes subalpine glacial grooving and mountaintop planing as well as a conglomeratic red bed containing erratic clasts. All indications point to this "unglaciated" region having been glaciated before the late Pliocene. It is suggested that in addition to Pliocene–Pleistocene glaciations, a northeastward advancing Miocene ice sheet seems plausible and, on the basis of palaeographic considerations and lithology, a Cretaceous glaciation is also not out of the question.

CONCLUDING DISCUSSION

CTOAE, CTAE and CTOAER

Our suggestion is that the CTOAE (or OAE 2) and the CTAE are records of two different aspects of a period some 94 Ma years ago that affected the $\delta^{13}C$ values of the organic matter and skeletons of plants and organisms that lived on the continents and in the oceans and their marginal seas. It was caused by the excessive production and burial of organic matter enriched in C^{12} in the proto-North Atlantic Ocean and probably, to a lesser extent in the proto-Pacific Ocean. This enhancement of the C^{13}/C^{12} ratio occurred both in the carbon dioxide in the atmosphere and in the bicarbonate of the oceans and seas. Evidence based on biostratigraphy, chemostratigraphy and radiometric dating of volcanic ash bands suggests that this linkage of the atmospheric and marine values of $\delta^{13}C$ started geologically simultaneously at the beginning of the *geslinianum* Zone, perhaps some ~94.4 Ma years ago. The linkage continued to the end of this zone perhaps representing 0.25 Ma. After that the $\delta^{13}C$ composition of the atmospheric carbon dioxide was unlinked from the marine system and rapidly returned to background values. In contrast the oceanic C^{13}/C^{12} ratios returned at variable rates to background values as a consequence of different and often sluggish circulation in the oceans and the recycling of enhanced C^{13} enriched organic matter within the marine environment. For example in the Northern Chalk Province of England the marine values of $\delta^{13}C$ returned to normal at the end of the *geslinianum* Zone whereas in the Southern Chalk Province this only happened well within the *devonense* Zone some ~ 0.60 Ma years later.

Three terms are needed to clarify this situation; (1) CTOAE – the Cenomanian–Turonian Oceanic Anoxic Event – to describe the marine record of the $\delta^{13}C$ Excursion including both the period when it was linked to the atmosphere as well as the variable period it took for the values to return to background, (2) CTAE – the Cenomanian–Turonian Anoxic Event – to describe the period when the marine and continental values of $\delta^{13}C$ were linked, and (3) CTOAER – the Cenomanian–Turonian Oceanic Anoxic Event Recovery – the time it took the $\delta^{13}C$ Excursion in

an area of the oceans or of their marginal seas to return to background values. Often associated with the CTAE are marine black bands, but their development continued not only to the end of the CTOAE but even beyond it after the $\delta^{13}C$ (calcite) Excursion had returned to background levels. For example at Flixton, Black Band F occurs at the Turonian–Cenomanian boundary (Text-fig. 14) with a $\delta^{13}C$ (calcite) value just hovering about the cut-off value (3.5‰) for the CTAE approximately 0.25 Ma after the CTOAE had come to an end. In the Wunstdorf borehole, northern Germany, not only did the $\delta^{13}C$ (calcite) Excursion of the CTOAE continued on until the lower part of the *Watinoceras devonense* Zone but black shale formation went on beyond this into the upper part of this zone (Voigt *et al*. 2008, fig.2).

Reconstructing paleoredox conditions in the Chalk Sea

The use of the cerium anomaly method (German and Elderfield 1990: Jeans *et al.* 2015; Liu *et al*. 2019) has proved successful in reconstructing the average palaeoredox conditions in the Chalk Sea during the CTOAE. This is independent of using the variations in the fossil floras and faunas associated with this event. It has allowed the separation of the palaeoredox conditions of the Chalk Sea from that of its sediment. In the three sequences – Flixton, Melton Ross and Dover – the consistency of the mineralogy and chemistry of the acid insoluble residue and its independence of variations in the two Ce anomalies is the basis of our interpretation. However this approach should not be applied to strata unless their mineralogy, chemistry and diagenesis have been thoroughly explored. In spite of our experience in this study and the previous field testing of the method on the Chalk (Jeans *et al.* 2015) it should not be assumed that variations in the REE composition of the Chalk's acid insoluble residues are so constant or their abundance is so low that they do not contribute to the pattern of variation recorded in the early diagenetic carbonate-fluorapatite. It would be unfortunate if its widespread use without such testing should mislead researchers in the manner that has occurred with $\delta^{13}C$ (calcite) and $^{34}S/^{32}S$ (CAS) and possibly other isotopic systems when applied to sedimentary rocks.

Source of the high concentration of atmospheric carbon dioxide during the CTAE

There is general agreement that a particularly high concentration of carbon dioxide in the global atmosphere was necessary to develop the linkage between the enhanced $\delta^{13}C$ values in the plants and organisms living on the continents and in the oceans. Estimates of the concentration of atmospheric carbon dioxide during this period range up to $\sim 500^{+400}/_{-180}$ ppm against a normal background of $370^{+100}/_{-70}$ ppm (Barclay *et al*. 2010). There is geochemical evidence that the CTAE was associated with enhanced rates of sea floor formation, volcanicity, and large igneous provinces (Black and Gibson 2019). A marked change in the $^{87}Sr/^{86}Sr$ ratio just prior to the initiation of the CTAE in southern Apennines, Italy, has been interpreted by Frijia and Parente (2008) as an increase in sea floor spreading associated with enhanced igneous activity and the release of radiogenic ^{87}Sr. Coinciding with the initiation of the CTOAE in Italy (Bonarelli Horizon) are parallel changes in the lead isotope composition of its silicate fraction towards values characteristic of contemporaneous flood basalts from the Caribbean and Madagascan large igneous provinces. This led Kuroda *et al.* (2007) to suggest that massive subaerial volcanism was responsible for the CTAE and its associated features with the release of huge amounts of carbon dioxide and particulate material into the atmosphere triggering significant climatic changes, inducing biotic crises and oceanic anoxia. More recently attention has been centred on the Caribbean Large Igneous Intrusion with its initial "improved" radiometric age of 94.58 Ma very close or similar to the "improved" radiometric age (datum A in Du Vivier *et al.* 2014 fig. 3) for the initiation of the "first build-up" phase of the $\delta^{13}C$ Excursion in the Cenomanian–Turonian sequence of the Western Interior Sea, Pueblo, USA. Previously the Caribbean intrusion has been linked to the relatively high concentrations of a range of trace metals in the upper part of this sequence (Snow *et al*. 2005). These may be related to the enhanced chromium contents reported from the Plenus Marls of the Southern Chalk Province, England (Pearce *et al.* 2009, fig.4) which are also known from unpublished analyses to be present at Flixton in the Northern Chalk Province up to the Cenomanian–Turonian boundary, but they are absent from the Wunstdorf sequence in northern Germany (Hetzel *et al*. 2011). Independent evidence of an age link with the Caribbean Large Igneous Province is the marked change from radiogenic to non-radiogenic osmium within the marine organic carbon fractions extracted from stratigraphically well-defined Cenomanian–Turonian marine sequences both in the ocean basins as well as onshore (Turgeon and Creaser 2008; Du Vivier *et al*. 2014, 2015a). The change from radiogenic to non-radio-

genic osmium takes place at or very close to the start of the CTOAE and the return to radiogenic osmium starts somewhat before the Cenomanian–Turonian boundary at locations in the proto-North Atlantic and proto-Pacific basins. There is also the suggestion that a large igneous province in northern Greenland (Tegner *et al*. 2011) of the same approximate age may have also been active at the time.

Triggering mechanism leading to the CTOAE

The association between the development of the CTOAE in Europe and one of the short-lived marine regression/transgression cycles, well known from the Cenomanian and Turonian sequences in North America, Europe, north Africa, and the Middle East (see *Stratgraphical setting*) is no coincidence. This suggests that the early stages of Cycle VII (Text-fig. 2) could have been the trigger mechanism that set off the cascade of processes in an atmosphere highly charged with carbon dioxide that ended up changing and linking the isotopic composition of the carbon dioxide in the atmosphere with that in the oceans (as bicarbonate ion). When viewed from the proto-Atlantic, Tethyan, north African and Middle East regions this initially involved a marked drop of sea level in the order of perhaps 43–86 metres. This would have restricted even further those areas of the oceans with limited circulation as was suggested in Jeans *et al.* (1991). A sea level recovery followed with a major transgression over areas exposed by the regression and beyond as well as resulting in the general deepening of the marginal seas and oceans. The $^{18}O/^{16}O$ record of bulk chalk samples above and below of the erosional contact between the base of the Plenus Marls and the underlying Ferriby Formation at Dover or the Grey Chalk at Eastbourne (Text-fig. 9: Paul *et al.* 1991 fig. 4) – that is the start of the positive part of the cycle – suggests a modest drop in sea water temperature recorded in the initial sediments (Bed 1) of the Plenus Marls. The nature of this transition in continuous sequences has been little explored. However in the Cenomanian–Turonian sequence in Hokkaido, Japan, just before the level at which the $\delta^{13}C$ Excursion begins there is a marked negative spike that Takashima *et al* (2011) suggest could be caused by a change in the global terrestrial climate or hydrological cycle including a massive input of carbon dioxide into the atmosphere. We suggest that it is comparable to the marked reduction in atmospheric carbon dioxide such has been intimated by Barclay *et al*. (2010) for the Plenus Cold Event, and that it may reflect the cooling associated with the 43–86 metres drop in sea level indicated for the Atlantic, Tethyan, North African, and Middle Eastern regions (see *Stratigraphical setting*). In the Wunstdorf borehole (Voigt *et al*. 2008, fig. 2) in northern Germany the pre-Plenus sequence displays a zone of low but variable values of $\delta^{13}C$ (calcite) down to ~ 2‰. Is this a diagenetic effect or does it reflect the drawdown of atmospheric carbon dioxide related to the same cooling we have proposed for the Hokkaido record?

Glacial associations

What remains of the glacio-eustatic hypothesis for the CTOAE? Our review of the Australian evidence leaves us in little doubt that there were glaciers and ice sheets and as these advanced and retreated they carried with them boulders and tree trunks as is so typical today when they impinge upon their marginal vegetated areas. Whether these ice sheets and glaciers were of sufficient dimension to cause the sea-level fluctuation is another matter. Recent modelling by Flögel *et al.* (2011) using an Atmospheric General Circulation Model suggested that under certain conditions large volumes of snow might accumulate even under Late Cretaceous greenhouse conditions with the possible build-up of an Antarctic ice sheet large enough to drive sea level fluctuations in the order of tens of metres within ~20,000 years. The six Cenomanian–Early Turonian cycles (II–VII, Text-fig. 2) have an average duration of 1.25 Ma and could easily accommodate glaciation of such a periodicity. The Plenus Cold Event (now with its three cold phases) was a cornerstone of the glacio-eustatic hypothesis. It is still so and it has become even more important in understanding the controlling mechanisms of the $\delta^{13}C$ Excursion. Detailed analysis of the relationship between its calcite geochemistry and the stepwise extinction of various marine micro-organisms living in the Chalk Sea leaves little doubt that they are directly related in a manner similar to, but perhaps only mimicking glacial cyclicity. Evidence from the neodymium isotope (^{144}Nd /^{143}Nd) record indicate that major modifications in ocean circulation were taking place during its deposition. How does the timing of the Plenus Cold Event with its northern boreal fauna fit in the midst of a major transgression possibly of global extent? Could it mean that the cold events and their pulse fauna represents a cold phase in the Arctic Polar regions whereas the transgression reflects an ice-melt phase in Antarctica? It is now known that phases of glaciations in the Northern and Southern hemispheres are not necessarily synchro-

nous (Blunier *et al.* 1998), and that within a single region there may be considerable variations in the timing of the maximum glacial phases (Stolldorf *et al*. 2012). An alternative possibility is an out-of-phase melting of a polar ice sheet, or, as we have considered earlier it may only represent a marine cooling caused by a slowing down of the volcanic contribution of carbon dioxide to the atmosphere. Future sea surface temperatures from the "trough" period in the proto-Pacific region may provide an answer. It is clear on present evidence that glacio-eustacy may have played a major role along with the degassing of large igneous intrusions and no doubt other factors in triggering the Cenomanian–Turonian Anoxic Event.

Acknowledgements

We wish to thank the following: Liam Gallagher for allowing the use of his nannofossil zonation of the Cenomanian–Turonian Chalk of the Northern Province; Rory Mortimore for providing notes and samples from the temporary excavations carried out at Melton Ross; Markus Wilmsen for bringing us up to date on advances in the stratigraphical framework and nature of the great Upper Cretaceous marine transgression; Graham Chinner, Sarah Humbert and Ken McNamara for help with the literature on the Cretaceous sediments of Australia; Philip Gibbard and Simon Crowhurst for discussions about glacial matters; Michael Hall and James Rolfe for carrying out stable isotope analysis of chalk samples; Ron Hardy of the University of Durham for analytical help. Stephen Reed for assistance with the photography; Hugh Jenkyns for providing sampling details of the black band sequence at South Ferriby, Lincolnshire reported in Owen *et al*. (2013). Vivien Brown for her skill and patience in interpreting hand written manuscripts; Philip Stickler, Silas Tull and Xu-Fang Hu for drafting figures; Ramues Gallois, Markus Wilmsen, Ian Platten, Peter Toft, Ian Jarvis and three anomymous referees for their helpful comments and suggestions.

REFERENCES

Adams, D.D., Hurtgen, M.T. and Sageman, B.B. 2010. Volcanic triggering of a biogeochemical cascade during Oceanic Anoxic Event 2. *Nature Geoscience*, **3**, 201–204.

Alley, N.F. and Frakes, L.A. 2003. First known Cretaceous glaciation: Livingston Tillite Member of the Adna-owie Formation, South Australia. *Australian Journal of Earth Sciences*, **50**, 139–144.

Arthur, M.A., Schlanger, S.O. and Jenkyns, H.C. 1987. The Cenomanian–Turonian Oceanic Anoxic Event, II. Palaeoceanographic controls on organic-matter production and preservation. In: Brooks, J. and Fleet, A.J. (Eds), Marine Petroleum Source Rocks. *Geological Society Special Publications*, **26**, 401–420.

Arthur, M.A., Dean, W.E. and Pratt, L.M. 1988. Geochemical and climatic effects of increased marine organic carbon burial at the Cenomanian–Turonian boundary. *Nature*, **335**, 714–717.

Barclay, R.S., McElwain, J.C. and Sageman, B.B. 2010. Carbon sequestration activated by a volcanic CO_2 pulse during Oceanic Anoxic Event 2. *Nature Geoscience*, **3**, 205–208.

Bice, K.L., Huber, B.T. and Norris, R.D. 2003. Extreme polar warmth during the Cretaceous greenhouse? Paradox of the late Turonian $\delta^{18}O$ record at Deep Sea Drilling Project Site 511. *Paleoceanography*, **18**, PA1029.18.10.1029. PA000848.

Bice, K.K., Birgel, D., Meyers, P.A., Dahl, K.A., Hinrichs, K.-V. and Norris, R.D. 2006. A multiple proxy and model study of Cretaceous upper ocean temperatures and atmospheric CO_2 conditions. *Palaeoceanography*, **21**, PA2002. 21.10.1029/2005 PA001203.

Black, B.A. and Gibson, S.A. 2019. Deep carbon and the life cycle of large igneous provinces. *Elements*, **15**, 319–324.

Black, M. 1980. On Chalk, Globigerina ooze and aragonite mud. In: Jeans, C.V. and Rawson, P.F. (Eds), Andros Island, Chalk and Oceanic Oozes. *Yorkshire Geological Society Occasional Publication*, **5**, 54–85.

Blätter, C.L., Jenkyns, H.C., Reynard, L.M. and Henderson, G.M. 2011. Significant increases in global weathering during Oceanic Anoxic Events 1a and 2 indicated by calcium isotopes. *Earth and Planetary Science Letters*, **309**, 77–88.

Blumenberg, M. and Wiese, F. 2012. Imbalanced nutrients as triggers for black shale formation in a shallow shelf setting during the OAE 2 (Wunstorf, Germany). *Biogeosciences*, **9**, 4139–4153.

Blunier, T., Chappellaz, J.,Schwander, J., Dällenbach, A., Stauffer, B., Stocker, T.F., Raynaud, D., Jouzel, J., Claussen, H.B., Hammer, C.U. and Johnsen, S.J. 1998. Asynchrony of Antarctic and Greenland climate change during the last glacial period. *Nature*, **394**, 739–743.

Bornemann, A., Norris, R.D., Friedrich, O., Beckmann, B., Schouten, S., Sinninge Damsté, J.S., Vogel, J., Hofmann, P. and Wagner, T. 2008. Isotopic evidence for glaciation during the Cretaceous supergreenhouse. *Science*, **319**, 189–192.

Boyd, P.W., Jickells, T., Law, C.S., Blain, S., Boyle, E.A., Buesseler, K.O., Coale, K.H., Cullen, J.J., de Baar, H.J.W., Follows, M., Harvey, M., Lancelot, C., Levasseur, M., Owens, N.P.J., Pollard, R., Rivkin, R.B., Sarmiento, J., Schoemann, V., Smetacek, V., Takeda, S., Tsuda, A., Turner, S. and Watson, A.J. 2007. Mesoscale iron enrichment experiments 1993–2005: synthesis and future directions. *Science*, **315**, 612–617.

Bralower, T.J. 1988. Calcareous nannofossil biostratigraphy and assemblages of the Cenomanian–Turonian boundary

interval: implications for the origin and timing of oceanic anoxia. *Paleoceanography*, **3**, 275–316.

Browning, J.V., Miller, K.G., Sugarman, P.J., Kominz, M.A., McLaughlin, P.P., Kulpecz, A.A. and Feigenson, M.D. 2008. 100 Myr record of sequences, sedimentary facies and sea level change from Ocean Drilling Program onshore coreholes, U.S. Mid-Atlantic coastal plain. *Basin Research*, **20**, 227–248.

Cassar, N., Bender, M.L., Harnett, B.A., Fan, S., Maxim, W.J., Levy, H. and Tilbrook, B. 2007. The Southern Ocean biological response to aeolian iron deposition. *Science*, **317**, 1067–1070.

Collins, A.1990. The 1–10 spore colour index (SCI) scale: a universally applicable colour maturation scale, based on graded, picked palynomorphs. *Mededelingen vant Rijks Geologischen Dienst*, **45**, 39–47.

Corfield, R.M., Hall, M.A. and Brasier, M.D. 1990. Stable isotope evidence for foraminiferal habitats during the development of the Cenomanian/Turonian oceanic anoxic event. *Geology*, **18**, 175–178.

Cornford, C. 1998. Source rocks and hydrocarbons of the North Sea. In: Glennie, K.W. (Ed.), Introduction to the Petroleum Geology of the North Sea, 4th Edition, 376–462. Blackwell Scientific Publications; Oxford.

David, T.W.E. and Browne, W.R. 1950. The geology of the Commonwealth of Australia (vol. 1), 747 pp. Edward Arnold; London.

De Lurio, J.L. and Frakes, L.A. 1999. Glendonites as a palaeoenvironmental tool: implications for the early Cretaceous high latitude climates in Australia. *Geochemica et Cosmochemica Acta*, **63**, 1039–1048.

Dodsworth, P. 1996. Stratigraphy, microfossils and depositional environments of the lowermost part of the Welton Chalk Formation (late Cenomanian to early Turonian, Cretaceous) in eastern England. *Proceedings of the Yorkshire Geological Society*, **51**, 45–64.

Du Vivier, A.D.C., Selby, D., Sageman, B.B., Jarvis, I., Gröcke, D.R. and Voigt, S. 2014. Marine $^{187}Os/^{188}Os$ isotope stratigraphy reveals the interaction of volcanism and ocean circulation during Oceanic Anoxic Event 2. *Earth and Planetary Science Letters*, **389**, 23–33.

Du Vivier, A.D.C., Selby, D., Condon, D.J., Takashima, R. and Nishi, H. 2015a. Pacific $^{187}Os/^{188}Os$ isotopic chemistry and U-Pb geochronology: synchroneity of global Os isotope change across OAE 2. *Earth and Planetary Science Letters*, **428**, 204–216.

Du Vivier, A.D.C., Jacobson, A.D., Lehn, G.O., Selby, D., Hurtgen, M.T. and Sageman, B.B. 2015b. Ca isotope stratigraphy across the Cenomanian–Turonian OAE2: links between vulcanism, seawater geochemistry, and the carbonate fractionation factor. *Earth and Planetary Science Letters*, **416**, 121–131.

Embleton, B.J.J. 1984. Past global settings. Continental palaeomagmatism. In: Veevers, J.J. (Ed.), Phanerozoic earth history of Australia, 11–16, Clarendon Press; Oxford.

Ernst, G., Schmid, F. and Seibertz, E. 1983. Event-Stratigraphie im Cenoman und Turon von NW Deutschland. *Zittelina*, **10**, 531–554.

Faucher, G., Erba, E., Bottini, C. and Gambacorta, G. 2017. Calcareous nannoplankton response to the latest Cenomanian Oceanic Anoxic Event 2 perturbation. *Rivista Italiana di Paleoontologia e Stratigrafia*, **123**, 159–176.

Filippelli, G.M. 2008. The global phosphorous cycle: past, present and future. *Elements*, **4**, 89–95.

Filippelli, G.M., Latimer, J.C., Murray, R.W. and Flores, J.-A. 2007. Productivity records from the Southern Ocean and the equatorial Pacific Ocean: testing the glacial shelf-nutrient hypothesis. *Deep Sea Research II: Topical studies in Oceanography*, **54**, 2443–2452.

Flögel, S., Wallmann, K. and Kuhnt, W. 2011. Cool episodes in the Cretaceous – Exploring the effects of physical forcings on the Antarctic snow accumulation. *Earth and Planetary Science Letters*, **307**, 279–288.

Forster, A., Schouten, S., Moriya, K., Wilson, P.A. and Sinninghe Damsté, J. S. 2007. Tropical warming and intermittent cooling during the Cenomanian/Turonian Oceanic Anoxic Event (OAE 2): Sea surface temperature records from the equatorial Atlantic. *Paleoceanography*, **22**, PA1219, doi:10.1029/2006PA001349.

Frakes, L.A. and Francis, J.E. 1988. A guide to Phanerozoic cold polar climates from high-latitude ice-rafting in the Cretaceous. *Nature*, **333**, 547–549.

Francis, J.E. and Frakes, L.A. 1993. Cretaceous climates. *Sedimentology Review*, **1**, 17–30.

Frijia, G. and Parente, M. 2008. Strontium isotope stratigraphy in the upper Cenomanian shallow-water carbonates of the southern Apennines: Short-term perturbations of marine Sr-87/Sr-86 during the Oceanic Anoxic Event 2. *Palaeogeography, Palaeoclimatology, Palaeoecology*, **261**, 15–29.

Gale, A.S. and Christensen, W.K. 1996. Occurrence of the belemnite *Actinocamax plenus* in the Cenomanian of SE France and its significance. *Bulletin of the Geological Society of Denmark*, **43**, 68–77.

Gale, A.S., Hancock, J.M. and Kennedy, W.M. 1999. Biostratigraphical and sequence correlation of the Cenomanian successions in Mangyshlak (W. Kazakhstan) and Crimea (Ukraine) with those in Southern England. *Bulletin de l'Institut Royal des Sciences Naturelles de Belgique Sciences de la Terre*, **69** (Supplément A), 67–86.

Gale, A.S., Smith, A.B., Monks, N.E.A., Young, J.A., Howard, A., Wray, D.S. and Huggett, J.M. 2000. Marine biodiversity through the Late Cenomanian–Early Turonian: palaeoceanographic controls and sequence stratigraphic biases. *Journal of the Geological Society, London*, **157**, 745–757.

Gale, A.S., Kennedy, W.J., Voigt, S. and Walaszczyk, I. 2005. Stratigraphy of the Upper Cenomanian–Lower Turonian

Chalk succession at Eastbourne, Sussex, UK: ammonites, inoceramid bivalves and stable carbon isotopes. *Cretaceous Research*, **26**, 460–487.

Gale, A.S., Voigt, S., Sageman, B.B. and Kennedy, W.J. 2008. Eustatic sea-level record for the Cenomanian (Late Cretaceous) – Extension to the Western Interior Basin, USA. *Geology*, **36**, 859–862.

Galeotti, S., Rusciadelli, G., Sprovieri, M., Lanci, L., Gaudio, A. and Pekar, S. 2009. Sea-level control on facies architecture in the Cenomanian–Coniacian Apulian Margin (Western Tethys); a record of glacio-eustatic fluctuations during the Cretaceous greenhouse? *Palaeogeography, Palaeoclimatology, Palaeoecology*, **276**, 196–205.

Gaunt, G.D., Fletcher, T.P. and Wood, C.J. 1992. Geology of the country around Kingston upon Hull and Brigg. *Memoir of the British Geological Survey*, sheets 80 and 89 (England and Wales), 172 pp. HMSO; London.

German, C.R. and Elderfield, H. 1990. Application of the Ce anomaly as a paleoredox indicator: the ground rules. *Paleoceanography*, **5**, 823–833.

Giraud, F., Reboulet, S., Deconinck, J.F., Martinez, M., Carpentier, A. and Bréziat, C. 2013. The Mid-Cenomanian Event in southeastern France: evidence from palaeontological and clay mineralogical data. *Cretaceous Research*, **46**, 43–58.

Gomes, M.L., Hurtgen, M.T. and Sageman, B.B. 2016. Biogeochemical sulphur cycling during Cretaceous oceanic anoxic events: A comparison of OAE1a and OAE2. *Paleoceanography and Paleoclimatology*, **31**, 233–251.

Gröcke, D.R. 1998. Carbon-isotope analyses of fossil plant as a chemostratigraphic and palaeoenvironmental tool. *Lethaia*, **31**, 1–13.

Gröcke, D.R., Price, G.D., Robinson, S.A., Baraboshkin, E.Y., Mutterlose, J. and Ruffell, A.H. 2005. The Upper Valanginian (Early Cretaceous) positive carbon-isotope event recorded in terrestrial plants. *Earth and Planetary Science Letters*, **240**, 495–509.

Hairapetian,V., Wilmsen, M., Ahmadi, A., Shojaei, Z., Berensmeier, M. and Majidifard, M.R. 2018. Integrated stratigraphy, facies analysis and correlation of the upper Albian–lower Turonian of the Esfahan area (Iran): Unravelling the conundrum of the so-called "Glauconitic Limestone". *Cretaceous Research*, **90**, 391–411.

Hancock, J.M. 1989. Sea-level changes in the British region during the late Cretaceous. *Proceedings of the Geologists' Association*, **100**, 565–594.

Hancock, J.M. and Kauffman, E.G. 1979. The great transgressions of the Late Cretaceous. *Journal of the Geological Society, London*, **136**, 175–186.

Hart, M.B. and Leary, P.N. 1991. Stepwise mass extinctions – the case for the Late Cenomanian event. *Terra Nova*, **3**, 142–147.

Hasegawa, T. 1997. Cenomanian–Turonian carbon isotope events recorded in terrestrial organic matter from northern Japan. *Palaeogeography, Palaeoclimatology, Palaeoecology*. **130**, 2273.

Hasegawa, T. 2003. Cretaceous terrestrial paleoenvironments of northeastern Asia suggested from carbon isotope stratigraphy: increased atmospheric ρCO_2-induced climate. *Journal of Asian Earth Sciences*, **21**, 849–859.

Hasegawa, T., Seo, S., Moriya, K., Tominaga, Y., Nemoto, T. and Naruse, T. 2010. High resolution carbon isotope stratigraphy across the Cenomanian/Turonian boundary in the Tappu area, Hokkaido, Japan. *Island Arc*, **2**, 181–191.

Hasegawa, T., Crampton, J.S., Schiøler, P., Field, B., Kukushi, K. and Kakizaki, Y. 2013. Carbon isotope stratigraphy and depositional anoxia through Cenomanian/Turonian boundary sequence (Upper Cretaceous) in New Zealand. *Cretaceous Research*, **40**, 6–80.

Hawkes, J.M. and Cramsie, J.N. 1984. Contributions to the geology of the Great Australian Basin, New South Wales. *Bulletin of the Geological Survey of New South Wales*, **31**, 1–295.

Hay, W.W, 2008. Evolving ideas about the Cretaceous climate and ocean circulation. *Cretaceous Research*, **29**, 725–753.

Henderson, P. and Williams, C.T. 1981. Application of intrinsic Ge detectors to the instrumental neutron activation analysis for rare earth elements in rocks and minerals. *Journal of Radioanalytical Chemistry*, **67**, 445–452.

Hetzel, A., März, C., Vogt, C. and Brumsack, H.-J. 2011. Geochemical environment of Cenomanian–Turonian black shale deposition at Wunstorf (northern Germany). *Cretaceous Research*, **32**, 480–494.

Holmden, C., Jacobson, A.D., Sageman, B.B. and Hurtgen, M.T. 2016. Response of the Cr isotope proxy to Cretaceous Ocean Anoxic Event 2 in a pelagic carbonate succession from the Western Interior Seaway. *Geochimica et Cosmochimica Acta*, **186**, 277–295.

Hu, X.-F., Jeans, C.V. and Dickson, J.A.D. 2012. Geochemical and stable isotope patterns of calcite cementation in the Upper Cretaceous Chalk, UK: Direct evidence from calcite-filled vugs in brachiopods. *Acta Geologica Polonica*, **62**, 143–172.

Hudson, J.D. 1977. Stable isotopes and limestone lithification. *Journal of the Geological Society, London*, **133**, 637–660.

Hut, P., Alvarez, W., Elder, W.P., Hansen, T., Kauffman, E.G., Keller, G., Shoemaker, E.M. and Weissman, P.R. 1987. Comet showers as a cause of mass extinction. *Nature*, **329**, 118–126.

Janetschke, N., Niebuhr, B. and Wilmsen, M. 2015. Interregional sequence stratigraphical synthesis of the Plänerkalk, Elbtal and Danubian Cretaceous groups (Germany): Cenomanian–Turonian correlations around the Mid-European Island. *Cretaceous Research*, **56**, 530–549.

Jarvis, I., Carson, G.A., Cooper, M.K. E., Hart, M.B., Leary, P.N., Tocher, B.A., Horne, D. and Rosenfeld, A. 1988. Microfossil assemblages and the Cenomanian–Turonian

(late Cretaceous) oceanic anoxic event. *Cretaceous Research*, **9**, 3–103.

Jarvis, I., Gale, A.S., Jenkyns, H.C. and Pearce, M.A. 2006. Secular variation in late Cretaceous carbon isotopes: a new $\delta^{13}C$ carbonate reference for the Cenomanian–Campanian (99.6–70.6 Ma). *Geological Magazine*, **143**, 561–608.

Jarvis, I., Lignum, J.S., Gröcke, R., Jenkyns, H.C. and Pearce, M.A. 2011. Black shale deposition, atmospheric CO_2 drawdown, and cooling during the Cenomanian–Turonian Oceanic Anoxic Event. *Paleoceanography*, **26**, PA3201, 1–17.

Jeans, C.V. 1967. The Cenomanian Rocks of England, 156 pp. Unpublished PhD thesis, University of Cambridge; Cambridge.

Jeans, C.V. 1968. The origin of the montmorillonite of the European Chalk with special reference to the Lower Chalk of England. *Clay Minerals*, **7**, 311–329.

Jeans, C.V. 1980. Early submarine lithification in the Red Chalk and Lower Chalk of eastern England; a bacterial control model and its implications. *Proceedings of the Yorkshire Geological Society*, **43**, 81–157.

Jeans, C.V. 2006. Clay mineralogy of the Cretaceous strata of the British Isles. *Clay Minerals*, **41**, 47–150.

Jeans, C.V. and Platten, I.M. 2021. The erratic rocks of the English Chalk: how did they get there, ice transport or other means? *Acta Geologica Polonica*, doi: 10.24425/agp.2020.134555.

Jeans, C.V., Merriman, R.J., Mitchell, J.G. and Bland. D.J.1982. Volcanic clays in the Cretaceous of southern England and Northern Ireland. *Clay Minerals*, **17**, 105–156.

Jeans, C.V., Long, D., Hall, M.A., Bland, D.J. and Cornford, C. 1991. The geochemistry of the Plenus Marls at Dover, England: evidence of fluctuating oceanographic conditions and of glacial control during the development of the Cenomanian–Turonian $\delta^{13}C$ anomaly. *Geological Magazine*, **128**, 604–632.

Jeans, C.V., Wray, D.S., Merriman, R.J. and Fisher, M.J. 2000. Volcanogenic clays in Jurassic and Cretaceous strata of England and the North Sea Basin. *Clay Minerals*, **35**, 25–55.

Jeans, C.V., Mitchell, J.G., Fisher, M.J., Wray, D.S. and Hall, I.R. 2001. Age, origin and climatic signal of English Mesozoic clays based on K/Ar signatures. *Clay Minerals*, **36**, 515–539.

Jeans, C.V., Hu, X.F. and Mortimore, R.N. 2012. Calcite cements and the stratigraphical significance of the marine $\delta^{13}C$ carbonate reference curve for the Upper Cretaceous Chalk of England. *Acta Geologica Polonica*, **62**, 173–196.

Jeans, C.V., Long, D., Hu, X.-F. and Mortimore, R.N. 2014a. Regional hardening of Upper Cretaceous Chalk in eastern England, UK: trace element and stable isotope patterns in the Upper Cenomanian and Turonian Chalk and their significance. *Acta Geologica Polonica*, **64**, 419–455.

Jeans, C.V., Tosca, N.J., Boreham, S. and Hu, X.F. 2014b. Clay mineral-grain size-calcite cement relationships in Upper Cretaceous Chalk, UK: a preliminary investigation. *Clay Minerals*, **49**, 299–325.

Jeans, C.V., Wray, D.S. and Williams, C.T. 2015. Redox conditions in the Late Cretaceous Chalk Sea: the possible use of cerium anomalies as palaeoredox indicators in the Cenomanian and Turonian Chalk of England. *Acta Geologica Polonica*, **65**, 345–366.

Jeans, C.V., Turchyn, A.V. and Hu, X.-F. 2016. Sulfur isotope patterns of iron sulphide and barite nodules in the Upper Cretaceous Chalk of England and their regional significance in the origin of coloured chalks. *Acta Geologica Polonica*, **66**, 227–256.

Jefferies, R.P.S. 1961. The palaeoecology of the Actinocamax plenus Subzone (Turonian) in the Anglo-Paris Basin. *Palaeontology*, **4**, 1–33.

Jefferies, R.P.S. 1963. The stratigraphy of the Actinocamax plenus Subzone (Turonian) in the Anglo-Paris Basin. *Proceedings of the Geologists' Association*, **74**, 1–30.

Jenkyns, H.C., Matthews, A., Tsikos, H. and Erel, Y. 2007. Nitrate reduction, sulfate reduction, and sedimentary iron isotope evolution during the Cenomanian–Turonian oceanic anoxic event. *Paleoceanography*, **22**, PA3208, doi:10.1029/2006PA0011355.

Jenkyns, H.C., Dickson, A.J., Ruhl, M. and Van den Boorn, S.H.J.M. 2017. Basalt-seawater interaction, the Plenus Cold Event, enhanced weathering and geochemical change: deconstructing Oceanic Anoxic Event 2 (Cenomanian–Turonian, Late Cretaceous). *Sedimentology*, **64**, 16–43.

Jones, C.E. and Jenkyns, H.C. 2001. Seawater strontium isotopes, Oceanic Anoxic Events, and seafloor hydrothermal activity in the Jurassic and Cretaceous. *American Journal of Science*, **301**, 112–149.

Keller, G., Han, Q., Adatte, T. and Burns, S.J. 2001. Palaeoenvironment of the Cenomanian–Turonian transition at Eastbourne, England. *Cretaceous Research*, **22**, 391–422.

Kominz, M.A., Browning, J.V., Miller, K.G., Sugarman, P.J., Mizintseva, S. and Scotese, C.R. 2008. Late Cretaceous to Miocene sea-level estimates from the New Jersey and Delaware coastal plain coreholes: an error analysis. *Basin Research*, **20**, 211–226.

Koutsoukos, E.A.M., Leary, P.N. and Hart, M.B. 1990. Cenomanian–Turonian low-oxygen tolerant benthonic foraminifera: a case study from the Sergipe basin (N.E. Brazil) and the Western Anglo-Paris basin (Southern England). *Palaeogeography, Palaeoclimatology, Palaeoecology*, **77**, 145–147.

Kuroda, J., Ogawa, N.O., Tanimizu, M., Coffin, M.F., Tokuyama, H, Kitazato, H. and Ohkouchi, N. 2007. Contemporaneous massive subaerial volcanism and late Cretaceous Oceanic Anoxic Event 2. *Earth and Planetary Science Letters*, **256**, 211–223.

Lamolda, M.A., Gorostidi, A. and Paul, C.R.C. 1994. Quantita-

tive estimates of calcareous nannofossil changes across the Plenus Marls (latest Cenomanian), Dover, England – implications for the generation of the Cenomanian–Turonian boundary event. *Cretaceous Research*, **15**, 143–164.

Leckie, R.M., Bralower, T.J. and Cashman, R. 2002. Oceanic anoxic events and plankton evolution: Biotic response to tectonic forcing during the mid-Cretaceous. *Paleoceanography*, **17**, 13.1–13.29.

Markwick, P.J. and Rowley, D.B. 1998. The geological evidence for Triassic to Pleistocene glaciations: implications for eustacy. In: Pindell, J. and Drake, C.L. (Eds), Paleogeographic evolution and non-glacial eustacy: northern South America. *SEMP Special Publication*, **58**, 17–43.

Martin, J.H. 1990. Glacial-interglacial CO_2 change: the iron hypothesis. *Palaeoceanography*, **5**, 1–13.

Meyers, S.R., Siewert, S.E., Singer, B.S., Sageman, B.B., Condon, D.J., Obradovich, J.D., Jicha, B.R. and Sawyer, D.A. 2012. Intercalibration of radioisotopic and astrochronologic time scales for the Cenomanian–Turonian boundary interval, Western Interior Basin, USA. *Geology*, **40**, 7–10.

Miller, K.G., Barrera, E. and Olsson, R.K. 1999. Does ice drive early Maastrichtian eustasy? Global $\delta^{18}O$ and New Jersey sequences. *Geology*, **27**, 783–786.

Miller, K.G., Sugarman, P.J., Browning, J.V., Kominz, M.A., Hernandez, J.C., Olsson, R.K., Feigenson, M.D. and Van Sickel, W. 2003. Late Cretaceous chronology of large, rapid sea-level changes: glacioeustasy during the greenhouse world. *Geology*, **31**, 585–588.

Miller, K.G., Sugarman, P.J., Browning, J.V., Kominz, M.A., Olsson, R.K., Feigenson, M.D. and Hernandez, J.C. 2004. Upper Cretaceous sequences and sea-level history, New Jersey Coastal Plain. *Geological Society of America Bulletin*, **116**, 368–393.

Mitchell, S.F., Paul, C.R.C. and Gale, A.S. 1996. Carbon isotopes and sequence stratigraphy. In: Howell, J.A. and Aitken, J.F. (Eds), Sequence stratigraphy: innovations and application. *Geological Society, London, Special Publications*, **104**, 349–377.

Mitchell, S.F., Ball, J.M., Crowley, S.F., Marshall, J.M., Paul, C.R.C., Veltkamp, C.J. and Samir, A. 1997. Isotope data from Cretaceous chalks and foraminifera: Environmental or diagenetic signals? *Geology*, **25,** 691–694.

Montoya-Pino, C., Wyer, S,, Anbart, A.D., Pross, J., Oschmann,W., Van de Schootbrugge, B. and Arz, H.W. 2010. Global enhancement of ocean anoxia during Oceanic Anoxic Event 2: a quantitative approach using U isotopes. *Geology*, **38**, 315–318.

Mort, H.P., Adatte, T., Föllmi, K. B., Keller, G., Steinmann, P., Matera, V., Berner, Z. and Stüben, D. 2007. Phosphorus and the roles of productivity and nutrient recycling during the oceanic anoxic event 2. *Geology*, **35**, 483–486.

Mort, H.P., Adatte, T., Keller, G., Bartels, D., Föllmi, K.B., Steinmann, P., Berner, Z. and Chellai, E.H. 2008. Organic carbon deposition and phosphorus accumulation during Oceanic Anoxic Event 2 in Tarfaya, Morocco. *Cretaceous Research*, **29**, 1008–1023.

Mortimore, R.N. 1986. Controls on Upper Cretaceous sedimentation in the South Downs, with particular reference to flint distribution. In: Sieveking, G. de G. and Hart, M.B. (Eds), The scientific study of Flint and Chert, 21–42. Cambridge University Press; Cambridge.

Mortimore, R.N., Wood, C.J. and Gallois, R.W. 2001. British Upper Cretaceous Stratigraphy. *Geological Conservation Review Series*, **23**, 558 pp.

Mortimore, R.N. 2014. Logging the Chalk, 357pp. Whittles Publishing; Caithness.

Mortimore, R.N. and Pomerol, B. 1998. Basin analysis in engineering geology: Chalk of the Anglo-Paris basin. In: Moore, D. and Hungr, O. (Eds), *Proceedings eighth international congress International Association for Engineering Geology and the Environment*, 3249–3268. Balkema; Rotterdam.

Nagm, E. 2015. Stratigraphic significance of rapid faunal change across the Cenomanian–Turonian boundary in the Eastern Desert. *Cretaceous Research*, **52A**, 9–24.

Nederbragt, A.J., Thurow, J., Vonhof, H. and Brumsack, H.-J. 2004. Modelling oceanic carbon and phosphorus fluxes: implications for the cause of the late Cenomanian Oceanic Anoxic Event (OAE2). *Journal of the Geological Society, London*, **161**, 721–728.

Nemoto, T. and Hasegawa, T. 2011. Submillennial resolution carbon isotope stratigraphy across the Oceanic Anox Event 2 in the Tappu section, Hokkaido, Japan. *Palaeogeography, Palaeoclimatology, Palaeoecology*, **309**, 271–280.

Oakman, C.D. and Partington, M.A. 1998. Cretaceous. In: Glennie, K.W. (Ed.), Petroleum geology of the North Sea: basic concepts and recent advances, 294–349. Blackwell Science; Oxford.

Ogg, J.G., Hinnov, L.A. and Huang, C. 2012. Cretaceous. In: Gradstein, F.M., Ogg, J.G., Schmitz, M.D. and Ogg, G.M. (Eds), The geological time scale 2012, Vol. 1, 794–814. Elsevier; Amsterdam.

Orth, C.J., Attrep, M., Quintana, L.R., Elder, W.P., Kauffman, E.G., Diner, R. and Villamil, T. 1993. Elemental abundance anomalies in the late Cenomanian extinction interval: a search for the source(s). *Earth and Planetary Science Letters*, **117**, 189–204.

Owen, J.D., Lyons, T.W., Li, X., Macleod, K.G., Gordon, G., Kuypers, M.M.M., Anbar, A., Kuhny, W. and Severmann, S. 2012. Iron isotope and trace metal records of iron cycling in the proto-North Atlantic during the Cenomanian–Turonian oceanic anoxic event (OAE-2). *Paleoceanography*, **27**, PA3223, doi:1029/2012PA002328.

Owen, J.D., Gill, B.C., Jenkyns, H.C., Bates, S.M., Severmann, S., Kuypers, M.M.M., Woodfine. R.G. and Lyons, T.W. 2013. Sulfur isotopes track the global extent and dynamics

of euxinia during Cretaceous Oceanic Anoxic Event 2. *Proceedings of the National Academy of Sciences*, **110**, 18407–1841

Paul, C.R.C. and Mitchell, S.F. 1994. Is famine a common factor in marine mass extinctions? *Geology*, **22**, 679–682.

Paul, C.R.C., Lamolda, M.A., Mitchell, S.F., Vaziri, M.R., Gorostidi, A. and Marshall, J.D. 1999. The Cenomanian–Turonian boundary at Eastbourne (Sussex, U.K.): a proposed European reference section. *Palaeogeography, Palaeoclimatology, Palaeoecology*, **150**, 83–121.

Paul, C.R.C., Mitchell, S.F., Marshall, J.D., Leary, P.N., Gale, A.S., Duane, A.M. and Ditchfield, P.W. 1994. Palaeoceanographic events in the Middle Cenomanian of northwest Europe. *Cretaceous Research*, **15**, 707–738.

Pearce, M.A., Jarvis, I. and Tocher, B.A. 2009. The Cenomanian–Turonian boundary event, OAE2 and palaeoenvironmental change in epicontinental seas: new insights from the dinocyst and geochemical records. *Palaeogeography, Palaeoclimatology, Palaeoecology*, **280**, 207–234.

Peryt, D and Wyrwicka, K. 1993. The Cenomanian/Turonian boundary event in Central Poland. *Palaeogeography, Palaeoclimatology, Palaeoecology*, **104**, 185–197.

Pogge von Strandmann, P.A.E., Jenkyns, H.C. and Woodfine, R.G. 2013. Lithium isotope evidence for enhanced weathering during Oceanic Anoxic Event 2. *Nature Geoscience*, **6**, 668–672.

Potts, P.J. 1987. A handbook of silicate rock analysis, 622 pp. Blackie & Son Ltd.; Glasgow.

Raven, M.R., Fike, D.A., Gomes, M.L., Webb, S.M., Bradley, S. and McClelland, H.L.O. 2018. Organic carbon burial during OAE2 driven by changes in the locus of organic matter sulfurization. *Nature Communications*, **9**, 3409, https://doi.org/10.1038/s41467-018-05943-6.

Raven, M.R., Fike, D.A., Bradley, A.S., and Gomes, M.L. 2019. Paired organic matter and pyrite $\delta^{34}S$ records reveal mechanism of carbon, sulphur, and iron cycle disruption during Oceanic Anoxic Event 2. *Earth and Planetary Science Letters*, **512**, 27–38.

Richardt, N., Wilmsen, M. and Niebuhr, B. 2013. Late Cenomanian–Early Turonian facies development and sea-level changes in the Bodenwöhrer Senke (Danubian Cretaceous Group, Bavaria, Germany). *Facies*, **59**, 803–827.

Robinson, N.D. 1986. Lithostratigraphy of the Chalk Group of the North Downs, southeast England. *Proceedings of the Geologists' Association*, **97**, 141–170.

Sahagian, D., Pinous, O., Olferiev, A. and Zakharov, V. 1996. Eustatic curve for the Middle Jurassic–Cretaceous based on Russian Platform and Siberian stratigraphy: zonal resolution. *AAPG Bulletin*, **80**, 1433–1458.

Savidge, R.A. 2000. Evidence of early glaciation of southeastern Beringia. *Canadian Journal of Earth Sciences*, 57, 199–226.

Schlanger, S.O., Arthur, M.A., Jenkyns, H.C. and Scholle, P.A. 1987. The Cenomanian–Turonian Oceanic Anoxic Event, 1. Stratigraphy and distribution of organic carbon-rich beds and the marine ^{13}C excursion. In: Brooks, J. and Fleet, A.J. (Eds), Marine Petroleum Source Rocks. *Geological Society Special Publications*, **26**, 371–399.

Scott, R.W., Oboh-Ikuenobe, F.E., Beson Jr., D.G., Holbrook, J.M. and Alnahwi, A. 2018. Cenomanian–Turonian flooding cycles: U.S. Gulf Coast and Western Interior. *Cretaceous Research*, **89**, 191–210.

Sepkoski, J.J. 1989. Periodicity in extinction and the problem of catastrophism in the history of life. *Journal of the Geological Society, London*, **146**, 7–19.

Sinninghe Damste, J.S., van Bentum, E.C., Reichart, G.J., Pross, J. and Schouten, S. 2010. A CO_2 decrease-driven cooling and increased latitudinal temperature gradient during the mid-Cretaceous Oceanic Anoxic Event 2. *Earth and Planetary Science Letters*, **293**, 97–103.

Snow, L.J., Duncan, R.A. and Bralower, T.J. 2005. Trace element abundances in the Rock Canyon Anticline, Pueblo, Colorado, marine sedimentary section and their relationship to Caribbean plateau construction and oxygen anoxic event 2. *Paleoceanography*, **20**, PA3005.

Stolldorf, T., Schenke, H.-W. and Anderson, J. B. 2012. LGM ice sheet extent in the Weddell Sea: evidence for diachronous behaviour of Antarctic Ice Sheets. *Quaternary Science Reviews*, **48**, 29–31.

Takashima, R., Nishi, H., Yamanaka, T., Hayashi, K., Waseda, A., Obuse, A., Tomosugi, T., Deguchi, N. and Mochizuki, S. 2010. High-resolution terrestrial carbon isotope and planktic foraminiferal records of the Upper Cenomanian to the Lower Campanian in the Northwest Pacific. *Earth and Planetary Science Letters*, **289**, 570–582.

Takashima, R., Nishi, H., Yamanaka, T., Tomosugi, T., Fernando, A.G., Tanabe, K., Moriya, K., Kawabe, F. and Hayashi, K. 2011. Prevailing oxic environments in the Pacific Ocean during the mid-Cretaceous Oceanic Anoxic Event 2. *Nature Communications*, **2**, 234.

Tegner, C., Storey, M., Holm, P.M., Thorarinsson, S.B., Zhao, X., Lo, C.-H. and Knudsen, M.F. 2011. Magmatism and Eurekan deformation in the High Arctic Large Igneous Province: ^{40}Ar-^{39}Ar age of Kap Washington Group volcanics, North Greenland. *Earth and Planetary Science Letters*, **303**, 203–214.

Tinsley, J. 1950. The determination of organic carbon in soils by dichromate mixtures. *Transactions 4*th *International Congress of Soil Science*, **1**, 161–164.

Tsikos, H., Jenkyns, H.J., Walsworth-Bell, B., Petrizzo, M.R., Forster, A., Kolonic, S., Erba, A., Premoli Silva, I., Baas, M., Wagner, T. and Sinninghe Damsté, J.S. 2004. Carbon-isotope stratigraphy recorded by the Cenomanian–Turonian Anoxic Event: correlation and implication based on three key localities. *Journal of the Geological Society, London*, **161**, 711–719.

Turgeon, S.C. and Creaser, R.A. 2008. Cretaceous oceanic anoxic event 2 triggered by a massive magmatic episode. *Nature*, **454**, 323–326.

Ulicný, D., Hladiková, J., Attrep, M.J. Čech, S., Hradecká, L. and Svobodová, M. 1997. Sea-level changes and geochemical anomalies across the Cenomanian–Turonian boundary: Pecínov Quarry, Bohemia. *Palaeogeography, Palaeoclimatology, Palaeoecology* **132**, 265–285.

Uramoto, G.I., Abe, Y.and Hirano, H. 2009. Carbon isotope fluctuations of terrestrial organic matter for the Upper Cretaceous (Cenomanian–Santonian) in the Obira area of Hokkaido, Japan. *Geological Magazine*, **146**, 761–774.

van Helmond, N.A.G.M., Ruvalcaba, I., Sluijs, A., Sinninghe Damsté, J.S. and Slomp, C.P. 2014a. Spatial extent and degree of oxygen depletion in the deep proto-North Atlantic basin during Oceanic Anoxic Event 2. *Geochemistry, Geophysics, Geosystems*, **15**, 4254–4266.

van Helmond, N.A.G.M., Sluijs, A., Reichart, G.-J., Sinninghe Damsté, J.S., Slomp, C.P. and Brinkhuis, H. 2014b. A perturbed hydrological cycle during Oceanic Anoxic Event 2. *Geology*, **42**, 123–126.

van Helmond, N.A.G.M., Sluijs, A., Sinninghe Damsté, J.S., Reichart, G.-J., Voigt, S., Erbacher, J., Pross, J. and Brinkhuis, H. 2015. Freshwater discharge controlled deposition of Cenomanian–Turonian black shales on the NW European epicontinental shelf (Wunstorf, northern Germany). *Climates of the Past*, **11**, 495–508.

van Helmond, N.A.G.M., Sluijs, A., Papadomanolaki, N.M., Plint, A.G., Gröcke, D., Pearce, M.A., Eldrett, J.S., Trabucho-Alexandre, J., de Walaszczyk van Schootbrugge, B. and Brinkhuis, H. 2016. Equatorward phytoplankton migration during a cold spell within the Late Cretaceous super-greenhouse. *Biogeosciences*, **13**, 2859–2872.

Voigt, S., Wilmsen, M., Mortimore, R.N. and Voigt, T. 2003. Cenomanian palaeotemperatures derived from the oxygen isotopic composition of brachiopods and belemnites: evaluation of Cretaceous palaeotemperature proxies. *International Journal of Earth Sciences*, **92**, 285–299.

Voigt, S., Erbacher, J., Mutterlose, J., Weiss, W., Westerhold, T., Wiese, F., Wilmsen, M. and Wonik, T. 2008. The Cenomanian–Turonian of the Wunstorf Section (North Germany): global stratigraphic reference section and new orbital time scale of Oceanic Anoxic Event 2. *Newsletters on Stratigraphy*, **43**, 65–89.

Wagreich, M., Lein, R. and Sames, B. 2014. Eustasy, its controlling factors, and the limno-eustatic hypothesis – concepts inspired by Eduard Suess. *Austrian Journal of Earth Sciences*, **107**, 115–131.

Wang, X., Reinhard, C.T., Planavsky, N.J., Owens, J.D., Lyons, T.W. and Johnson, T.M. 2016. Sedimentary chromium isotopic compositions across the Cretaceous OAE2 at Demerara Rise Site 1258. *Journal of Chemical Geology*, **429**, 85–92.

Westermann, S., Caron, M., Fiet, N., Fleitmann, D., Matera, V., and Föllmi, K.B. 2010. Evidence for oxic conditions during the oceanic anoxic event 2 in the northern Tethyan pelagic realm. *Cretaceous Research*, **31**, 500–514.

Wiese, F. 2009. The Söhlde Formation (Cenomanian, Turonian) of NW Germany: shallow marine pelagic red beds. In: Scott, R.W., Jansa, L., Wang, C., Hu, X. andWagreich, M. (Eds), Cretaceous oceanic red beds: stratigraphy, composition, origins, and palaeographic and paleoclimatic significance. *SEPM Special Publications*, 150170.

Wilmsen, M. 2003. Sequence stratigraphy and palaeoceanography of the Cenomanian Stage in northern Germany. *Cretaceous Research***, 24**, 525–568.

Wilmsen, M., Niebuhr, B. and Hiss, M. 2005. The Cenomanian of northern Germany: facies analysis of a transgressive biosedimentary system. *Facies*, **51** (1-4), 242–263.

Wilmsen, M. and Nagm, E. 2013. Sequence stratigraphy of the lower Upper Cretaceous (Upper Cenomanian–Turonian) of the Eastern Desert, Egypt. *Newsletters on Stratigraphy*, **46**, 23–46.

Wilmsen, M., Niebuhr B., Chellouche, P., Purner, T. and Kling, M. 2010a. Facies patterns and sea-level dynamics of the early late Cretaceous transgression: a case study from the lower Danubian Cretaceous Group (Bavaria, southern Germany). *Facies*, **56**, 483–507.

Wilmsen, M., Niebuhr, B. and Chellouche, P. 2010b. Occurrence and significance of Cretaceous belemnites in the lower Danubian Cretaceous Group (Bavaria, southern Germany). *Acta Geologica Polonica*, **60**, 231–241.

Wilson, P.A., Norris, R.D. and Cooper, M.J. 2002. Testing the Cretaceous greenhouse hypothesis using glassy foraminiferal calcite from the core of the Turonian tropics on Demerara Rise. *Geology*, **30**, 607–610.

Wohlwend, S., Hart, M. and Weissert, H. 2015. Ocean current intensification during the Cretaceous oceanic anoxic event 2 – evidence from the northern Tethys. *Terra Nova*, **27**, 147–155.

Wood, C.J. and Smith, E.G. 1978. Lithostratigraphical classification of the Chalk in North Yorkshire, Humberside and Lincolnshire. *Proceedings of the Yorkshire Geological Society*, **42**, 263–287.

Wood, C.J. and Mortimore, R.N. 1995. An anomalous Black Band succession (Cenomanian–Turonian boundary interval) at Melton Ross, Lincolnshire, eastern England and its international significance. *Berliner Geowissenschaftlichte Abhandlungen Reihe*, **E16** (Gundolf Ernst Festschrift), 277–287.

Wood, C J., Batten, D.J., Mortimore, R.N. and Wray, D.S. 1997. The stratigraphy and correlation of the Cenomanian–Turonian boundary interval succession in Lincolnshire, eastern England. *Freiberger Forschungsheft*, **C468**, 333–346.

Woolnough,W.G. and David, T.W.E. 1926. Cretaceous glacia-

tion in Central Australia. *Quarterly Journal of the Geological Society, London*, **82**, 332–351.

Worssam B.C. and Taylor, J.H. 1969. Geology of the country around Cambridge. *Memoir of the Geological Survey of Great Britain*, sheet 188 (England and Wales), 159 pp. HMSO; London.

Zheng, X.-Y., Jenkyns, H.C., Gale, A.S., Ward, D.J. and Henderson, G.M. 2013. Changing ocean circulation and hydrothermal inputs during Ocean Anoxic Event 2 (Cenomanian–Turonian): Evidence from Nd-isotopes in the European shelf sea. *Earth and Planetary Science Letters*, **375**, 338–348.

Zheng, X.-Y., Jenkyns, H.C., Gale, A.S., Ward, D.J. and Henderson, G.M. 2016. A climatic control on reorganization of ocean circulation during the mid-Cenomanian event and Cenomanian–Turonian oceanic anoxic event (OAE 2): Nd isotope evidence. *Geology*, **44**, 151–154.

Manuscript submitted: 27th December 2018
Revised version accepted: 31th August 2020